Health Indicator construction for health assessment and fault identification of compressors

Master Thesis

Julian Tas

Delft University of Technology

TU Delft

Health Indicator construction for health assessment and fault identification of compressors

by

Julian Tas

Master Thesis

in partial fulfilment of the requirements for the degree of

Master of Science
in Mechanical Engineering

at the Department Maritime and Transport Technology of Faculty Mechanical, Maritime and Materials Engineering of Delft University of Technology
to be defended publicly on Tuesday September 3, 2024 at 12:00 AM

Student number:	4371194
MSc track:	Multi-Machine Engineering
Report number:	2024.MME.8975
Supervisor:	
Thesis committee:	Prof. dr. R.R. Negenborn, TU Delft committee Chair, 3mE
	Dr. ir. X. Jiang, TU Delft supervisor, 3mE
	Dr. M.A. Mitici, external committee member, Utrecht University
	B. van den Bogerd, company Supervisor, Nobian
Date:	August 26, 2024

TU Delft

Preface

With this thesis I will complete my Master of Science in Mechanical Engineering at the University of Technology in Delft. Within the master Mechanical Engineering I have specialised in the track Multi Machine Engineering. This thesis is written as part of the graduation project, with the purpose of applying the theory and knowledge gained during the master program in a real-world problem situation. In this thesis I will cover the topic of Health Indicator construction for health assessment and fault identification of industrial compressors. This topic brought me the challenge of combining machine learning with the world of maintenance and reliability. It was a though challenge, nevertheless it has awakened my curiosity in the subject and I can see myself already tackling the next challenge. I am proud of what I have achieved and and learned during this period.

This research was conducted for Nobian in Rotterdam, here I have spent most of my time during this journey. I would like to start with thanking the staff of Nobian for their support and collegiality. I would like to specially thank Bart van den Bogerd for providing the opportunity to execute my work, and for the support and guidance during this challenge. Furthermore, I would like to thank Xiaoli Jiang for all her guidance, feedback, patience and unlimited support during this journey, I am very grateful for having you as my supervisor and motivator. Lastly, I would like to thank Rudy Negenborn for his feedback during the meetings which helped me multiple times staying on track towards the final goal.

Also, I would like to thank my parents, brother, friends and other family for all their unlimited support during this graduation project and my entire study at the TU Delft. Finally, I would like to thank my girlfriend for giving me the all love, perseverance, emotional support and patience to full bring this difficult task. This achievement is for all of you and your unconditional support, positivity and pleasant distractions.

Julian Tas
Delft, August 2024

Summary

A new industrial revolution is ongoing, namely Industry 4.0. This revolution focuses on using resources more efficiently and leveraging data, communication, and new technology to achieve this goal. Industry 4.0 covers all fields of industry and is becoming increasingly relevant and required to compete in today's market. This research focuses on the maintenance part of Industry 4.0, specifically on fault diagnostics methods for turbomachinery such as compressors. Compressors play a crucial role in the industry, and maintaining high reliability and availability is desirable. In the chemical industry, dealing with toxic and corrosive products, maintenance of compressors on-site presents difficulties and is preferably scheduled far in advance. Furthermore, compressors are machines with multiple possible failure mechanisms and different degradation patterns. The mean time between failures is not reliable; the deviation between life cycles is widely spread and highly dependent on the production process, where errors in previous process stages impact the degradation of the compressor. This degradation behavior means that a time-based approach to maintenance could be too late or a waste of time and resources on a well-operating machine. Therefore, developing a fault diagnostic model that provides insight into the health condition of machinery could be beneficial. This opportunity is well known in the industry, and a lot of research is being done in this direction.

The aim of this research is to develop a diagnostic model for the chlorine compressor that is able to asses the health, which could be used to optimize the maintenance strategy in order to reduce downtime and improve the performance of the production line with the use of data collected by multiple sensors. The focus is establishing a model that gives insight in the health of the asset and is able to detect degradation and failures. To achieve this goal the available measurement data and failure history is studied to get an understanding of what failure mechanisms could occur and how the degradation pattern of these mechanisms could be detected.

To find the best method for this problem literature is reviewed to find possible solutions, from which the method with the best fit for this research is selected. Condition monitoring includes the observation of the operational parameters and condition of equipment to detect anomalies that could indicate potential faults. The increasing availability of condition monitoring on systems has facilitated the increasing research in fault diagnosis techniques. FDD takes the information from condition monitoring and applies diagnostic algorithms to detect, isolate, and identify the faults. FDD gives insight in the state of equipment and is important to maintain high productivity, efficiency and safety in production plants (Arias Chao et al., [2022]). A lot of the research is focused on a single failure mechanism, for example: the study into fouling mechanism by deriving the equivalent compressor performance map at various degrees of fouling with a consideration of gas properties and stage efficiency variation and without prior knowledge of the detailed geometrical features Al-Busaidi and Pilidis, (2016).

An approach that is able to assess the machine as a whole is the construction of a health indicator (Lei et al., [2018]Jardine et al., [2006]Schwartz et al., [2022]Wang et al., [2012]). Well constructed Health indicators could also be used as basis for remaining useful life prediction methods. HIs can be divided into two categories based on their construction strategies: physical HIs (PHI) and virtual HIs (VHI) (Lei et al., [2018]). PHI correspond to direct underlying degradation factor and the physics of failure and are generally directly extracted from monitoring signals. VHIs are generally built by fusing multiple PHIs or multi-sensor signals. VHIs describe the degradation trend of the equipment, but loses the direct physical meaning. For this research there are no monitoring signals available that directly correspond to a physical degradation, so a VHI should me constructed using multi-sensor signals. This could be achieved by statistical approaches, in Wang et al., (2012) the framework for constructing generic HIs is provided by employing a linear data transformation method. This method is suitable for continuously collected measurements and is a process of information fusion which provides a unified measure being used to characterize the health condition of the system. Schwartz et al., (2022) uses kernel functions in combination with principal component analysis to provide a non linear approach to data fusion as

basis for the HI construction. These methods are trained with the help of failure data. Due to preventive maintenance approach limited failure data of compressors is available. This gives the challenge of learning the degradation and failure behaviour without having training data of this. Model should be able to learn the characteristics of a healthy compressor.

A different approach is provided using a machine learning method, where the HIs are constructed with the help of neural networks (NN) Kim et al., (2019). This has the advantage of not requiring the exact failure threshold and does not limit the application of the method for a specific degradation process. Another study uses Semi-Supervised Deep Neural Network (SSDNN) for data fusion in order to create HIs Moradi et al., (2023). Here the model is trained to construct HIs with high prognosability by using evaluation metrics for HIs during the training process, these are often used for this practice (Eleftheroglou et al., [2018]). Liu et al., (2020) proposes the use of a Long-Short Term Memory AutoEncoder (LSTM-AE). The structure of LSTM predicts the next time steps and is able to learn long-term memory information to provide a solution to long-term dependencies X. Chen et al., (2023), this makes it functional for using the dtaa in an optimal manner. The AE is a reconstruction method that recovers the original input from its compressed representation to measure the reconstruction error. This reconstruction error is used as the basis for the HI. HIs are not only sensitive to degradation, but they also might be influenced by abnormalities in environmental conditions and operations. de Pater and Mitici, (2023) extends on this method by making the LSTM-AE feasible for varying operation conditions and applying attention to increase accuracy. Most of these use the same type of data set, which are created by a simulation using a degradation function (Arias Chao et al., [2021]) and thus providing a clear degradation behaviour the challenge is to construct accurate HIs for real world applications which are robust enough to deal with impurities in data. Malhotra et al., (2016) also uses LSTM-AE to construct HIs with a different approach. Their goal is to construct a mapping of the reconstruction losses over time, resulting in a HI function that is used for RUL prediction. The limitation here is that the model only assumes one type of degradation curve, which does reflect the occurrence of multiple degradation mechanisms in reality. This highlights the difficulties of performing fault diagnosis and identification in real world cases. The considered methods should meet the following criteria to be considered feasible:

- Can be trained with limited or without failure data.
- Is able to deal with changing operating conditions.
- Is capable of detection and identification of the degradation by multiple faults simultaneously.

This has resulted in the selection of the LSTM-AE as foundation for the methodology of this research.

To study the selected method for the purpose of fault detection and identification, a case study is conducted at Nobian Rotterdam. The research question that will be answered with this tudy is as follows: *How can the failure mechanisms of chlorine compressor be diagnosed and the health of the compressor be monitored?* The scope of this research are the chlorine compressors that are used in the chlorine production plant. The compressor is a complex system with a lot of inlet, outlets and subsystems, this provides many boundary uncertainties. The most difficult part of the compressor system to replace or repair is the compressor itself and the internal parts, this due to the corrosive nature of chlorine and the precision requirements for the turbomachinery. To limit the scope of the study, the system boundaries of the compressor are chosen to be at the coupling between the rotor and the gearbox and at the flanges of the inlets and outlets of the compressor. The main focus of this research is on developing a fault diagnosis model that is able to identify the chosen failure mechanisms by constructing health indicators for the compressor. The contribution to the prognostic part of predictive maintenance is limited in this research due to limited recorded failure instances of the compressors, with this lack of data it is at this moment not possible to develop a reliable prognostic model. The steps that will be executed are presented in Figure 1.

First the characteristics and failure mechanisms of the compressor are described. The compressor used for chlorine liquefaction consists of four compressing stages with cooling between the stages, except after the first stage. It operates at a high rotational speed and is considered as turbomachinery. The compressor is driven by an electrical engine, which is coupled by a gearbox to the rotor of the compressor. The rotor is hold in place by journal bearings on both ends of the compressor and an axial bearing on the non driven end to limit axial movement. These bearing are fed from an auxiliary

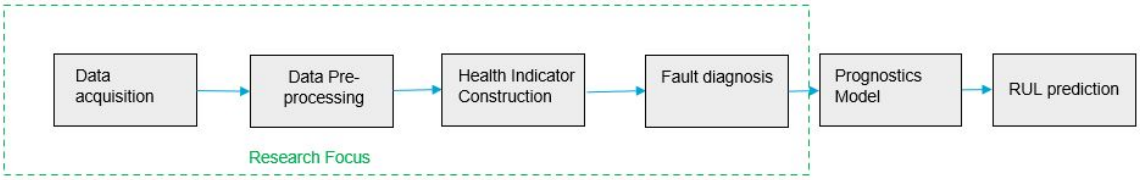

Figure 1: The steps of PHM with encircled in green the focus of this research.

oil system, this oil functions as both lubricant and coolant of the bearings. Labyrinth seals are used to separate the stages and prevent leakages. At both ends where the rotor leaves the compressor casing a labyrinth gas seal is applied.
The failure mechanisms that are included into this research are selected based on occurrence, severity and the ability to be detected with the available data. The following failure mechanisms are included into the fault identification model: leakages, fouling and bearing failures. Due to the corrosive and toxic nature of chlorine leakages are a great risk for compressors. Leakages have effect on the temperature and pressure in the compression stages and on the pressure difference between the dry air and chlorine feedback in the gas seal. Fouling occurs when contaminants enter the compressor system, this results in performance losses of the compressor. The main cause of fouling in chlorine compressors is the presence of moisture in the chlorine which in combination with the cast iron casing and chlorine reacts to ferrochlorine's. These particles can deposit inside the compressor and lead to internal blockages. The effect of fouling is decreasing efficiency of the compressor and is noticeably in the temperature between stages as well by the increase of power consumption. Bearing failure is the best known failure mechanism when dealing with rotary equipment and is normally detected with high frequency vibration measurements, these are not included in this case study. The purpose of the axial bearing is to absorb the axial forces and prevent axial movement, so out of bound axial displacement is a sign of a defect. Furthermore, defects on the bearings create extra friction and lead to increasing temperatures.

The next steps are data acquisition and data preprocessing. The data of 5 compressor lifecycles is available with length varying between 2.5 and 5.5 years. The sensor measurements are collected and stored each minute, this rate results in a large amount of data. In this case study the change in measurement values is slow, therefore the measurements are aggregated per hour by considering the mean per hour. There are 56 functional sensors outputting data, resulting in a total of almost 9 million sensor measurements. To reduce the data input for the model, sensor selection is performed. Following industry safety standards critical sensor measurements are executed twice or even three times to implement a safety factor, this brings sensor duplicates of which only one is selected. Also non identical sensors can have a high correlation, only one of two is selected if the correlation is 0.95 or higher. There are a total of $a^s = 16$ sensors selected and $a^o = 3$ are considered as the operation conditions. To train a model to recognise the health state of a system a footprint of the state where the system is considered healthy is required. To establish time intervals in the data from where the training data can be acquired an assumption has to be made. It is assumed that the compressor data is considered healthy the first few months after the compressor is replaced.

The preprocessing of the raw data is required to make the model functional by giving it clean data as input. The preprocessing of raw data consists of multiple steps including: outlier removal, noise reduction, normalization and sequencing. The acquired data contains outliers that could be caused by various reasons for example sensor failures. The assumption is made that the training sets do not contain outliers, since these sets are of created of data during relatively short healthy period. To identify potential outliers in the test sets the overall mean and standard deviation of the training sets is used to establish the operation boundaries of the parameters that are measured. To find the potential outliers the data of the test sets is subjected to these boundaries, in case of outliers the data is replaced by interpolating between the neighbouring non outlier data points. The noise reduction will be performed with the moving average method, this makes the time series more smooth and will give a better performance for the model. Standardisation is performed on the data. Here the the mean μ and standard deviation std are calculated from the data and used for standardization. It is important to note that the mean value and standard deviation of the training sets is also used on the testing set, for the reason that these are considered to be the values of the healthy state of the compressor. The time series of a data set can not be fed to the LSTM-AE at once and is therefore split in smaller sequences. The sequences are extracted with a rolling window. The stride and length of this rolling window is different for the training and testing set.

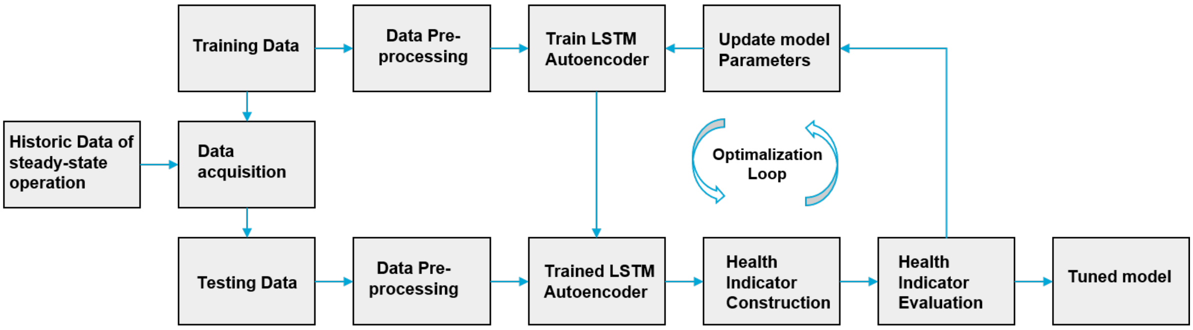

Figure 2: The approach for tuning the model.

After the implementation of the model is verified the optimal parameters of the model are determined, these are acquired by performing a grid-search. This optimization loop is shown in the schematic Figure 2. This optimization loop is executed with the help of grid search, where systematically each logical combination of parameters is evaluated. The model parameters in the grid search that had the highest fitness overall are considered to be the optimal parameters. The weights of the training epoch with the lowest validation losses are applied to the model. Only sensors with a high trendability are included in the construction of the HI. The trendability provides information over the difference in reconstruction loss at start of a lifecycle and the end of a lifecycle. For features with high trendability it is expected that the reconstructed signal deviation is minimal in the early stage of a lifecycle, this deviation increases with increasing time in the lifecycle, this corresponds to the increasing degradation. The final verification steps compares the proposed method to two different approaches of LSTM-AE. One approach ignores the operating conditions, analysing this version by comparing its metrics with that of the proposed method it is clear that the evaluation metrics decrease significantly. This result emphasize the effect of training the model independently from the operating conditions has positive impact on the performance of the HI construction. The proposed model is trained with the training data of all compressors and could therefore be applied immediately for a newly placed compressor. The version of the method where the weights are trained for each compressor lifecycle separately could only be a applied to a new compressor when the months that are used for collecting training data are passed. However when dealing with real world data each compressor could have a different initial state, which brings extra noise and offsets to the HI construction. This expected difference in performance is visible in Table 1, where the evaluation metrics increase with this approach.

Table 1: Evaluation of the different version of LSTM-AE architecture. Here the sets corresponds to the compressor lifecycle. Mon, Tre and Pro stand for the monotinicity, trendability and prognosability respectively, which are the evaluation metrics for the constructed HIs.

	Set 1		Set 2		Set 3		Set 4		Set 5		Mean			
	Mon	Tre	Mon	Tre	Mon	Tre	Mon	Tre	Mon	Tre	Mon	Tre	Pro	Fitness
proposed LSTM-AE	0.01	0.88	0.02	0.87	0.02	0.51	0.00	0.91	0.03	0.86	0.02	0.81	0.519	0.612
proposed LSTM-AE without operating conditions	0.03	0.79	0.05	0.91	-0.01	0.51	-0.01	0.65	0.05	0.47	0.02	0.67	0.398	0.525
proposed LSTM-AE with trained weights per compressor lifecycle	0.03	0.94	0.05	0.88	0.04	0.72	0.04	0.88	0.08	0.92	0.05	0.87	0.704	0.764

The validation of the results is conducted by evaluating the health assessment and fault identification. Health assessment is performed to divide the health state of the compressor using the constructed HI. There is no nuance in health state, there is only healthy or unhealthy, this has as result that the compressor are considered unhealthy relatively early on their lifecycle and operate for a long time before they are overhauled, see Figure 3.

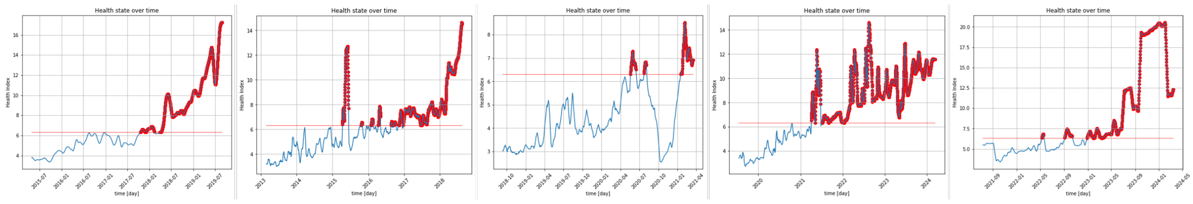

Figure 3: The health state division of the compressor lifecycles sets 1 to 5 from the left to the right. The unhealthy state is marked by the red circles.

The HI is based on the reconstruction losses of a subset of sensors that are considered for each HI of a failure mechanism. These subsets are based on the expected effect and location of the failure mechanism as previously described. Furthermore the trendability of the reconstruction loss has to be higher than 0.5 for the sensor to be included. The HI for detecting leakages will be constructed from the sensors that are relevant to the gas sealing. The selected sensor for fouling are measuring parameters of the gas path in the compressor. The subset for the bearing HI includes the temperature and pressure of the oil, the bearing temperatures and the position of the rotor. The identification is performed by checking whether the separate HIs of the test sets cross the health threshold, that is determined for each failure mechanism. The fault identification is performed by analysing the failures per set for each constructed HI, the results of analysis is presented in Table 2. The results of the fault identification are used to calculate the KPIs and are shown in Table 6.7. The first instance of an compressor marked as unhealthy triggers the start of the fault identification, which has resulted in a identification with an accuracy of 73% and a precision of 56% for the three considered failure mechanisms. The performance of the model is increased by training the weights of the model for each compressor lifecycle separately. The trade-off using this approach is that health assessment and fault identification is not possible in the start of a new lifecycle, because this period is used to acquire the training data. To overcome this trade-off a combination of both approaches should be used, where the health assessment during this first period of a new compressor is performed original model and after this initial period the model specifically trained for this lifecycle is used for fault identification with higher accuracy.

Table 2: Confusion matrix of the fault identification

Confusion matrix		Diagnosed Fault	
		Fault is present	*Fault is absent*
Identified fault	*Fault is identified*	5 TP	4 FP
	Fault is not identified	0 FN	6 TN

Table 3: Case study results of the fault identification.

KPI	Score
Accuracy	0.73
Precision	0.56
Recall	0.45
F1-score	0.5

To conclude, the proposed LSTM-AE method is able to correctly detect and thereafter identify single or multiple failure mechanism present in chlorine compressors with an accuracy of 73 %, while only being trained with healthy data and is therefore applicable for real world cases with unlabeled data.

Therefore the goal of this study has been achieved.

The main contributions of this research are:

- A method is proposed for health indicator construction for compressors with the purpose of health assessment and fault identification. By constructing health indicators for each detectable failure mechanisms the model is able to perform fault identification even when multiple faults are developing. The model is tested with a real world case study of chlorine compressors of which little failure data is available so the model is trained to learn the healthy characteristics of the compressor. In this study it is shown that this method is able to correctly identify the failure mechanism present in the compressor and is therefore applicable for real world cases.
- The health indicators are constructed with the reconstruction loss of the LSTM-AE. The model is trained to reconstruct the measurements independently of the operation conditions, which increases the robustness of the model.
- The collected real world data requires extensive preprocessing to reduce the effect of corrupted data and format it to the correct form before it is used as input to the LSTM-AE. This research proposes the tools to realise this and shows the effect of the quality of the preprocessing.

Contents

List of Figures

List of Tables

1 Introduction

1.1. Industry 4.0

A new industrial revolution is ongoing, namely Industry 4.0. This revolution focuses on using resources more efficiently and leveraging data, communication, and new technology to achieve this goal. Industry 4.0 covers all fields of industry and is becoming increasingly relevant and required to compete in today's market. This research focuses on the maintenance part of Industry 4.0, specifically on fault diagnostics methods for turbomachinery such as compressors.

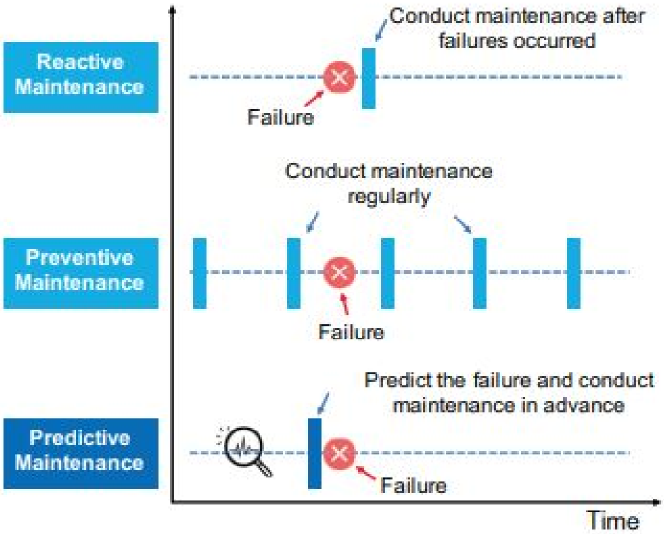

Figure 1.1: An overview when maintenance takes places based on a failure Ran et al., (2019).

In industry there are three main maintenance strategies: reactive maintenance, preventive maintenance and predictive maintenance, see Figure 1.1. By reactive maintenance the action to repair or replace components takes place at he moment of a failure. With preventive maintenance the equipment is maintained periodically. This has the advantage that the unexpected failures are largely reduced, however this also means that the cost of the maintenance strategy increases, because the equipment is not used for its full useful lifetime. Predictive maintenance uses condition monitoring techniques in combination with fault diagnosis and the prediction of the remaining useful lifetime (RUL). One of the main advantages of adapting this strategy is that incipient faults can be detected, which allows time to come up with an optimal plan for maintaining the system. The disadvantage of predictive maintenance are the costs upfront to establish a system of sensors so the condition of the equipment can be assessed and for implementing a predictive model, however the availability and reliability of equipment increases considerably that for critical systems it quickly becomes profitable. In the industry complex and critical equipment is usually already monitored for process control and safety measures, these sensors could also be used to further reduce implementation costs. Predictive condition monitoring and preventive maintenance are both used to achieve high reliability and availability of complex rotating machinery, and to reduce unplanned production shutdowns. To achieve these goals, it is not only necessary to implement effective fault detection and diagnosis, but also respond to the detected faults by continuously assessing and predicting the health status of the system. As previously mentioned predictive maintenance consists of condition monitoring and a prediction of the RUL, this can be elaborated with the help of figure Figure 1.2. The step that are executed includes: data acquisition, data processing, detection, fault diagnosis, prognosis and maintenance decision making. To refer back to the industry 4.0, big data is a term often used in this context and means analysing the data industrial companies already continuously collects. However, to gain value out of this big data the approach for data analysis should structuralized, hence the introduction of the workflow in Figure 1.2.

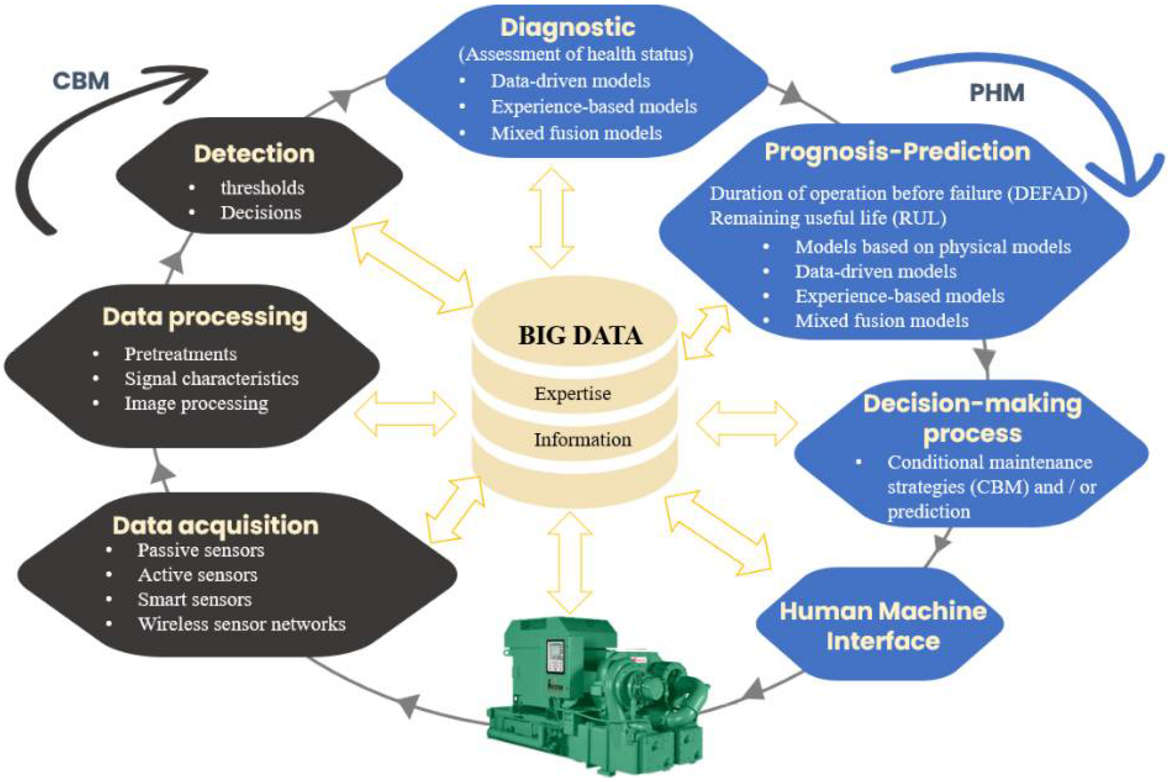

Figure 1.2: The worklfow of predictive maintenance (Achouch et al., [2022])

1.2. Nobian Rotterdam

Nobian is a company specialised in the production of essential chemicals for industries and has production plants in the Netherlands, Germany and Denmark. Their core business is the production of salt, chlorine and caustic soda. The plant in Rotterdam is the largest chlorine producer of the company. The plant has been modernised several times and has also increased its production capacity. This has influenced the usage of assets in the plant. The object for this research are the chlorine compressors, that are used in the process of liquefying the chlorine and are critical to the plants capacity. The compressors are parallel to one another and originally only one was operating, while the other was on stand-by. Due to the increase of the production capacity of the plant both compressors are required to be operated at maximum capacity to reach the target production capacity of the plant. This change results in the loss of the redundancy of the chlorine compressors, this situation makes the need for an efficient maintenance strategy high.

1.3. Problem description

The compressor is a critical part in the plants process to liquefy chlorine, which is necessary to store and transport the chlorine. Therefore stopping one of the compressors means losing 50% of production capacity, the company desires an optimized maintenance strategy for the chlorine compressors. Furthermore, the chlorine compressor is a complex machine with multiple possible failure mechanisms and different degradation patterns. The mean time between repair (MTBR) is not reliable, the deviation between life cycles is spread widely and highly depended on the production process, where errors in previous process stages have an impact the degradation of the chlorine compressor. In the current situation a preventive maintenance strategy is used with an time-based interval of 6 years, in this interval failures still occur. Two compressors operate continuously at full capacity without redundancy. The plant has an turnaround interval of 2 years, in the turnaround the production is stopped entirely. The moment is coordinated with the customers, who rely on the supply of chlorine. The turnaround is an ideal moment to replace the chlorine compressor without losing any unplanned production capacity. Furthermore there are moments of opportunity in the interval between turnarounds where the production demand is relatively low, this moment is used if the condition of the compressor is degraded that an overhaul within this opportunity moment is beneficial. Maintenance of the compressor means exchanging the operating compressor with the spare compressor, because opening the compressor in the field and executing repairs locally is not an option, due to the corrosive nature of chlorine and short period of time during the turnaround. That is why the compressor is taken out of the field and revised in a workshop and the spare compressor is placed in the same location. The time the compressor placed on its location is from now on referred to compressor lifecycle. Thus, the ideal situation would be to make predictions for the asset whether it can operate optimally till the next turnaround.

1.4. Research Objective

The aim of this research is to develop a diagnostic model for the chlorine compressor that is able to asses the health, which could be used to optimize the maintenance strategy in order to reduce downtime and improve the performance of the production line with the use of data collected by multiple sensors. The focus is establishing a model that gives insight in the health of the asset and is able to detect degradation and failures. To achieve this goal the available measurement data and failure history is studied to get an understanding of what failure mechanisms could occur and how the degradation pattern of these mechanisms could be detected. The research objective is formulated into a main research question and several sub research questions that contribute to reaching the objective:

Main research question

How can the failure mechanisms of chlorine compressor be diagnosed and the health of the compressor be monitored?

Sub-research questions

1. What are characteristics and the failure mechanisms of the chlorine compressor and which will be included in the model?
2. What is the current state of failure diagnosis methods in literature and what method is best applicable to this case study?
3. How to develop the proposed fault detection and indication model for the chlorine compressor?
4. What data is available and how can it be retrieved and analysed for the purpose of fault detection and diagnosis?
5. How to verify and validate the proposed method?

1.5. Research Scope

The scope of this research are the chlorine compressors that are used in the chlorine production plant of Nobian Rotterdam. The compressor is a complex system with a lot of inlet, outlets and subsystems, this provides many boundary uncertainties. The most difficult part of the compressor system to replace or repair is the compressor itself and the internal parts, this due to the corrosive nature of chlorine and the precision requirements for the turbomachinery. To limit the scope of the study, the system boundaries of the compressor are chosen to be at the coupling between the rotor and the gearbox and at the flanges of the inlets and outlets of the compressor.

The chlorine compressor is a turbomachinery dealing with a highly corrosive medium and has therefore multiple possible separate or combination of failure mechanisms. Not all of the mechanisms occur as frequently, to limit the scope of this research there is chosen to only include three main failure mechanisms.

Nowadays a lot of mechanical failures are identified by vibration monitoring, however vibrations measurements are performed by a third party and the raw data is not available for the entire chosen research period, so high freq vibration data is not included in the scope.

The main focus of this research is on developing a fault diagnosis model that is able to identify the chosen failure mechanisms by constructing health indicators for the compressor. The contribution to the prognostic part of predictive maintenance is limited in this research due to limited recorded failure instances of the compressors, with this lack of data it is at this moment not possible to develop a reliable prognostic model. The steps that will be executed are presented in Figure 1.3.

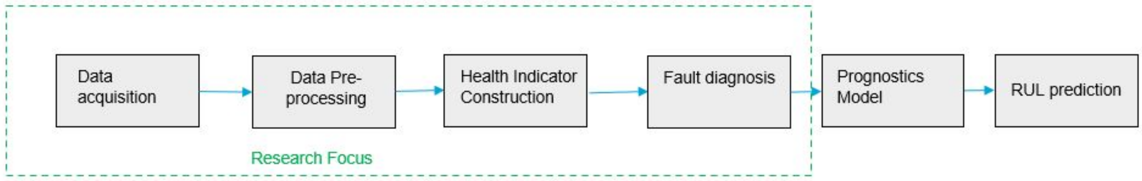

Figure 1.3: The steps of PHM with encircled in green the focus of this research.

1.6. Report outline

The each chapter of this research provides the answer of a research subquestion. Chapter 2 contains the background information of the production process, the characteristics of the compressor and the failure mechanisms. Chapter 3 gives an overview of fault detection and diagnosis methods in literature, and the method selection is presented here. In Chapter 4 the methodology of the proposed method is described and the tools the evaluate the outputs. Chapter 5 gives an overview of the data acquisition and preprocessing. Chapter 6 contains the implementation and verification of the proposed methodology along with the validation of the results. Chapter 7 answers the main research question by providing the conclusion of the research and its limitations.

2

Background information

The goal of this chapter is to answer the following research question: *What are characteristics and the failure mechanisms of the chlorine compressor?* This goal is achieved by firstly emphasizing the criticality of the chlorine compressor by describing the production process, thereafter the characteristics of the compressor and in it auxiliary system are described. Then an overview of the possible failure mechanisms of the chlorine compressor are provided and at last with this basis the failure mechanism that are included in this research are selected.

2.1. Production process

In this section the production process of chlorine is shortly described to empathise the criticality of the compressor and to provide an understanding of the production process it is integrated in. The process from salt to chlorine has the following steps:
Salt-> Brine -> Electrolyse -> Chlorine gas -> Cooling -> Drying -> Pre Cooling -> Compression -> Condensation -> Liquid chlorine -> Storage/ Distribution

2.1.1. Electrolysis process

At Nobian vacuum salt is used to create chlorine, this is a high quality salt and has the advantage that it does not require a purification process at the plant. The brine is prepared from depleted brine circulating back from the electrolysis process, which is re-saturated by adding salt and water. The depleted brine is saturated with chlorine and is de-chlorinated to prevent corrosion and chlorine emissions. The chlorine extracted from the brine are fed to the quench. After dissolving the salt and water in the brine, impurities originating from the salt are removed in several purification steps, before being fed to the electrolysers. The purity of the brine has effect on the degradation and efficiency of the electrolysers. Currently the most used method for electrolyse is the membrane technique, this is also used at the plants of Nobian. The membrane cell process has an ion-exchange membrane that separates the anode and cathode of the electrolyser. Only sodium ions and water pass through the membrane in one direction. The saturated brine is fed to the anode side of the electrolyse cell, here the chloride ions react to chlorine:
$2Cl^- \rightarrow Cl_2 + 2e^-$
The electric field causes the sodium ions to migrate through the membrane into the cathode compartment. The cathode is the negative electrode of the electrochemical cell and supplies electrons to the medium, causes the following reaction:
$2H_2O + 2e^- \rightarrow H_2 + 2\,OH^-$
The hydroxyl ions together with the sodium ions forms caustic soda, which is also processed towards an final product of Nobian. The hydrogen is released as a gas and is distributed towards costumers and power facilities. At the anode side the chlorine in gas form saturated with water leaves the compartment and travels towards the anolyte tower via a cyclone, where it is separated from the depleted brine. Chlorine gas that holds water is called wet chlorine and is highly corrosive. The chlorine gas has a high temperature of around 85 degrees Celsius when leaving the electrolyser and is saturated with water vapor. The wet chlorine requires cooling to prepare it for the drying and to purify it. The

first cooling takes place in the anolyte tower where the gas passes purified brine which acts as coolant and decreases the temperature towards around 70 degrees Celsius. In this process the chlorine gas stream is also cleaned by the brine. Hereafter the gas travels into the quench where it is cooled and cleaned on multiple packed beds by a reversed stream of chilled brine towards 15 degrees Celsius. By cooling the chlorine stream is separated from a large part of the present water, this is condensed and added to the brine streams.

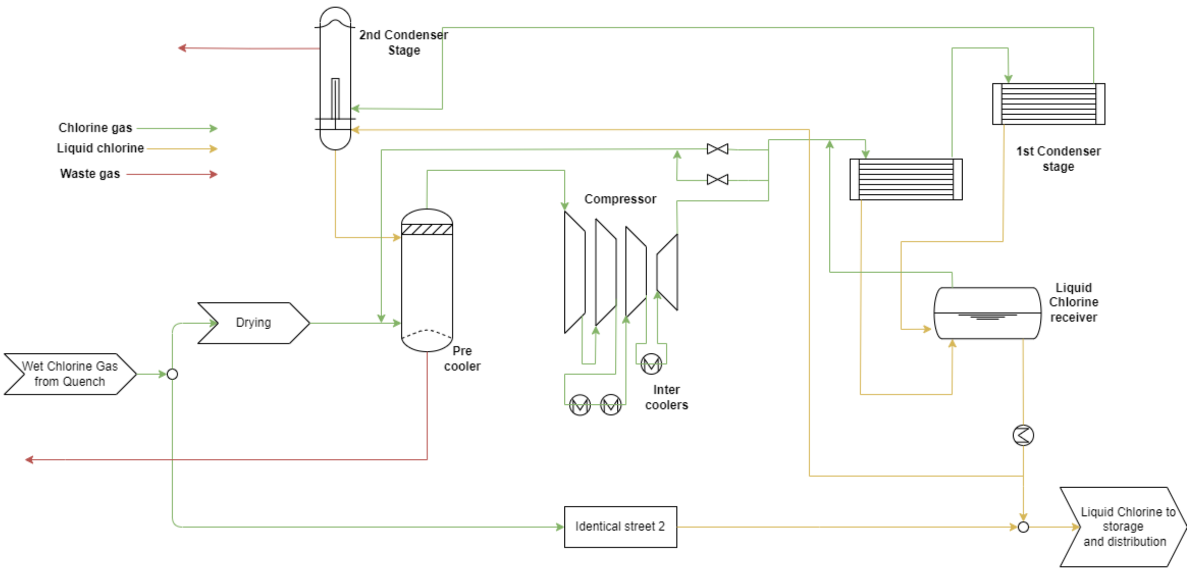

Figure 2.1: Flow diagram of the chlorine street

2.1.2. Chlorine street

The chlorine leaves at the top of the quench and flows towards the drying unit. Here the stream is divided over two identical streets, presented in a schematic overview in Figure 2.1.

Drying

At the start of the street the stream passes through a wet demister where contaminants and small droplets are removed. The chlorine contains to much water and is still considered wet, before the chlorine is considered dry the moisture content should be lower than 10 ppm. The drying process occurs in two consecutive drying towers where sulphuric acid flows in opposite direction of the chlorine gas and absorbs the water. At the end of the drying process a dry demister is located, which removes the fine sulphuric acid mist.

Pre cooling

The dry chlorine leaving the demister is cooled down to around -32 degrees Celsius before entering the compressor to reduce the compression load. This cooling takes places with the use of liquid chlorine, which also cleans the chlorine gas ones more. The liquid chlorine is returning from the liquefaction process. This technique increases the flow through the compressor and it removes no heat from the process. One of the contaminants that is removed from the gas stream here is nitrogen trichloride, which is a hazardous compound. The concentration of NCl_3 should not exceed 2% according to the chlorine institute (Brinkmann et al., [2014]). In the bottom of the precooler NCl3 accumulates in the liquid chlorine, therefore the bottom of the cooling installation is coupled to a NCl3 decomposer.

Compression
The cooled chlorine enters the multistage centrifugal compressor at the suction side, the ideal suction pressure is 1.368 bar. The compressor consist of four stages, with a double intercooler between stage 2 and 3 and single intercooler between stage 3 and 4. The intercoolers are in place to avoid overheating of the chlorine, this is an issue because chlorine reacts combustively with most metals. The temperature is kept below 110 degrees Celsius, which is considered a safe margin for prevention of iron chlorine fire (Dokter, [1985]). Due to the precooling no intercooler is required between the first and second stage. The ideal pressure on the pressure side after the last stage is 11 bar. After the compression of the chlorine gas, it travels towards the first condenser of the first condensation stage. On this path there is also a branch for recirculation to the precooler, this is used for pressure control and surge prevention.

Condensation
The liquefaction of the chlorine occurs in two steps to reach a high liquefaction degree. The first step consists of two condensers in series that use water as cooling medium, here the largest part of the chlorine is condensed. The liquid chlorine is collected in a receiver and is transferred towards the storage and distribution section via an aftercooler. The remaining chlorine gas that leaves the second condenser flows to the second condensation step where it is condensed with the use of evaporating cold chlorine. The liquid chlorine flows from the second condensation step to the precooler, while the remaining tail gas is diluted with air to avoid explosion risk and sent to the chlorine destruction.

Distribution
The liquid chlorine of both liquefaction street is combined and can be stored under pressure in two large tanks or directly distributed towards the costumers by the long distance pipe network.

2.2. Characteristics of the chlorine compressor

The centrifugal compressor is a dynamic machine that uses rotation energy to compress gasses. The impeller rotates at high speed and through the impellers design the gasses are driven from the center to the outside edge, this creates an under pressure in the center and draws gasses through the inlet towards the impeller, so the pressure of the gas is increased by the spinning of the impeller. The gas at the outside with the high velocity is directed into a diffuser. The shape of the diffuser reduces the velocity of the gas resulting in an additional increase of pressure. It is possible to add multiple stages of this process by leading the gas from the diffuser into the next impeller. Centrifugal turbo compressors with a mono or multi-stage can have a throughput up to 1800 tons per day and a discharge pressure up to 16 bar. In the large industry, the multi stage centrifugal compressor is most commonly installed, as is the case at Nobian (Talk, [2020]).

The components, subsystems and auxiliary systems of the centrifugal multi stage compressor are discussed here. In Figure 2.2 an intersected compressor is shown, where the internals are visible in their operating location. This specific figure provides a clear cross sectional view of the compressor and is retrieved from compressor manufacturer Group, (2014).

2.2.1. Casing

The casing is the outermost pressure containing part of the compressor and includes the inlet and outlet nozzles. There are two types of casings used for centrifugal compressors that differ in the way how they are opened; the horizontal split casing and vertical split casing, also known as the barrel type. The vertical split casing is suited for high pressure applications. The horizontal split casing is the one used in this case study. Horizontal split casing consists of a top and bottom half which are bolted together along the center line and is shown in figure Figure 2.3. The internals can be accessed by removing the top half. To ease maintenance the piping connections are mostly on the bottom half, so it can stay in place. This type of casing is used for low pressure application up to 40 bar discharge pressure (Talk, (2020)). With higher pressures the possibility exist that the two parts break up and leaks occur. This should be prevented at all cost when dealing with chlorine, luckily for the liquefaction of chlorine is a pressure of

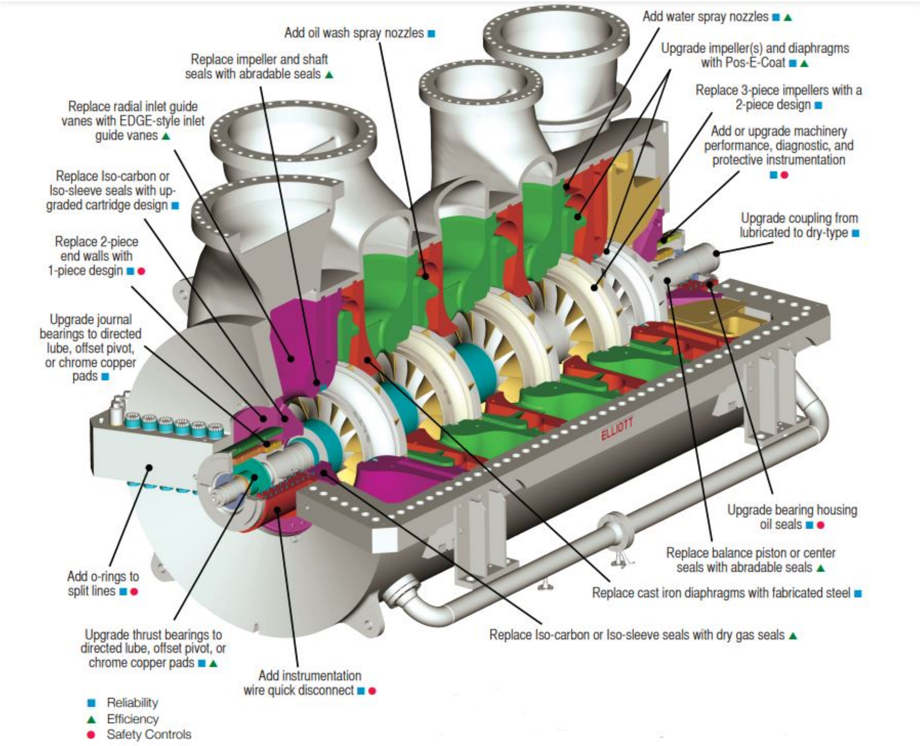

Figure 2.2: New modifications made on the chlorine compressor produced by Elliot Engineered Solutions Group, (2014)

16 bar sufficient. To ensure the prevention of chlorine leaks a sealing is applied between the two halves.

2.2.2. Rotor

The rotor of a centrifugal compressor is an assembly of the shaft and impellers. The rotor should be perfectly balanced for the high speed rotations and is hold in place by bearings on either side.

Shaft

The shaft consists of a stiff solid rod, that is machined to fit all the parts. The impellers are mounted on the shaft even as the spacers. Towards both ends of the shaft it contains grooves, these are functional for the labyrinth seal.

Impeller

The impellers provide the head pressure and are available in different designs. For multi stage turbo machinery enclosed impellers are most of the time the best choice. This type functions well at the high rotation speeds of the compressor that is required in the industry.

2.2.3. Bearings

Two types of bearings are required to hold the rotor in position and make it functional. Journal bearings are placed to let the rotor rotate, while the thrust bearings are used to hold the rotor in position axially. The journal bearings operate as radial bearings and make use of a pressurized oil fluid films between the shaft and the bearing itself to support the rotating shaft. The most commonly type of journal bearing that is used is the the tilting pad journal bearing. These can handle the unbalancing action of the oil film. The thrust bearing operates as axial bearing and are suitable of resisting axial motion. The inner part of the bearing, the thrust collar is hydraulically fitted on the shaft, so it is fixed and rotates along. Thrust bearings have a stationary thrust surface, thrust pads and a thrust collar which revolves with the shaft. In normal condition there is a thin layer of oil in between thrust collar and thrust shoe. Any axial

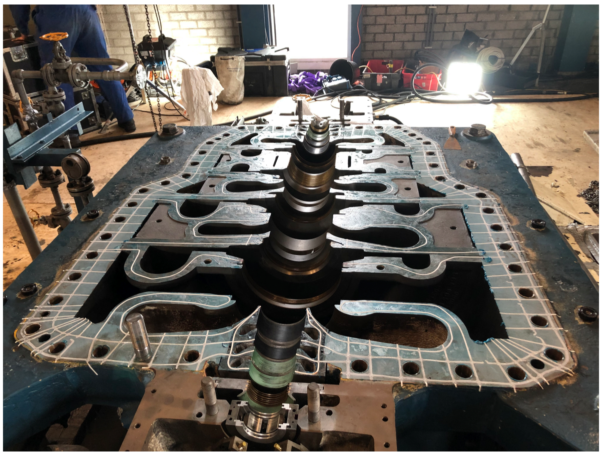

Figure 2.3: The lower half of the casing with the tefloncoard and Hylomar applied for a sealing layer.

motion is prevented by the thrust shoes.
Both type of bearings make use of oil as lubricant, for continuous lubrication this requires a lubrication system which maintain the oil levels. Mixing of oil with the operating gas should not occur due to the reactive nature of chlorine, which has a negative effect on the lubrication, therefore the bearings have to be properly sealed from the medium.

2.2.4. Diaphragm

The diaphragm are placed in the casing and are stationary. It contains the the diffuser in which the impeller discharges the gasses and and a channel to redirect the gasses to the next stage. The diaphragm are fabricated in halves to ease the installation and are bolted together. The two halves want to move away from one another due to the pressurized gasses inside, therefore the assembly is important to prevent leakage.

2.2.5. Sealing

Operating with chlorine brings risks due to reactive nature of the element, therefore choosing the correct materials it contacts is important. Also, the sealing of the entire system should be sufficient to prevent the chlorine of making contact with different components or leaking out of the casing. Different type of seals are used inside the compressor. As stated above the diaphragms and the casing consist of two halves which are bolted together, to make sure no leakage can occur a seal is applied between the two halves, so the chlorine is contained, see figure 2.3. Labyrinth dry gas sealing called a tandem seal is in place to keep the gas in the process area and is placed along the shaft between the bearings and the process area. The labyrinth seals used for chlorine compressors has three chambers where dry air is lead through to create an over pressure and ensure that the chlorine is prevented from leaving the compressor, this type of sealing is shown in Figure 2.4.

2.2.6. Power

Consistent power is required to operate the compressor efficiently, nowadays the most commonly used power source is an electrical engine. These can provide a consistent power input to the compressor with stable amount of revolutions. The option exist to have an variable frequency driver that makes it possible to have different operating points of the compressor, which could benefit the efficiency. This is however not the case for this particular compressor.

2.2.7. Gearbox

The centrifugal multistage turbo compressor requires high rotation speeds, to increase the rpm delivered by the engine a gearbox is set in place to realise this. The type of gearbox that is commonly used is one made of planetary gears. The gearbox also includes the coupling between the driving engine and the compressor rotor.

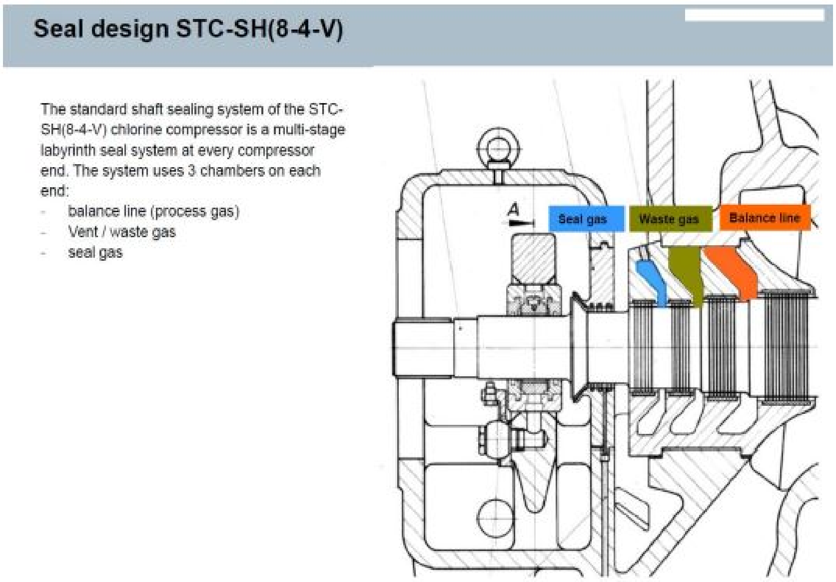

Figure 2.4: Type of labyrinth seal that uses three chambers with gasses.

2.2.8. Auxiliary units

For the compressor to function it requires extra inputs from auxiliary systems. The seals require dry air or nitrogen to function, which is supplied by the dry air system. Furthermore the compressor requires interstage cooling for improved efficiency and the bearings require oil for lubrication.

Intercoolers

In the case the compressor consists of multiple stages it is often usual to cool the chlorine in between stages. This method increases the efficiency of the compressors. The gas is then lead to the intercooler after it passes the diffuser and lead back to the next impeller stage after it is cooled down. The advantage of pressurized chlorine is that it can be cooled at ambient temperatures.

Oil system

A machine with moving and rotating parts requires oil. This oil is multifunctional, it is used for lubrication in the bearings and gearbox and circulating the oil through the system it also dissipates the heat produced at those locations. The oil system consists of pumps, coolers, filters and a reservoir.

2.3. Failure mechanism

The failure mechanisms that are included into this research are selected based on occurrence, severity and the ability to be detected with the available data. The following failure mechanisms are included into the fault identification model.

2.3.1. Fouling

Fouling occurs when contaminants enter the compressor system, this results in performance losses of the compressor. Fouling can be divided in two groups, the first being non reactive contaminants that enter the compression circuit and do not change state Barnard, (2001). This group typically settles in calm places, erode labyrinths and the edges of impeller blades. The other group consists of contaminates in gas or liquid form and these cause problems if they change state as they pass through the compression circuit. The main cause of fouling in chlorine compressors is the presence of moisture in the chlorine which in combination with the cast iron casing and chlorine reacts to ferrochlorines (Brinkmann et al., [2014]). These particles can deposit inside the compressor and lead to internal blockages. For example see figure 2.5a where fouling has occurred and the diffuser of the third stage is clogged, which results in a smaller diffuser and effects the performance of the compressor. The effect of fouling is decreasing efficiency of the compressor and is noticeably in the temperature between stages as well

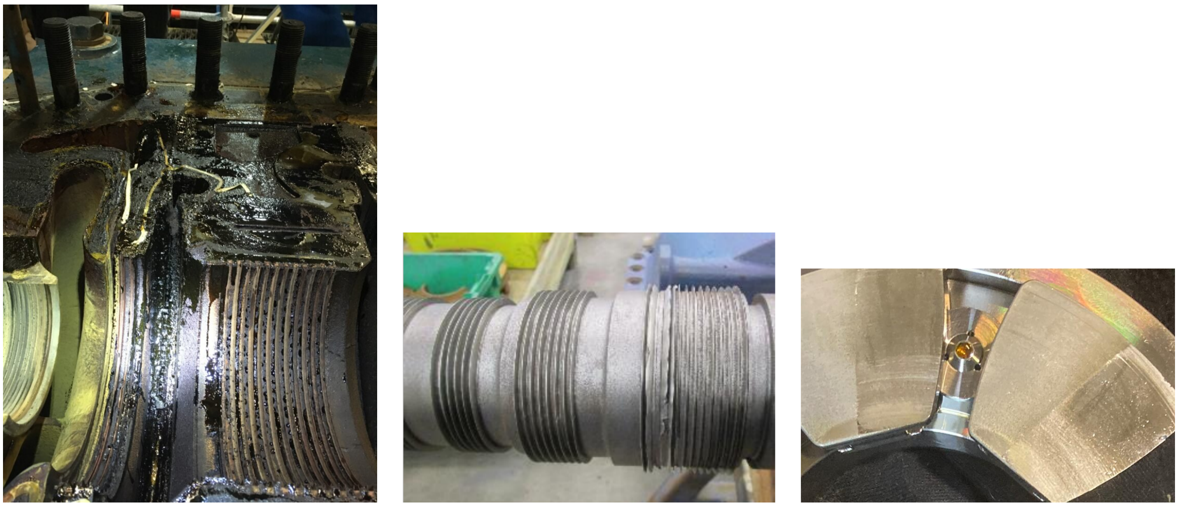

(a) Fouling in the diffuser of the third stage **(b)** Labyrinth Damage **(c)** Damaged axial bearing pads

Figure 2.5: Representations of the selected failure mechanisms

by the increase of power consumption.

2.3.2. Leakages

Due to the corrosive and toxic nature of chlorine leakages are a great risk for compressors. Most important is that external leakages of chlorine are prevented, since it has a large influence on the direct environment and personnel. Multiple types of leakage can occur in the compressor, namely between the two halves of the horizontal split casing and in the cavities between the rotor and stator. The leakage between the casing halves can occur due to the temperature and pressure causing the flanges to not be tight anymore Bidaut et al., (2013). The cavities between rotor and stator exist between compressor stages, between the first stage and the bearing and also between the last stage and other bearing. The leakage through this cavities influence the flow in the compressor circuit and therefore also the performance of the compressor decreases Qiao et al., (2019). The leakage towards the bearings and through the casing halves are disastrous when dealing with chlorine due to the toxic behaviour of the gas. These types of leakages are prevented by using the correct type of sealing. Between the two halves of the casing a thin film can be applied to seal the the casing Bidaut et al., (2013). The corrosive chlorine limits the types of sealing that can be used in this application. Leakages have effect on the performance of the compressor, it can effect the flow rate of the chlorine or it can raise temperatures in the compressor stages. The possibility exist that part of the sealing could fail as shown in Figure 2.5b, here the labyrinth is damaged which caused an internal leakage that effected the performance of the compressor.

2.3.3. Bearing failures

Bearing failure is the best known failure mechanism when dealing with rotary equipment and is normally detected with high frequency vibration measurements, these are not included in this case study. The purpose of the axial bearing is to absorb the axial forces and prevent axial movement, so out of bound axial displacement is a sign of a defect. Furthermore, defects on the bearings create extra friction and lead to increasing temperatures. Bearing failures could be caused by contaminated oil, a deviation of the prescribed oil pressure or uneven divided stress in the bearing. In Figure 2.5c axial bearing pads are shown with the effects of pitting and scratching, this was caused by chlorine contamination in the oil in combination with a decreased oil pressure. This is an example of one failure mechanism causing another, since the oil contamination was caused by a leakage.

2.3.4. Unbalance and misalignment

Rotor stability is essential for turbomachinery, an instability can occur due to unbalance and misalignment. The rotor misalignment is the misalignment of the axis of the compressor rotor and the axis of the output shaft of the gearbox, this misalignment can occur in the form of an offset, inclination or combination of the two. The main types of misalignment are defined by this study Manikandan and Anwar, (2018):

- Parallel: The axes of the driving and driven shafts are parallel but have a laterally displacement.
- Angular: The axes of the shafts cross each other and are not parallel.
- Axial: The compressor rotor is not in its correct axial position on the bearing.

Misalignment has an influence on the compressor performance, however it can also cause extra stress and fatigue in the bearings.
Every rotating machine has an inherent degree of unbalance, therefore unbalance as fault can be redefined as unbalance outside of a given tolerance level (Walker et al., [2013]). To prevent unbalance the rotor center of mass axis should coincides with geometric central axis. Unbalance does not necessarily directly lead to machine failure, however overtime it can induce vibrations which lead to failures as rub and wear.

2.3.5. Wear

Wear is the erosion of components in compressor. The erosion occurs due to particles in gas flow and is hard to completely prevent. Recognising the points sensitive to erosion would lead to more accurate determination of the components life times. High erosion rates mainly occurs at the impeller eye and the blade roots according to Biglarian et al., (2019). Wear can also be caused by rubbing of rotating and stationary parts of the compressor. This should be prevented at all times, but due to large tolerances, large vibrations, external forces it could occur. Wear has multiple effects that depend on the location of the mechanism. Wear can lead to performance decrease of the compressor, however due to the destructive nature of wear it can also cause direct mechanical failures. The particles that erode due to wear act as contaminants and can lead to more erosion and fouling. If wear occurs in the labyrinth sealing it can lead to less effective sealing and even internal leakages. Wear is also one the major causes to bearing defects.

2.3.6. Selection of failure mechanisms

Not all previously described failure mechanisms occur frequently, which makes it hard to include those in the research. Moreover, some measurements to acquire essential data are lacking which makes it not feasible to identify these mechanisms. The selection is based on the severity, frequency of occurrence and the possibility to detect them with available sensors. The mechanisms that are selected to be included in this research are the following:

- Leakages
- Fouling
- Bearing failures

2.4. Concluding remarks

With the overview of the production process the criticality of the compressors is emphasized. The characteristics of the compressor are presented by describing all important parts of the system. Lastly, the failure mechanisms that could occur in the compressor are presented. The insight into these factors resulted in the selection of the three failure mechanisms that are considered for diagnosis.

3
Literature review

In this chapter the answer is provided to the following research question: *What is the current state of failure diagnosis methods in literature and what method is best applicable to this case study?* This question is answered in steps, starting with understanding Fault detection and diagnosis (FDD) in general. Then the possible approaches for health indicator construction are presented and finally the method best applicable to this study is selected.

3.1. Fault detection and diagnosis

Condition monitoring includes the observation of the operational parameters and condition of equipment to detect anomalies that could indicate potential faults. The increasing availability of condition monitoring on systems has facilitated the increasing research in fault diagnosis techniques. FDD takes the information from condition monitoring and applies diagnostic algorithms to detect, isolate, and identify the faults. FDD gives insight in the state of equipment and is important to maintain high productivity, efficiency and safety in production plants (Arias Chao et al., [2022]). A lot of the research is focused on a single failure mechanism, for example: the study into fouling mechanism by deriving the equivalent compressor performance map at various degrees of fouling with a consideration of gas properties and stage efficiency variation and without prior knowledge of the detailed geometrical features Al-Busaidi and Pilidis, (2016). An improved qualitative simulation (QSIM) based fault diagnosis method is proposed to diagnose the faults of centrifugal compressors in Lu et al., (2016). This study uses the thermal parameters to detect the occurrence of faults in the gas flow path. The method presented in Luo et al., (2022) is a Dynamic Recurrence Index (DRI) and is used to detect the occurrence and quantify the evolution of oil film instability in the journal bearing system. However, as stated in the previous Chapter 2, the compressor is a complex machine where often multiple degradation modes are developing. This means these approaches of fault diagnosis for single failure mechanism are not sufficient. A different approach is the construction of health indicators and using them as tool to assess the machine in its entirety (Lei et al., [2018]) (Jardine et al., [2006]) (Schwartz et al., [2022]) (Wang et al., [2012]).

3.2. Health indicator construction

The aim of using a HI in the PdM model is capturing the degradation process of a complex machine into a single function, so FDD becomes feasible. HIs are often applied for anomaly detection and as a basis for prognosis. HIs can be classified in two categories based on their construction strategies: model based HIs and data driven HIs(Lei et al., [2018]) (K. T. P. Nguyen, [2022]), the categories are shown in Figure 3.1. A model based HI correspond to direct underlying degradation factor and the physics of failure and are generally directly extracted from monitoring signals. Thus, the construction of a model based HI requires an understanding of the working principle of the system and the possible deviation from expected behaviour. A data driven HI describes the degradation trend of the equipment, but loses the direct physical meaning. The underlying assumption of data-driven approaches is that the relevant information concerning the evolution of the system health and the failure time can be learned from past data (Arias Chao et al., [2022]). For the construction of data driven HIs the fusion of multi-sensor measurements is required. The techniques for accomplishing this fusion could be divided in

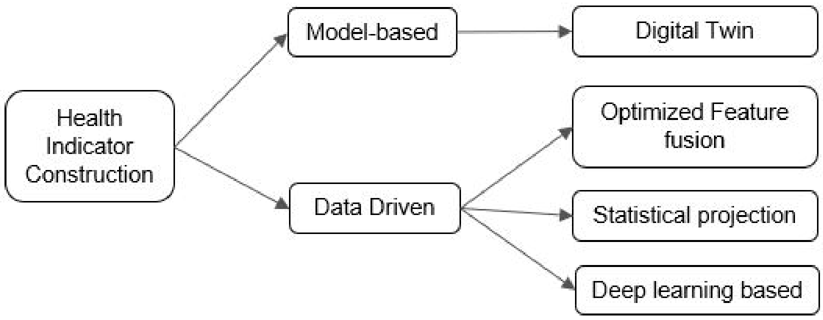

Figure 3.1: Overview of health indicator construction methods split into model based and data driven approaches (K. T. P. Nguyen, [2022]).

three categories: optimization methods for feature combination, statistical projection and deep learning based (Arias Chao et al., [2022]). The first group, optimization method of feature fusion want to find the best mathematical expressions that produces high-level diagnostic and prognostic features by combining low level features, for example by using genetic algorithms (Firpi & Vachtsevanos, [2008]). These methods require expertise knowledge about the HI formulation, which is limited with complex machinery, where multiple degradation patterns could occur simultaneously. The next group based on statistical projection aims to project high-dimensional multivariate data to a lower dimensional space. This method is suitable for continuously collected measurements and is a process of information fusion which provides a unified measure being used to characterize the health condition of the system. For example, in the study of Wang et al., (2012) the framework for constructing generic HIs is provided by employing a linear data transformation method. These methods are trained with the help of failure data. Due to preventive maintenance approach limited failure data of compressors is available. This gives the challenge of learning the degradation and failure behaviour without having training data of this. Model should be able to learn the characteristics of a healthy compressor. The final group deep learning methods, provides a different data driven approach for automatically extracting and constructing useful information, without the necessity for expertise knowledge in presence of big data. However, a disadvantage of using machine learning for FDD is the need for data on failure instances to learn the correlation between the multi-sensor measurements. This data if often not widely available for complex and expensive machinery due to preventive measures. The model based approaches and optimization methods for feature combination are not compatible with the research scope. These are not further looked into due to the lack of required measurements for the model based approach and the lack of required expertise knowledge about the HI formulation, where multiple degradation patterns could occur simultaneously. Hereafter, extra insight is gathered on the statistical projections and deep learning based method to provide the basis for the optimal chose of proposed methodology.

3.2.1. Statistical approach for HI construction

One of the methods for data reduction that is often proposed is the Principal Component Analysis (PCA) (Jolliffe, [2002]). Using PCA for data-driven analysis and empirical modelling is a promising approach as it gives the ability to learn different operating condition of the machinery without the need for any physical understanding of the process. PCA is a valuable technique for compressing a large amount of information in a compact and easily interpretative form, therefore is the PCA a popular option as feature extraction method for fault diagnosis methods (He et al., [2009]) (H. Chen et al., [2020]). The PCA technique is a linear projection that is standardized and which maximizes the variance in the projection space. The main advantage of PCA is the reduction of the data dimension and therefore reduction of the computation time, while losing minimal information. However PCA is limited, since it only allows linear dimensionality reduction. Therefore different derivations of the PCA method are developed over time which can solve this limitation, examples are: Probabilistic PCA (PPCA) and Kernel PCA (KPCA).

Kernel PCA
KPCA is described by Schölkopf et al., (1999) and is a tool to generalize standard PCA to nonlinear dimensionality reduction, this is required when dealing with more complicated structures that cannot be presented in a linear subspace. An example of the adaptation of KPCA by Feng et al., (2016), here KPCA is use to establish a basis for the health index and RUL estimation for a turbofan engine. The principal idea of KPCA is to go to a higher dimension space in which the decision boundary becomes linear (Feng et al., [2016]) . However, by doing this the generic non-linear combination of the original variables will have a huge number of new variables which will overload the computational complexity of the problem. The exact combination of non-linear terms needed is unknown, that is why the large number of combinations that are required. This can be overcome by using the kernel trick (Schölkopf et al., [1999]), which enables us to get to the eigenvalues and eigenvector without actually calculating it explicitly, by using the kernel function.

Probabilistic PCA
PPCA is established by deriving PCA within a density estimation framework. The main advantages of PPCA is that multiple PCA models can be combined as a probabilistic mixture and the possibility to obtain PCA projections while data is missing (Tipping & Bishop, [1999]). Also it is capable of reduction of dimension and can be used as a constrained Gaussian density model, where maximum likelihood estimates for the parameters can be efficiently computed from the data principal components. This has the benefit that PPCA can be used for classification and novelty detection.

Canonical Variate Analysis
Canonical Variate analysis (CVA) is also referred to in literature as Canonical Correlation Analysis and is in the basis a method for analysing the correlations between two data sets. CVA searches for linear combinations which are responsible for the most correlation in two data sets, where PCA only focuses on the linear combinations with the most variance in one data set. This gives the advantage that this method could handle two data sets with different origins and format. The use of the CVA method has the benefit that it is possible to combine process data with vibration and electric current data (Ruiz-Cárcel et al., [2016]). The goal of CVA is to find linear combinations between two sets of variables that maximize the correlation. CVA is capable to detect and diagnose faults in systems with dynamically changing conditions, which is its main advantage compared to other methods. The working principal of CVA according to literature Ruiz-Cárcel et al., (2016), Pilario and Cao, (2018), Larimore, (1983) is explained next. CVA takes time correlations in account by expanding the observation vector $\mathbf{y}(\mathbf{k}) \in R^m$ at each time point k of the training period with considering p previous and f future measurements. This creates the past and future observation vectors $\mathbf{y}_{\mathbf{p},\mathbf{k}}$ and $\mathbf{y}_{\mathbf{f},\mathbf{k}}$.

Support Vector Machine
A support vector machine (SVM) is a method that is useful when the underlying process of the real-world system is unknown or to complex to sufficiently model. It is mostly used for classification tasks due to its high accuracy even for non linear problems. For fault diagnosis support vector regression (SVR) is used in combination with the HilbertHuang transform to extract health indicator. In this form SVR is capable of determining the RUL of machinery with time series data.

3.2.2. Deep learning for data driven HI construction
In this section deep learning approaches for constructing HIs are explored and described. Also the important aspects of machine learning in general all researched to gain an understanding of the matter. A different approach is provided using a machine learning method, where the HIs are constructed with the help of neural networks (NN) Kim et al., (2019). This has the advantage of not requiring the exact failure threshold and does not limit the application of the method for a specific degradation process. Neural Networks use nodes in hidden layers in combination with weights to give an output. These nodes can activate when the input surpasses a certain threshold, most often this threshold is connected with a sigmoid function. The input of every node is an product of the original input and a weight factor. These weight factors are the learning parameters of the network and makes that a NN requires historic knowledge to function. The NNs basic learning procedure cannot effectively extract the informative features hidden in raw data and therefore require additional feature selection Ran et al., (2019). NNs can have good approximations of non linear functions, however this technique is limited since a lot

weight parameters need to be trained, it is easily possible to over-fit by choosing to many layers and nodes and might require large computational power.
Many adaptions of NNs are constructed to deal with these limitations, such as convolutional neural network (CNN) and the recurrent neural network (RNN).

Convolutional neural network
CNN normally consists of multiple layers; the input layer, convolution layer, pooling layer, fully connected layer and the output layer. This setup makes it possible to extract local features of the input data and combine them layer by layer to generate high-level features (Ran et al., [2019]).

Recurrent neural network
RNNs is capable of dealing with sequential data such as time series. RNN can build circular connections in its hidden layers and use that feature to keep memory of previous inputs in the networks internal state (Ran et al., [2019]). The limitation of the RNN is that the gradient can be unstable and explode or disappear due to the back propagation used during training.

Long Short-Term Memory Network
Long Short-Term Memory (LSTM) neural network is an improvement of the RNN and consist of multiple connected recurrent units recursively. LSTM was introduced as an efficient gradient based method by Hochreiter and Schmidhuber, (1997). The recurrent unit has three gating structures, namely a forgetting gate, an input gate and an output gate (X. Chen et al., [2023]). The two main advantages of LSTM are the following; the structure of LSTM can learn long-term memory information and provide a solution to long-term dependence. Also LSTM has an activation function that combines the sigmoid function and tanh function, which avoids explosion or disappearance of the gradient, while also accelerating the convergence speed of the model. This all makes the LSTM network valuable for applications with time series predictions.

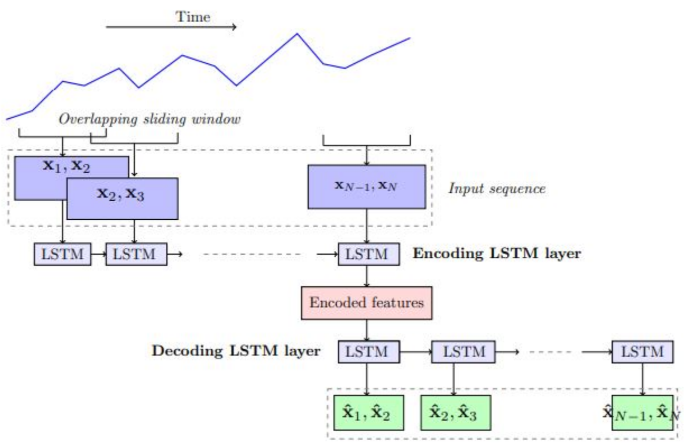

Figure 3.2: Network of LSTM cell that encodes and decodes multivariate time series H. D. Nguyen et al., (2020).

LSTM Autoencoder
The LSTM cells are often used in a LSTM-autoencoder (LSTM-AE) network, see Equation (4.3), which is a variation of an autoencoder that uses an Encoder-Decoder LSTM architecture to process sequence data (de Pater & Mitici, [2023]) (H. D. Nguyen et al., [2020]). This is an unsupervised machine learning method that encodes a sequence to an embedding with a smaller dimension and decodes this embedding to the reconstructed sequence. The goal of this process is to learn the important aspects of the system by reducing the dimension of the data, while maintaining the important information structure. The possibility to learn patterns and dependencies between features over longer periods makes LSTM-AE relevant for time series prediction and anomaly detection.

3.3. Method selection

In this section the methods will be compared on their strong points and weaknesses for the adaption to this research and taken in account the scope. The selection of methods will be made on the basis of criteria that are important to the research. The methods are described above along with their characteristics, advantages and limitations.

3.3.1. Selection criteria

The selection criteria are based on the requirements of the methods for this research. In the optimal case the criteria are fully independent of one another, so the selection of methods is fully objective. The criteria are as follows: Accuracy, Feasibility, Computational effort and Robustness. Below the criteria are described concisely along with the reasoning of the importance for this selection procedure.

Accuracy : The output should be accurate enough useful for the research
Feasibility :It is important that the proposed method can be applied and executed with the available resources
Computational effort :The cost to implement the method in the model should be reasonable, these costs are mainly the time to understand and adapt the method for the model and the calculation time
Robustness :The method should easily adapt to minor changes or the loss of a measurement, it would not be beneficial if the model based on this method should be entirely reconstructed all the time.

Feasibility for the purpose of this research is a limiting factor for many of the considered methods. The selected method should be able to deal with the following requirements to be feasible:

- Can be trained with limited or without failure data.
- Is able to deal with changing operating conditions.
- Is capable of detection and identification of the degradation by multiple faults simultaneously.

Scores are provided in a range of one to five based on the characteristics of the method and the results of consulted literature. The final scores of the methods are presented in table 3.1. The best option is the LSTM-Autoencoder, which is selected as the foundation of the proposed methodology in the next chapter.

Table 3.1: Evaluation matrix for methods vs selection criteria

Statistical projection methods	Robustness	Accuracy	Ease of implementation	Feasibility	Total Score
Kernel-PCA	3	4	4	2	13
Probability-PCA	3	3	3	1	10
Canonical Variate Analysis	3	4	4	2	13
Support Vector Machine	3	4	4	2	13
Deep learning based methods					
Convolutional-NN	4	4	2	2	12
Recurrent-NN	2	3	5	4	14
LSTM-RNN	3	3	4	3	13
LSTM-AutoEncoder	4	4	2	5	15

3.4. Concluding remarks

In this chapter literature that focuses on FDD and HI construction is consulted to get an understanding of what techniques are available and suitable for this research subject. It has become clear that the best approach for machine diagnosis of a compressor with limited recorded failure instances, is health assessment by constructing of health indicators. The construction of health indicators requires fusion of the multivariate data, which provides four groups of health indicator construction methods: Model based, optimization methods for feature combination, statistical projection and deep learning based. The last two groups are subjected to case specific selection criteria: Accuracy, Feasibility, Computational effort and Robustness. The considered methods should meet the following criteria to be considered feasible:

- Can be trained with limited or without failure data.
- Is able to deal with changing operating conditions.
- Is capable of detection and identification of the degradation by multiple faults simultaneously.

This has resulted in the selection of the LSTM-AE as foundation for the methodology of this research, which provides the answer to the question; *What is the current state of failure diagnosis methods in literature and what method is best applicable to this case study?*

4
Methodology

In this chapter the following subquestion is answered: *How to develop the proposed fault detection and indication model for the chlorine compressor?*, by firstly introducing the LSTM-AE, along with the format of the time series data. Secondly, the reconstruction loss is used to construct the HIs. Then the training and the tuning process for the optimal parameters is described. At last the application of the HIs for health assessment and fault identification is presented, along with the key performance indicators (KPIs).

4.1. LSTM Autoencoder

In this section the characteristics of the LSTM-AE are described. Let $\vec{X}^{c,d} = \vec{X}_t^{c,d}, t \in \{1, 2, ..., n^{c,d}\}$ be the multi-sensor measurement of compressor lifecycle c during sequence d , where t denotes the time step during this sequence. The compressor lifecycle c refers to period that the compressor starts operating after placement till it either fails or is replaced. The input for the LSTM-AE should have a limited length for the model to function effectively, therefore the lifecycle are split in sequences d of size $n^{c,d}$ which are used as input. The $\vec{X}_t^{c,d} = [X_t^{c,d,1}, X_t^{c,d,2}, ..., X_t^{c,d,a^s}]$ is the multi-sensor measurement at time step t, with a^s the amount of considered sensors. Furthermore, the amount of sequences in a compressor lifecycle c is indicated as D^c. The operation conditions are separated with the purpose of developing a model that constructs the HI independent of these conditions. The sensors that qualify for this purpose are the ones measuring the inlet conditions of the chlorine gas and oil, more precise: the inlet temperature and pressure of the chlorine gas and the inlet temperature of the oil. These are the parameters that could change depending on the season or the production process that precedes the compression and influence the other parameters in the system. The measurements of the operation conditions have their own notification. Let $\vec{O}^{c,d} = \vec{O}_t^{c,d}, t \in \{1, 2, ..., n^{c,d}\}$ be the conditions of sequence d of compressor lifecycle c, then $\vec{O}_t^{c,d} = [O_t^{c,d,1}, O_t^{c,d,2}, ..., O_t^{c,d,a^o}]$ refers to the conditions at time step t of this sequence d and a^o correspond to the amount of operating conditions. The LSTM-AE consists of an encoder part and a decoder part, which recurrent layers exist of enrolled series of LSTM cells and encodes the input data to the repeat vector and reconstruct the time series at the decoder part, see Figure 4.1 where the architecture with one layer is shown.

4.1.1. LSTM cell

The LSTM technique is an adapted version of the original LSTM structure by Hochreiter and Schmidhuber, (1997). This version described by de Pater and Mitici, (2023) consists of two variable states that are updated by every cell and than past on to the next cell, these states are the memory state c_t and the hidden state h_t. This results in the situation that every cell has four inputs; the features and operation conditions at the current time step $\vec{X}_t^{c,d}$ and $\vec{O}_t^{c,d}$, the initial memory c_{t-1} and hidden state h_{t-1} and two outputs; the updated memory and hidden state. The LSTM cell is shown in figure 4.2 and consists of three gates that update the variable states with the use of the inputs and an activation function. The two types of activation functions that are used in the LSTM cell are the simgoid function σ and the tanh function, see Equations (4.1) and (4.2).

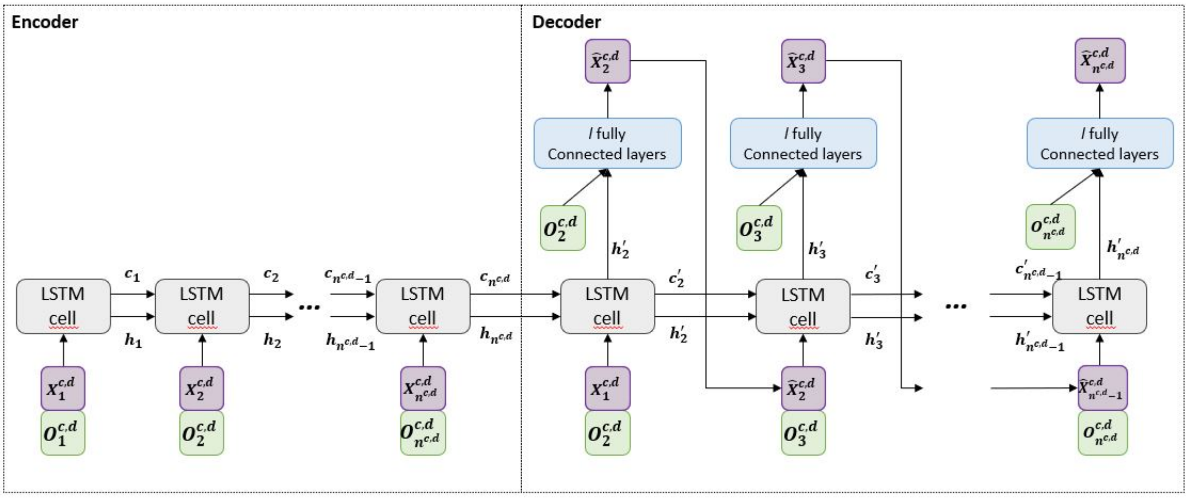

Figure 4.1: Architecture of the LSTM-AE

$$\sigma(x) = \frac{e^x}{e^x + 1} \tag{4.1}$$

$$tanh(x) = \frac{e^x - e^{-x}}{e^x + e^{-x}} \tag{4.2}$$

The first operation in the LSTM cell is the forget gate, here is decided what old information is removed of the previous memory state. The portion of the memory state that should be forgotten is determined by passing the inputs through the sigmoid function as shown in Equation (4.3), here W_g, V_g, U_g are the weights and b_g is the bias of the forget gate.

$$g_t = \sigma(W_g\vec{X}_t^{c,d} + V_g\vec{O}_t^{c,d} + U_g h_{t-1} + b_g) \tag{4.3}$$

Secondly the input gate provides a potential memory state c_t^{pot} and simultaneously an input state i_t that will decide what part of the potential memory state will be added to update the memory state, see Equations (4.4) and (4.5) . Here $W_c, V_c, U_c, W_i, V_i, U_i$ are the weights and b_c and b_i are the biases of the input gate.

$$c_t^{pot} = tanh(W_c\vec{X}_t^{c,d} + V_c\vec{O}_t^{c,d} + U_c h_{t-1} + b_c) \tag{4.4}$$

$$i_t = \sigma(W_i\vec{X}_t^{c,d} + V_i\vec{O}_t^{c,d} + U_i h_{t-1} + b_i) \tag{4.5}$$

The new memory state c_t is determined with the information of the forget and input gate by, see Equation (4.6).

$$c_t = (c_{t-1} \otimes g_t) \oplus (i_t \otimes c_t^{pot}) \tag{4.6}$$

At last, the output gate generates the new hidden state h_t by determining what part of the new memory state should be used, see Equations (4.7) and (4.8). Here W_p, V_p, U_p are the weights and b_p is the bias of the output gate.

$$p_t = \sigma(W_p\vec{X}_t^{c,d} + V_p\vec{O}_t^{c,d} + U_p h_{t-1} + b_p) \tag{4.7}$$

$$h_t = p_t \otimes tanh(c_t) \tag{4.8}$$

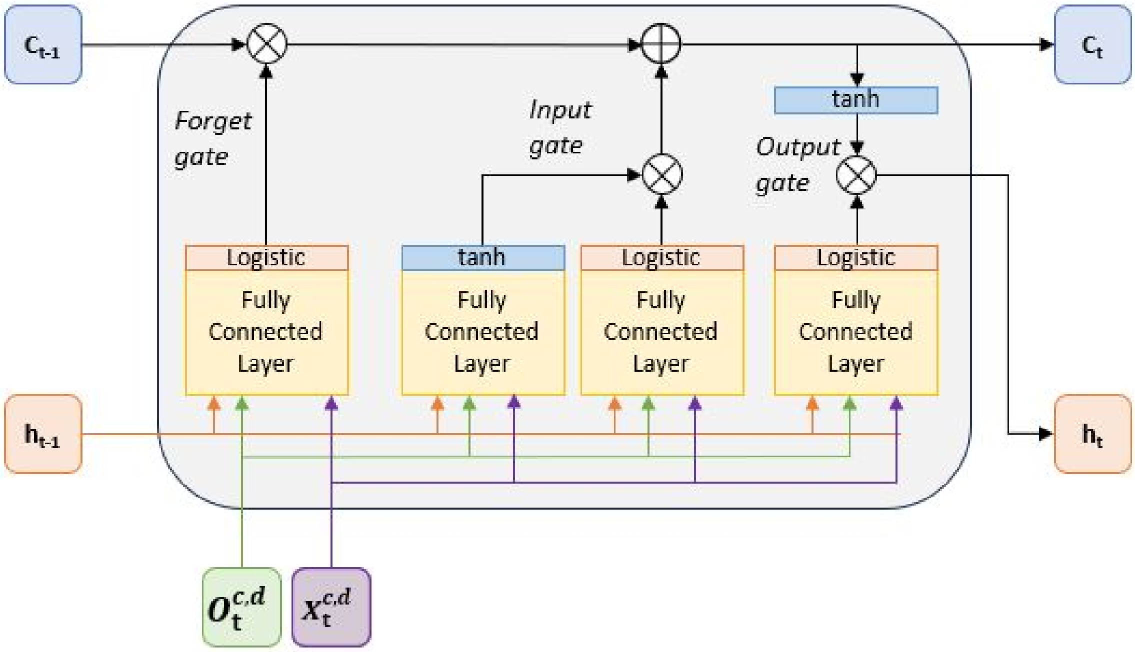

Figure 4.2: Schematic overview of the LSTM cell structure.

4.1.2. Encoder

At the encoder side of the LSTM-AE the sequences are imported into a LSTM cell for every time step together with the hidden and memory state of the previous LSTM cell, see Figure 4.1. The operation conditions and the sensors measurements are separate inputs so the reconstruction of the data is independent of the operation conditions. The last hidden and memory state at time point $n^{c,d}$ are the starting conditions of the decoder.

4.1.3. Decoder

The decoder uses the reconstructed measurements of the previous time step $\hat{X}_{t-1}^{c,d}$ as input, except at $t = 1$, here the original data is used. Furthermore, it also uses the previous hidden and memory state and the operation conditions as inputs. The reconstructed measurement $\hat{X}_t^{c,d}$ is the output of this network and is generated by a fully connected layers of a neural network. This network consist of three layers where the last layer has an output of a^s, corresponding to the number of input sensors. The fully connected layers have the hidden state of the recurrent layer and the original operation conditions as input. By separating the operation conditions the autoencoder is forced to learn that the reconstruction of the sensor data is independent of the operation conditions.

4.1.4. Reconstruction losses

The reconstruction loss is determined by the difference between the input measurements and the reconstructed measurements. The mean reconstruction loss $RL_d^{c,s}$ of sensor s in sequence d of compressor lifecycle c is equal to:

$$RL_d^{c,s} = \frac{1}{n^{c,d}-1} \sum_{t=2}^{n^{c,d}} \left| \hat{\vec{X}}_t^{c,d,s} - \vec{X}_t^{c,d,s} \right| \tag{4.9}$$

$$HI_d^c = \sum_{s=1}^{m^s} RL_d^{c,s} \tag{4.10}$$

The LSTM-AE is trained to minimize the reconstruction error, so it learns to capture the essential characteristics of the healthy chlorine compressor, while discarding noise and irrelevant information. During training phase teacher forcing will be applied to improve the training efficiency. Teacher forcing is performed by giving the original $X_{t-1}^{c,d}$ as input at the decoder side of the reconstructed measurements. In this manner the parameters further down the recurring LSTM cells are determined with the exact values instead of the predicted values.

4.2. Health Indicator construction

The data driven health indicators are based on the reconstruction loss of the LSTM-AE. As previously described there will be constructed four different data driven HIs with the use of the model.

4.2.1. Sensor selection

As shown in Equation (4.10) the HI is a summation of the reconstruction losses for set of sensors. This subset is specific for a HI. The usefulness of a sensor is dependent on the change of the reconstruction loss towards failure. This can be determined in an objective manner by using the trendability, which will be explained further in section 4.2. The sensors that are included in Equation (4.10) to construct the HI have a high trendability.

4.2.2. Health Indicator Evaluation Metrics

To evaluate the health indicators three metrics are defined: the monotonicity (M), trendability (T) and prognosability (P). These metrics are adopted from the work of Liu et al., (2020) and de Pater and Mitici, (2023) to test the behaviour of the HI during a compressor lifecycle.

Monotonicity. The general increasing or decreasing pattern of a feature over time. For a HI the monotonicity should increase when a incipient fault occurs and evolves.

$$M = \frac{1}{D^c - 1}\left|\sum_{d=1}^{D^c-1} I(HI_{d+1}^c - HI_d^c) - I(HI_d^c - HI_{d-1}^c)\right|, \quad \text{where } I(x) = \begin{cases}1, & \text{if } x > 0\\ 0, & \text{if } x \le 0\end{cases} \tag{4.11}$$

Trendability. The Spearman correlation coefficient is used between the HI and the sequences $\{1, 2, ..., D^c\}$ to define the trendability.

$$T = \frac{D^c \sum_{d=1}^{D^c} r_d^{HI^c} d - (\sum_{d=1}^{D^c} r_d^{HI^c})(\sum_{d=1}^{D^c} d)}{\sqrt{(D^c \sum_{d=1}^{D^c} (r_d^{HI^c})^2) \times \sqrt{(D^c \sum_{d=1}^{D^c} d^2) - (\sum_{d=1}^{D^c} d)^2}}} \tag{4.12}$$

Prognosability. The prognosability is the variance of the final state of the HI for each compressor lifecycle divided by the average lifecylce length. This metrics tells how well the HI could be used to detect the fault.

$$P = exp\left[\frac{-std(HI_{D^c}^c, e \in C^{test}}{\frac{1}{|C^{test}|}\sum_{e \in C^{test}} |HI_1^c - HI_{D^c}^c|}\right] \tag{4.13}$$

4.2.3. Tuning

The architecture of the LSTM-AE depends on the chosen model parameters, these are presented in Table 4.1. The settings of the model parameters have a big influence on the behaviour of the model and The optimal parameters are found using the approach presented in Figure 4.3, where the model parameters are updated after each training process. This optimization loop is executed with the help of grid search, where systematically each logical combination of parameters is evaluated.

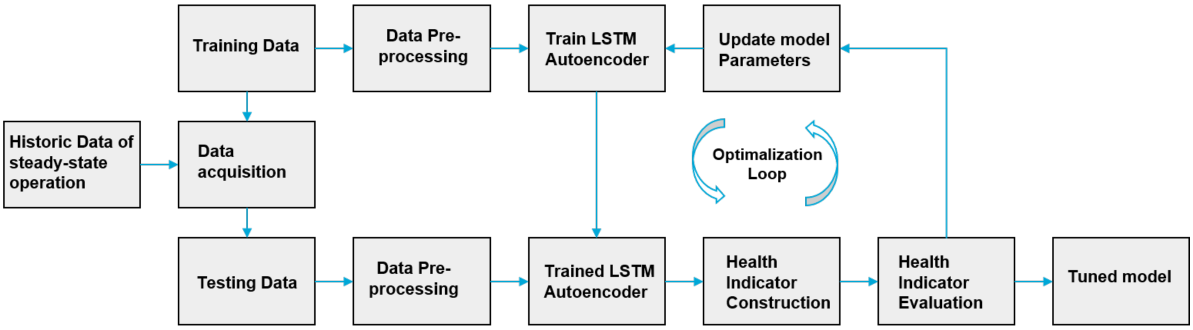

Figure 4.3: The approach for tuning the model.

Table 4.1: The model parameters of the LSTM-AE that are included in the grid search for the optimal model.

Architecture parameters
Number of stacked LSTM layers
Size of hidden and memory state
Sequence length of test data
Number of fully connected output layers

4.3. Health Assessment

The purpose of constructing the HI of the compressor is the ability to diagnose the state of the compressor. To determine the difference in the state of the compressor a fault threshold for the HI is proposed. When the upper bound of this threshold is passed the HI is considered unhealthy. The threshold is determined following Equation (4.14), which corresponds to the Chebyshev's inequality (Kong & Yang, [2019]).

$$P(|HI_d^c - \mu \geq k\sigma) \leq \frac{1}{k^2}, \tag{4.14}$$

where $P()$ is the probability, k determines the confidence interval, μ is the mean and σ is the standard deviation. The mean and standard deviation are retrieved from the healthy training sets. The condition of the threshold is adapted from Chebyshev's inequality to Equation (4.15).

$$HI_d^c \geq k\sigma + \mu \tag{4.15}$$

To filter out outliers of the HI the condition should be met v times in a row for the compressor to be diagnosed as unhealthy. This condition is used for the general HI to determine the state of the entire compressor and to determine whether fault identification is necessary.

4.4. Fault Identification

HIs are constructed in the same manner as described in Section 4.2 for each failure mechanism. Here, the sensor selection for the subset that is used in Equation (4.10) is based on both system knowledge and trendability. For each HI of the included failure mechanisms a threshold is determined in the same way as described in Section 4.3. Fault identification takes place if the compressor is considered unhealthy and is the process assess the health of the HIs corresponding to each failure mechanism. Note, by performing the fault identification in this way it is possible to detect multiple developing faults simultaneously. The assess the performance of the fault identification key performance indicators (KPIs) are introduced, that are frequently used in this research field (Bohutska, [2021]), (Al, [2021]). These KPIs are based on the confusion matrix, which is a visualisation of the fault identification results in a tabular representation, see Figure 4.4.
The outcome of the classification is split in four categories:

- True positive (TP)
    - Correctly identified positive prediction

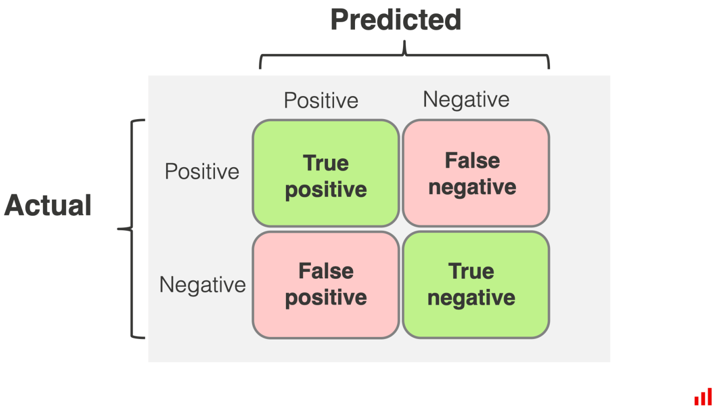

Figure 4.4: The confusion matrix presents an overview the results of a classification problem (AI, [2021]).

- True negative (TN)
  - Correctly identified negative prediction
- False positive (FP)
  - Incorrectly identified positive prediction
- False negative (FN)
  - Incorrectly identified negative prediction

The confusion matrix presents the absolute results, however it is desired for the KPIs to be relative metrics. These can easily be derived from the matrix:

- *Accuracy*
  - the number of correct predictions made by the model Equation (4.16).
- *Precision*
  - how correctly the model has detected positive outcomes Equation (4.17).
- *Recall*
  - evaluates the effectiveness of a classification model in identifying all positive instances. It is calculated as the proportion of relevant instances that were correctly detected Equation (4.18).
- *F1-score*
  - identifies overall performance by combining precision and recall Equation (4.19).

$$Accuracy = \frac{TP + TN}{TP + TN + FP + FN} \tag{4.16}$$

$$Precision = \frac{TP}{TP + FP} \tag{4.17}$$

$$Recall = \frac{TP}{TP + FN} \tag{4.18}$$

$$F1 - score = 2 * \frac{Precision * Recall}{Precision + Recall} \tag{4.19}$$

4.5. Concluding remarks

In this chapter the research sub question: *How to develop the proposed fault detection and indication model for the chlorine compressor?* is answered by describing the methodology. The main part is about the characteristics of LSTM-AE model which is the foundation of the proposed method. Then it is described how the health indicators are constructed based on the reconstruction error of the autoencoder. To evaluate the developed model three metrics are proposed are proposed that determine the characteristics of the development of the HI over time, namely; Monotonicity, trendability and prognosability. Furthermore, Chebychev's inequality is introduced to establish the threshold for health state division between the healthy and unhealthy state of the compressor. Hereafter the verification steps of the model are described, which includes:

- The implementation of the model with a different dataset that is frequently used in literature.
- Parameter tuning with the help of a grid search.
- Sensor selection for HI construction.

At the end the methods for health assessment and fault identification are described.

5 Case Study: Data

Goal of the of the chapter data handling is to answer the following sub question: *What data is available and how can it be retrieved and analysed for the purpose of fault detection and diagnosis?* This question is answered in multiple sections; The proposed method is tested on the case study of a chlorine production plant, where two chlorine compressors operate parallel to pressurize and cool down chlorine with the purpose of liquefaction. First, the data acquisition is described this includes the description of historic data and the sensor selection. Then data preprocessing is described, which is an important aspect when real world data is used as input for the model.

5.1. Data Acquisition

The compressor is handling a toxic substance and is qualified as a turbomachinery with a high rotational speed, to ensure the safety of the machine their are multiple measures to make the system shut off when certain parameters reach a threshold. To keep track of these critical parameters sensors are installed in system to conduct measurements. Besides these sensors for safety needs, there are also sensors that are used to indicate the state of the system and ongoing process. The main types of parameters that are measured are the following: temperature, pressure, pressure difference, flow, displacement.
The database stores the measurements at a frequency of 1 measurement per 5 seconds. However after storage for a few months the time span between data points is changed to a minute by averaging the data, this is done to reduce the required storage space. The degradation of the compressor is a slow process, therefore a lower sampling rate should also be sufficient. The only exception for this statement are the vibration measurements, they require a high frequency in the order of 10 times the rpm to capture all information hidden in the vibrations, which comes close to 1800 measurements per second. These measurements are executed by a third party and are not directly stored in the database and therefore not available for this research. The sampling at which the data is retrieved from the database is chosen to be 1 measurement per hour, which is sufficient for capturing slow changes in the behaviour of the compressor and limits the data size, while having sufficient data to train and test the model. The data of 5 compressor lifecycles is available with length varying between 2.5 and 5.5 years.
The sensor measurements are collected and stored each minute, this rate results in a large amount of data. In this case study the change in measurement values is slow, therefore the measurements are aggregated per hour by considering the mean per hour.

Table 5.1: Selected failure mechanisms with their effect on the compressor and the affected sensor measurements.

Failure mechanism	Effect on compressor	Affected sensor measurements
Fouling	Reduced performance Increasing stage temperatures	Critical temperature inside compressor
Bearing damage	Increasing bearing temperature Increasing rotor displacements	Maximum axial displacement Critical bearing temperature
Leakage	Reduced performance Increasing stage temperatures	Critical temperature inside compressor Critical chlorine concentration outside compressor

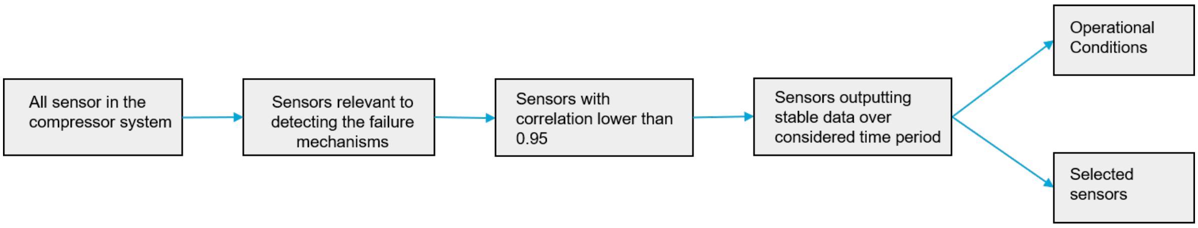

Figure 5.1: Overview of the sensor selection, the final two blocks present the sensor that will be used as input for the model.

5.1.1. Sensor Selection

There are more than a 100 sensors of different types in the compressor system that log measurements to the database. To limit the amount of unnecessary data analysis a selection of sensors is made to be considered as input for the model. The sensor selection occurs in multiple steps, a schematic of these steps is shown in Figure 5.1. The first step is to only include the sensors relevant to detecting the included failure mechanisms, in Table 5.1 the affected sensor measurements are presented. This is used as basis for the selection criteria:

- Only sensors that measure parameters in the gas path, oil circuit, bearings and engine are included.
- The sensors measure one of the following types of parameters: temperature, pressure, displacement and engine power.

Applying this criteria on the sensor set is reduced to 56 functional sensors that are outputting data, resulting in a total of almost 9 million sensor measurements. Following industry safety standards critical sensor measurements are executed twice or even three times to implement a safety factor, this brings sensor duplicates of which only one is selected. Also non identical sensors can have a high correlation, only one of two is selected if the correlation is 0.95 or higher, the correlation matrix can be reviewed in Appendix B. The next step is analysing the data on the stability of the output of the sensor over the considered period, with the purpose of eliminating sensors that have failed in parts of this period. The last step is to determine which sensor measurements are considered as operation conditions of the compressor. There are a total of $a^s = 16$ sensors selected and $a^o = 3$ are considered as the operation conditions, see Table 5.2 and Figure 5.2.

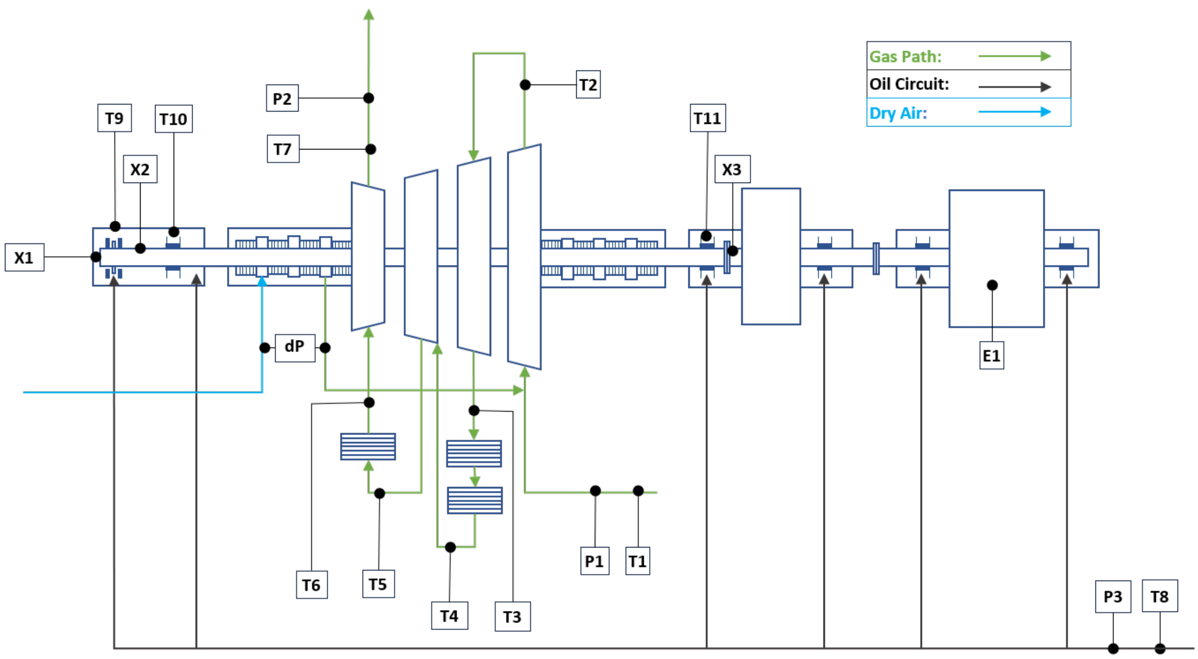

Figure 5.2: Schematic of the compressor with the location of the sensors.

Table 5.2: The operation conditions and selected sensors. DE stands for Driven End and NDE for non driven end.

Sensor	Description	Unit
Operation conditions		
P1	Suction pressure	barg
T1	Inlet temperature	°C
T8	Oil temperature	°C
Selected sensors		
dP	Pressure difference dry air and labyrinth	mbar
E1	Power consumption	Amp
P2	Press pressure	barg
P3	Oil pressure	barg
T2	Temperature outlet stage 1	°C
T3	Temperature outlet stage 2	°C
T4	Temperature inlet stage 3	°C
T5	Temperature outlet stage 3	°C
T6	Temperature inlet stage 4	°C
T7	Discharge temperature	°C
T9	Axial bearing temperature	°C
T10	NDE journal bearing temperature	°C
T11	DE journal bearing temperature	°C
X1	Axial displacement NDE	mm
X2	Rotor vibration NDE	µm
X3	Rotor vibration DE	µm

5.1.2. Historic data

The previous named database first recordings that are accessible are from around 2008, however not all measurements of the sensors in the compressor system are stable or recorded in the first years, this group is so large that the data of this first period can not be used. The data is acquired in intervals that correspond to the stand time of the equipment, from now one referred to as compressor lifecycles. In total 5 compressor lifecycles covering both functional locations are included in this research. Furthermore to simplify the model the two parallel compressor systems are considered identical and the sensors of both systems are considered the same. Data is not labeled, the correlation between data and the failures are not recorded, most of the time the compressors have not failed but are overhauled in the interest of preventive maintenance. So a direct relation between sensor readings and the degradation or failure pattern is unknown, dealing with this fact is one of the main reasons for the choice of the proposed method.

Lifecycle data

The lifecycle data is used as test data and is collected during the stand time of the compressor on a functional location, in Table 5.3 the period of the lifecycles are shown. For reference the functional locations are in short called K8411 and K8421 for street 1 and 2 respectively. The aim is to have both compressors operating continuously at steady-state during their lifecycle. However, there have been moments the compressor is out of operation for maintenance or process safety, so to ensure the correct data is used the data is only included when the compressor is operating at steady-state. Unfortunately there is no rotational speed measurement that could be used to indicate the steady-state operation. Instead the requirement for steady-state is that the inlet pressure P1 and the amperage of the engine E1 are between the boundaries of the normal operation.

Healthy data

To train a model to recognise the health state of a system a footprint of the state where the system is considered healthy is required. To establish time intervals in the data from where the training data can be acquired an assumption has to be made. It is assumed that the compressor data is considered healthy the first few months after the compressor is replaced. After installation of a new or overhauled compressor the possibility exist that system has to deal with infant diseases due to errors during the installation. To limit the possibility of having corrupted data in the healthy state data the healthy periods are all checked by hand, the cut off date for this period is present Table 5.3.

Table 5.3: Compressor lifecycles along with the corresponding cut off date for the healthy period .

Data set	Compressor	start date	end date	healthy date
1	K8421	24-4-2015	29-8-2019	23-8-2015
2	K8421	13-7-2019	14-3-2024	20-2-2020
3	K8411	20-2-2013	17-8-2018	3-8-2013
4	K8411	9-9-2018	17-3-2021	25-11-2018
5	K8411	8-7-2021	14-3-2024	13-10-2021

5.2. Data preprocessing

When using real world data, it is important to clean the input data to ensure that the measurements best represent the compressor behaviour. The preprocessing of raw data consists of multiple steps including: outlier removal, noise reduction, normalization and sequencing. The function and method of the preprocess step will be described in this section in the order of application, see Figure 5.3.

Figure 5.3: The order of the preprocessing steps that are applied to prepare the data for the model.

Outlier Removal

The possibility exist that dataset contain extreme values that are outside the range of what is expected and unlike the other measurements. These values are called outliers and often machine learning modeling could be improved by understanding and even removing these outlier (Sharma, [2018]). Outliers can have different possible causes, such as: measurement or input error and data corruption. If it assumed that the distribution of values in the sample is Gaussian or Gaussian-like, there can be made use of the standard deviation of the healthy data as a cut-off for identifying outliers (de Cheveigné & Arzounian, [2018]). The acquired data contains outliers that could be caused by various reasons for example sensor failures. The assumption is made that the training sets do not contain outliers, since these sets are of created of data during relatively short healthy period. To identify potential outliers in the test sets the overall mean and standard deviation of the training sets is used to establish the operation boundaries of the parameters that are measured. The upper and lower boundaries are equal to the mean plus/minus three times the standard deviation. To find the potential outliers the data of the test sets is subjected to these boundaries and the data points outside these boundaries are checked by hand to confirm whether they are outliers or not. In case of outliers the data is replaced by interpolating between the neighbouring non outlier data points.

Noise Reduction

When dealing with real world data noise is present in the raw data, this could give disturbances to the output of a fault diagnosis model. Different types of noise exist, in this research it is assumed the noise is primarily caused in measurement equipment, which results in Gaussian noise. A simple method for denoising time-series data involves using a rolling window to compute summary statistics (Bilogur, [2018]). A rolling window groups observations into sets of size n. These groups shift by one observation at a time, creating a moving ”window” across the dataset. Each observation belongs to $n-1$ groups, except those near the beginning or end, which may appear in fewer groups unless adjusted.

Any summary statistic, such as the average, median, minimum, or maximum, can be used within the rolling window to aggregate the data, with the average being the most commonly used.

Advantages of Rolling Windows:

- Simplicity and Ease of Computation: Rolling windows are straightforward to understand and computationally simple.
- Adjustable Smoothing Factor: By varying n, you can significantly increase or decrease the smoothing effect.
- Flexibility: You can use any aggregation function (mean, median, min, max, quantile, etc.).
- Familiarity: They extend familiar record-oriented algorithms to time-series data without additional complexity.

Disadvantages of Rolling Windows:

- Edge Clipping: They clip the beginnings and ends of the observations, reducing the total number of observations. This can be significant if the window is large or the dataset is small.
- Periodic Limitation: They cannot capture macro periodicity without losing micro periodicity

The noise reduction will be performed with the moving average method, which replaces data points with the local mean of the window around the point. The window rolls through the time series with the data of each point as middle point and a size $D = 48$. This operation smooths the time series and reduces the noise.

Normalization
Normalization is used to scale all sensor to the same standard. Standardizing a dataset involves rescaling the distribution of values so that the mean of the set of values is 0 and the standard deviation is 1 (Brownlee, [2020]). This can be thought of as subtracting the mean value or centering the data. Standardization is useful in cases where time series data has input values with differing scales. Standardization assumes that the multi-variate data fit a Gaussian distribution, the results are of lower quality if this expectation is not met. Standardization requires knowing or being able to accurately estimate the mean and standard deviation of observable values. The type of normalisation that will be used is the mean normalisation, also known as standardisation. Here the the mean μ and standard deviation std are calculated from the data and used to normalize the set as shown in Equation (5.1). It is important to note that the mean value and standard deviation of the training sets is also used on the testing set, for the reason that these are considered to be the values of the healthy state of the compressor. In Figures 5.4a and 5.4b the time series of temperature T2 is visualised before and after the preprocessing steps, except sequencing. The value of preprocessing is clearly visible in the in significantly cleaner curve of the after plot. Also, in Appendix C the data of all sensors is presented before and after preprocessing, where mainly the effect of standardization is noticeable.

$$X_t^{c,s} = \frac{X_t^{c,s} - \mu^{c,s}}{std^{c,s}} \tag{5.1}$$

Sequencing
The time series of a data set can not be fed to the LSTM-AE at once and is therefore split in smaller sequences d of size $n^{c,d}$. The sequences are extracted with a rolling window. The stride and length of this rolling window is different for the training and testing set. The training data has sequences with a length of 48, which corresponds to 2 days worth of data. For the training data the order of the sequences does not matter and overlapping windows are useful to increase the amount of training data. The length of the sequences of the test data is set to $n^{c,d} = 12$, which means that the HI is constructed for every 12 hours.

5.3. Concluding remarks

This chapter describes the acquisition of the real world data of the case study. There are in total 16 sensors and 3 operation conditions selected to be used as input for the model. The multivariate

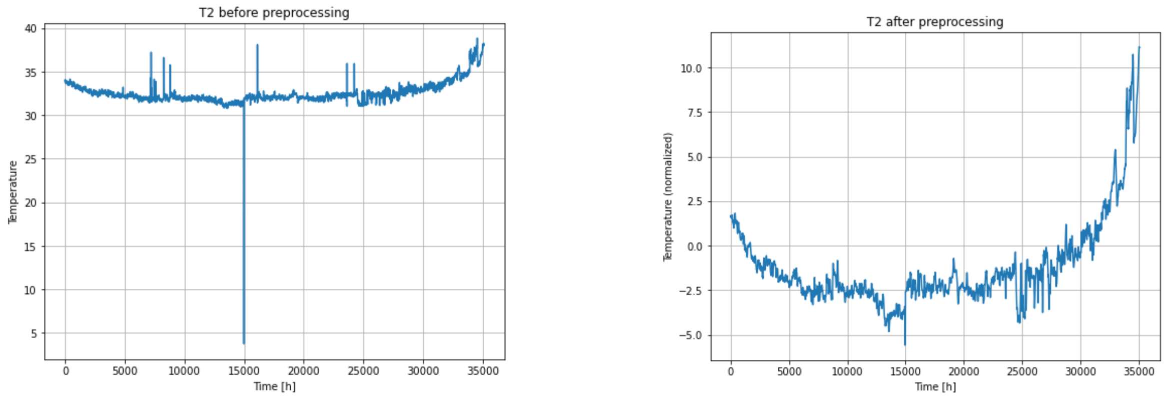

(a) T2 of compressor lifecycle set 1 before preprocessing.

(b) T2 of compressor lifecycle set 1 after preprocessing steps.

measurements of these sensors are collected of five compressor lifecycles with a sampling rate of one hour, this collected data is the testing data. The training data is collected from the first months of each lifecycle that are considered healthy, this data will be used to train the LSTM-AE. The data sets are prepared for usage as input to the proposed model. The preprocessing steps include:

- Outlier removal by a assuming a Gaussian distribution of the data.
- Noise reduction will be performed with the moving average method, which replaces data points with the local mean of the window around the point.
- Standardization for both training and testing data, the mean and standard deviation of the training sets is used.
- Sequencing are extracted with a rolling window. The stride and length of this rolling window is different for the training and testing set.

6 Verification & Validation

The goal of this chapter is to answer the following sub question: *How to verify and validate the proposed method?* The solution is provided in multiple verification and validation steps following the overview in Figure 6.1. First the implementation of the model in python and the functioning of the method is verified. Then the model is subjected to the validation steps to check if it is providing the expected outputs. Lastly the verification and validation of the model are evaluated and discussed.

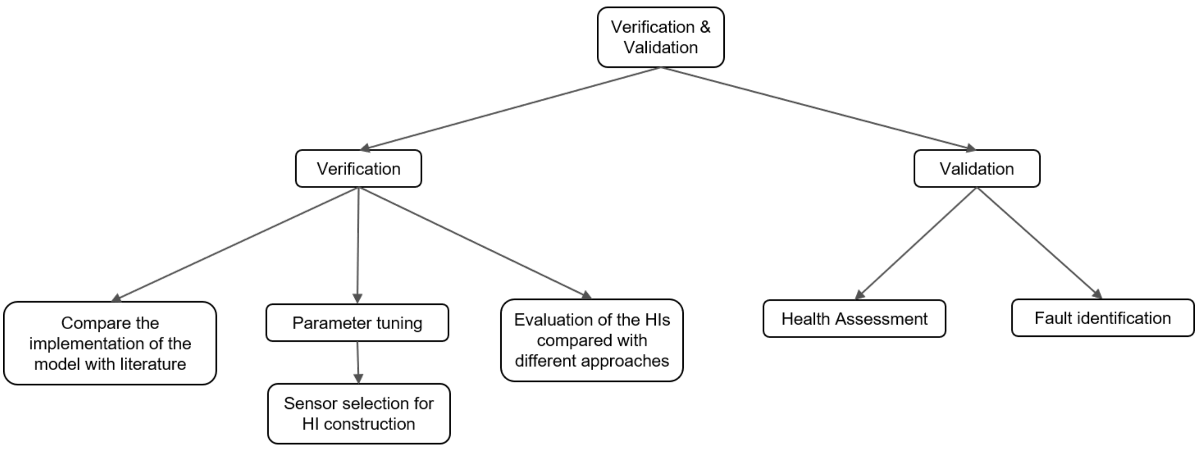

Figure 6.1: Overview of verification and validation steps that are executed

6.1. Verification

After and also during the implementation of the model verification takes place to ensure the model functions as it is designed. As described previously the functioning model is checked during the developing process with the help of the NASA data set (Arias Chao et al., [2021]), since this is a simulation data set with a known degradation pattern. To verify that the model is also applicable to the data of this research it is subjected to some logical tests. First a reconstructed sequence is compared to its original sequence by plotting them.

6.1.1. Implementation

The deep learning library of Pytorch is used to construct the autoencoder in python, the author has no experience in programming with this tool, so online libraries are consulted (Vasilev, [2019]) and the construction of the autoencoder is based on the work found on github by Vincrichard, (2020). The model is constructed in multiple versions where new features are added to the architecture in the newer versions. First the basic LSTM-AE is constructed, followed by the separation of the operation conditions and the addition of the fully connected layers. At last a different version is constructed where teacher forcing is applied to train the model.

Separation of the operation conditions
To program the structure as described in the methodology (see Figure 4.1) the operation conditions are separated from the features to be used as an input in both the encoder and decoder side. This action is performed to make the LSTM-AE model independent of the operation conditions.

Fully connected layers
The fully connected layers on top of the decoder outputs provide an extra step for reconstructing the time series. These make the model more robust to changing conditions and increase the reconstruction accuracy overall.

Teacher Forcing
To speed the training of the model teacher forcing is applied, by using the replacing the inputs of the features for the LSTM cells on the decoder side with the original input of the encoder. So at every enrolled LSTM cell the true inputs are used instead of the predicted ones.

Training
During training an initial set of weights and biases are set, which are updated with the use of back propagation on the error of the training loss. How large the adjustments of the weights and biases are is depended on the set learning rate. The training loss is determined with the mean squared error between the input and the reconstructed output. The model is trained for a predetermined amount of epochs, where for each epoch the training loss and validation loss is calculated, see figure 6.2. The validation losses should decrease per epoch, when the decrease becomes to small the training is stopped early to prevent overfitting.

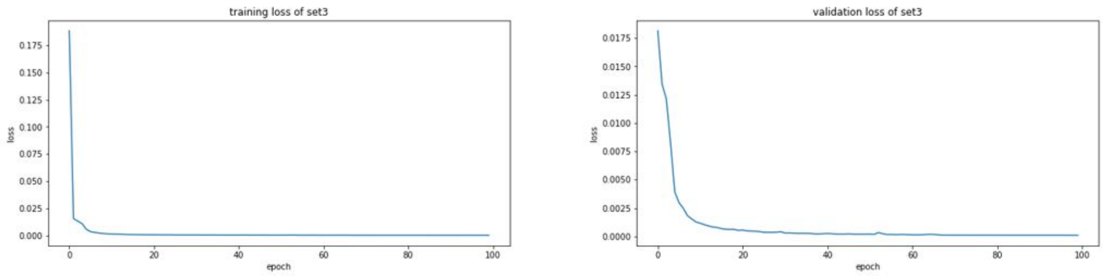

Figure 6.2: Training and validation loss

6.1.2. Model verification with N-CMAPSS data set
To help building and verifying the model the NASA dataset for jet engines by Arias Chao et al., (2021) is used as study material. A lot of research in the predictive maintenance part of literature is based on this dataset and therefore is ideal to verify the model implementation in python.
The dataset is created by simulating the flights of aircraft engines until failure, so no real world data. The data has a very slow degradation for the first flights till flight from this flight on the degradation pattern follows and exponential trend. The first part of the data is used as training data. Health Indicators generated for this data should therefore be predictable. Since the dataset is predictable and the outputs are known it is used as a tool during the building of the LSTM-AE model in python. It is used to give insight in functions that are required for development of the autoencoder model.

The model implementation steps described previously are verified with the use of the NASA data, because the expected degradation are known for these outputs as opposed to the real world data of the case study. If the model with the complete architecture functions as intended, then it is expected that the evaluations metrics should increase for every addition. In table Table 6.1 it is shown that indeed the mean values of the metrics are higher for the full version than for the basic LSTM-AE, which means that the model functions as expected. As can be seen in Table 6.1, according to the metrics the additions to the architecture improves the performance of the model, except for the addition of the teacher forcing. The explanation of this because the amount of training epochs are large enough to reach the optimum with conventional training, however it does increase the speed of the training. Furthermore, it should be noted that the NASA dataset the operation conditions fluctuate heavily and thus have a large influence on the reconstruction losses, for the version without the separation of operations conditions the HI construction will perform bad, see Figure 6.3. A different explanation for unexpected trend of the HI is not taking in account the varying length of each flight during the training phase.

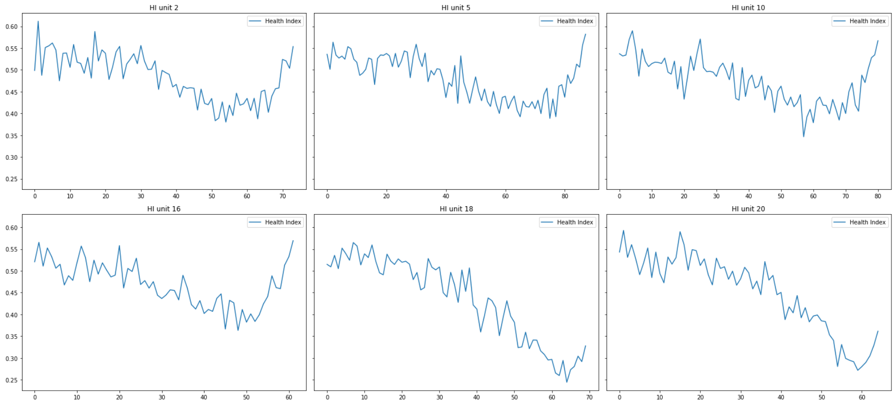

Figure 6.3: The constructed HIs of the test engines of the NASA data set constructed with basic LSTM-AE.

Table 6.1: Evaluation of the different LSTM-AE architectures, where the first five columns describe the differences in the architecture and the last three columns present the evaluation metrics.

Model version	seperate OC	FC layers	Teacher Forcing	Stacked layer	Mean values of the metrics		
					Monotinicity	Trendability	Prognosability
Basic LSTM-AE	No	No	No	No	-0.03	0.01	0.11
LSTM-AE-OC	Yes	No	No	No	0.16	0.77	0.67
LSTM-AE-OC-FC	Yes	Yes	No	No	0.21	0.82	0.72
LSTM-AE-OC-FC with TF	Yes	Yes	Yes	No	0.15	0.84	0.73
Proposed LSTM-AE	Yes	Yes	Yes	Yes	0.19	0.95	0.8

Sequence reconstruction
Another way to visualise that the model functions properly is plotting the reconstructed time series together with the original input. For the healthy state of the compressor the difference between these plots should be minimal. In Figure 6.4 the reconstructed sequence of the compressor in a assumed healthy state is shown, note that the reconstruction is similar to the original input, which provides evidence that the autoencoder functions as supposed.

6.1.3. Parameter Tuning

After the verification of the implementation of the model, the optimal parameters of the model are determined, these are acquired by performing a grid-search. This optimization loop is shown in the schematic Figure 4.3. The grid search is evaluated with the metrics described in the methodology; monotonicity (M), trendability (T) and prognosability (P), the results of the grid search are shown in Appendix D. The fitness of the model is added to the evaluation metrics, this is equal to the sum of the other metrics. The model parameters in the grid search that had the highest fitness overall are considered to be the optimal parameters, these are presented in Table 6.2 along with the other important hyperparameters. The weights of the training epoch with the lowest validation losses are applied to the model.

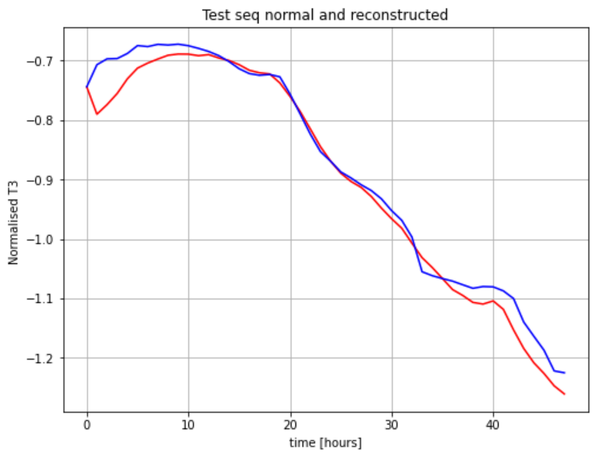

Figure 6.4: A reconstructed sequence (blue line) of T3 from the training set compared with the original sequence (red line).

Table 6.2: The hyperparameters that are applied to this case study and optimized by performing a grid search.

Architecture parameters	value
Number of stacked LSTM layers	3
Size of hidden and memory state	128
Sequence length of test data	12
Number of fully connected output layers	3
Hyperparameters	
Optimizer	Adam
Initial learning rate	0.001
Number of epochs	100
Patience before decreasing the learning rate	5
Decrease the learning rate by factor	0.1

6.1.4. Sensor selection for HI construction

Only sensors with a high trendability are included in the construction of the HI. These sensors are added to subset S_{HI} which will be the input for Equation (4.10). The trendability provides information over the difference in reconstruction loss at start of a lifecycle and the end of a lifecycle. For sensor with high trendability it is expected that the reconstructed signal deviation is minimal in the early stage of a lifecycle, this deviation increases with increasing time in the lifecycle, this corresponds to the increasing degradation. On the left in Figure 6.5 a feature is shown with a high trendability, this corresponds to described expectation. On the right in Figure 6.5 a feature is shown with low trendability, this does not correspond to described expectation and looks more like random noise. The sensor that are used for the construction of the HI have a high trendability and are included in subset S_{HI}.

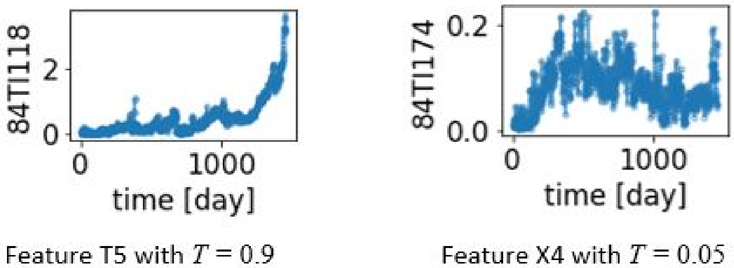

Figure 6.5: Reconstruction loss per sequence of compressor lifecyle set 1.

The HI is based on the reconstruction losses of a subset of sensors that are considered for each HI of a failure mechanism. These subsets are based on the expected effect and location of the failure mechanism as described in section 2.3. Furthermore the trendability of the reconstruction loss has to be higher than 0.5 for the sensor to be included. The HI for detecting leakages will be constructed from the sensors that are relevant to the gas sealing. The selected sensor for fouling are measuring parameters of the gas path in the compressor. The subset for the bearing HI includes the temperature and pressure of the oil, the bearing temperatures and the position of the rotor. The subsets of the selected sensors are shown in Table 6.3 and Figure 6.6.

Table 6.3: The subsets for each type of constructed health indicator (HI).

Health indicator	Sensor subset
General HI	{dP, P2 T2, T4, T5, T6, T7,T9, T10, T11, X2}
Leakage HI	{dP, P2}
Fouling HI	{P2, T2,T3, T4, T5, T6, T7}
Bearing HI	{P3, T9, T10, T11, X1, X2, X3}

6.1.5. Health indicator evaluation

The metrics of the HIs of the proposed method are compared with those of different versions of the method, see Table 6.4. The version of LSTM-AE without the operation conditions ignores the operating conditions. Analysing this version by comparing its metrics with that of the proposed method it is clear that the evaluation metrics decrease significantly. This result emphasize the effect of training the model independently from the operating conditions has positive impact on the performance of the HI construction.

The proposed model is trained with the training data of all compressors and could therefore be applied immediately for a newly placed compressor. The version of the method where the weights are trained for each compressor lifecycle separately could only be a applied to a new compressor when the months that are used for collecting training data are passed. However when dealing with real world

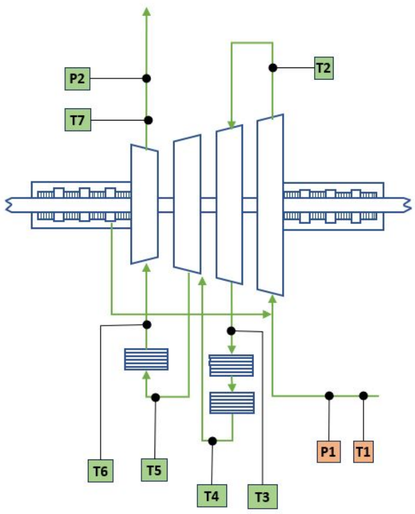

(a) A schematic overview of the gas path in the chlorine compressor and the sensors that are involved.

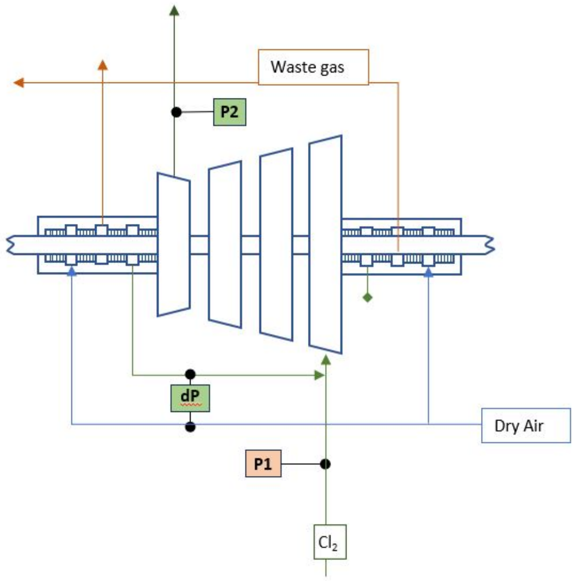

(b) Gas path through the compressor with location of sensors

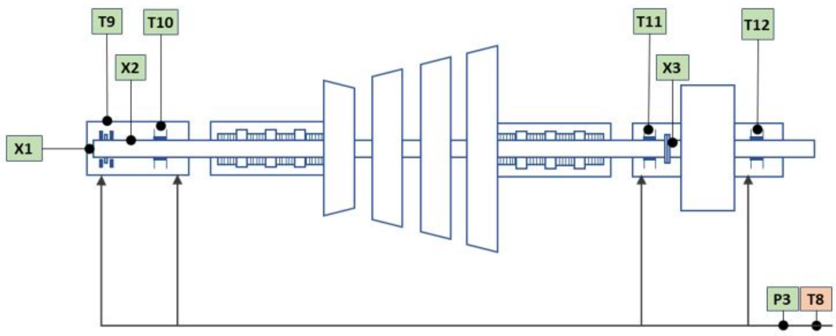

(c) A schematic view of the oil supply, axial bearing, journal bearings, gearbox and the location of the corresponding sensors

Figure 6.6: The selected sensor for the HI construction of failure specific HIs

data each compressor could have a different initial state, which brings extra noise and offsets to the HI construction. This expected difference in performance is visible in Table 6.4, where the evaluation metrics increase with this approach.

Table 6.4: Evaluation of the different version of LSTM-AE architecture. Here the sets corresponds to the compressor lifecycle. Mon, Tre and Pro stand for the monotinicity, trendability and prognosability respectively.

	Set 1		Set 2		Set 3		Set 4		Set 5		Mean			
	Mon	Tre	Mon	Tre	Mon	Tre	Mon	Tre	Mon	Tre	Mon	Tre	Pro	Fitness
proposed LSTM-AE	0.01	0.88	0.02	0.87	0.02	0.51	0.00	0.91	0.03	0.86	0.02	0.81	0.519	0.612
proposed LSTM-AE without operating conditions	0.03	0.79	0.05	0.91	-0.01	0.51	-0.01	0.65	0.05	0.47	0.02	0.67	0.398	0.525
proposed LSTM-AE with trained weights per compressor lifecycle	0.03	0.94	0.05	0.88	0.04	0.72	0.04	0.88	0.08	0.92	0.05	0.87	0.704	0.764

6.2. Validation of the results

After the implementation and verification of the model, the validation takes place. Since the model has two main purposes, namely assessment of the health and fault identification, the validation should cover both of these purposes.

6.2.1. Health Assessment

The health state division of the compressor lifecycle is shown in Figure 6.7. There is no nuance in health state, when applying the threshold for the division between a healthy and unhealthy state as proposed in the methodology, this has as result that the compressor are considered unhealthy relatively early and operate for a long time before they are overhauled. The threshold could be increased or established in an entire different way to overcome this. The health state division could be used as bases for RUL prediction, since it indicates that degradation is taking place. To realise RUL prediction for this case study more failure data is required and in the best case addition of run-to-failure data. For generalisation and ease of implementation the original method has advantages over the method where for each lifecycle the model has to be retrained, while the latter has better performance.

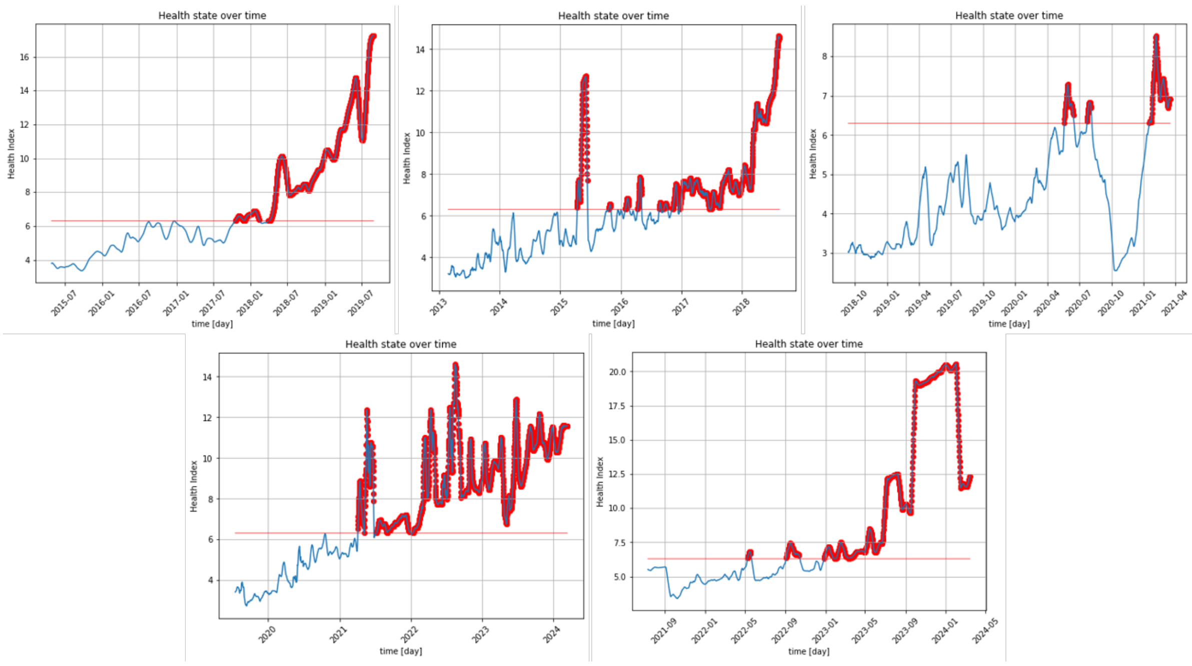

Figure 6.7: The health state division of the compressor lifecycles sets 1 to 5 from the left to the right. The unhealthy state is marked by the red circles.

6.2.2. Fault Identification

The process of fault identification is started from the moment the compressor lifecycle is marked unhealthy for the first time. This model has the possibility to identify what fault is developing in the compressor. As mentioned multiple times before there is no clear data of failures available, adding to this the documentation of failures that occurred in the compressors are also lacking. This makes it hard to objectify this validation step, therefore it is chosen to discuss the occasions where the fail mechanisms of the compressor are known to a certain degree. These are found by analysing the notifications and inspection reports of the compressors. These are found by analysing the notifications and inspection reports of the compressors and are presented in Table 6.5. The identification is performed by checking whether the separate HIs of the test sets cross the health threshold. Instances of the passing the threshold for each HI are shown in Figure 6.8. In the left graph of Figure 6.8 fouling HI of set 1 is shown, it is clearly visible that the HI passes the threshold, so fouling is identified. This lifecycle has been diagnosed with fouling so this identification is correct. The middle and right graph of Figure 6.8 are both of lifecycle set 5 and show the presence of bearing damage and leakage respectively. These failure mechanisms are diagnosed for this compressor lifecycle so the identification is correct. The fault identification is performed by analysing the failures per set for each constructed HI, the results of analysis are presented in a confusion matrix (Table 6.6). In Appendix E the results of the same validation task are presented, however here the fault identification is performed by hand and trends of the HIs are analysed instead of the crossing of thresholds. This has resulted in a similar outcome. The results of the fault identification are used to calculate the KPIs proposed in Section 4.4 and are shown in Table 6.7.

Table 6.5: The fail mechanisms that have developed during the corresponding compressor lifecycle.

Dataset	**Compressor**	**Fail mechanism**
Compressor lifecycle 1	K8421	Fouling
Compressor lifecycle 2	K8411	Fouling
Compressor lifecycle 3	K8411	Unknown
Compressor lifecycle 4	K8421	Fouling
Compressor lifecycle 5	K8411	Bearing and Leakage

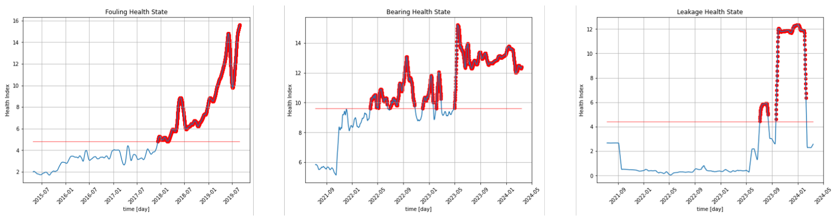

Figure 6.8: Fault identification instances. The left figure shows that fouling is detected in lifecycle set 1. The figure in the middle and on the right show that bearing damages and leakage are detected in compressor lifecycle set 5.

Table 6.6: Confusion matrix of the fault identification

Confusion matrix		Diagnosed Fault	
		Fault is present	*Fault is absent*
Identified fault	*Fault is identified*	5 TP	4 FP
	Fault is not identified	0 FN	6 TN

6.3. Discussion

The results of the case study are validated to determine the quality of the model. In section 6.1.5 the performance of the proposed method is presented. The LSTM-AE which is trained for each compressor lifecycle separately performs considerably than the original proposed method, it has a mean monotonicity of 0.05, a mean trendability of 0.87 and a prognosability of 0.704. The health assessment and fault

Table 6.7: Case study results of the fault identification.

KPI	Score
Accuracy	0.73
Precision	0.56
Recall	0.45
F1-score	0.5

identification are therefore executed with this version. The health state division as shown in Figure 6.7 functions as start signal for the fault identification. The HIs behave as expected with increasing reconstruction losses towards the end of life, however it is noticeable that the HI is not only increasing over time. The HI corresponds to the degradation of the compressor and degradation can not be undone without repairs, therefore this decreases of the HI are in theory not logical. However, they can be explained acknowledging that this is real data of compressors in a controlled process, this means that performance can be boosted by changing the process parameters. For the fault identification it is required to identify and couple the failure mechanism for each test set. However, there is no clear data of failures available, adding to this the documentation of failures that occurred in the compressors are also lacking, this has the effect that is hard to objectively quantify the performance. To make the validation of the fault identification possible educated assumptions based on the data that is available, are made on the failure mechanism of the compressor lifecycles. These are then analysed for compressor lifecycle and the results are presented in a confusion matrix (see Table 6.6). This results in a identification with an accuracy of 73% and a precision of 56%, which means that the proposed method could successfully identify faults in real world compressors even when multiple faults are occurring simultaneously. The use of the HI construction as basis for RUL prediction is not possible to be tested with the lack of run to failure instances in the available data.

7 Conclusion and recommendations

This chapter presents the final conclusion of the research by answering the main research question. The sub-questions have been answered the previous chapters. Furthermore it provides recommendations on future research on this topic and lastly a section is devoted on how this work could be implemented at Nobian.

7.1. Conclusion

The main research question that is asked to achieve the goal of this study is as follows:

How can the failure mechanisms of chlorine compressor be diagnosed and the health of the compressor be monitored?

This main question is concluded by answering the sub research question one by one.

Sub-research questions 1: *What are characteristics and the failure mechanisms of the chlorine compressor and which will be included in the model?*

The chlorine compressor is a critical part of the chlorine liquefaction unit, if one of the two compressors is not available the production capacity of the plant reduces to 40%. Therefore reducing the downtime by optimizing the maintenance strategy is beneficial to the whole production plant. The first step towards this goal is determining what the main failure mechanisms of the compressor are. By researching the literature for compressor failures in general and researching the database of the company it is found that the main failure mechanisms are: fouling, leakages and damaged bearings.

Sub-research questions 2: *What is the current state of failure diagnosis methods in literature and what method is best applicable to this case study?*
Literature tis reviewed hat focuses on FDD and HI construction is consulted to get an understanding of what techniques are available and suitable for this research subject. It has become clear that the best approach for machine diagnosis of a compressor with limited recorded failure instances, is health assessment by constructing of health indicators. The construction of health indicators requires fusion of the multivariate data, which provides four groups of health indicator construction methods: Model based, optimization methods for feature combination, statistical projection and deep learning based. The last two groups are subjected to case specific selection criteria: Accuracy, Feasibility, Computational effort and Robustness. The considered methods should meet the following criteria to be considered feasible:

- Can be trained with limited or without failure data.
- Is able to deal with changing operating conditions.
- Is capable of detection and identification of the degradation by multiple faults simultaneously.

This has resulted in the selection of the LSTM-AE as foundation for the methodology of this research, which provides the answer to the question.

Sub-research questions 3: *How to develop the proposed fault detection and indication model for the chlorine compressor?*

This answer is provided by describing the methodology of the proposed method. The main part is about the characteristics of the LSTM-AE model which is the foundation of the proposed method. Then it is described how the health indicators are constructed based on the reconstruction error of the autoencoder. To evaluate the developed model three metrics are proposed are proposed that determine the characteristics of the development of the HI over time, namely; Monotonicity, trendability and prognosability. Furthermore, Chebychev's inequality is introduced to establish the threshold for health state division between the healthy and unhealthy state of the compressor. Hereafter the verification steps of the model are described, which includes:

- The implementation of the model with a different dataset that is frequently used in literature.
- Parameter tuning with the help of a grid search.
- Sensor selection for HI construction.

At the end the methods for health assessment and fault identification are described.

Sub-research questions 4: *What data is available and how can it be retrieved and analysed for the purpose of fault diagnosis?*

The used database is considered to provide stable data for the period of the past ten years. The available measurements have the function to provide insight in the process and driving alarms when the parameters are out of bound. The types of parameters that are included are the following: temperature, pressure, pressure difference, and displacement. There are in total 16 sensors and 3 operation conditions selected to be used as input for the model. The multivariate measurements of these sensors are collected of five compressor lifecycles with a sampling rate of one hour, this collected data is the testing data. The training data is collected from the first months of each lifecycle that are considered healthy, this data will be used to train the LSTM-AE. The datasets are prepared for usage as input to the proposed model. The preprocessing steps include:

- Outlier removal by a assuming a Gaussian distribution of the data.
- Noise reduction will be performed with the moving average method, which replaces data points with the local mean of the window around the point.
- Standardization for both training and testing data, the mean and standard deviation of the training sets is used.
- Sequencing are extracted with a rolling window. The stride and length of this rolling window is different for the training and testing set.

Sub-research questions 5: *How to verify and validate the proposed method?*

At first, the implementation of the model is verified by analysing it with the help of simulated public data. The usage of this data set for verification purposes has as advantage that the expected outputs such as the degradation pattern are known. The results using this dataset are comparable with a reference paper, although of less quality, which can be explained by the lack the attention mechanism and the selection of a uniform length for all flights. The next verification steps are parameter optimization with a grid search and sensor selection for HI construction, which are heavily depended of one another. The optimal architecture, according to the considered variable parameters, is determined with the grid search and has been implemented for the following steps. Also, the sensors with high trendability that will be used for the HI construction are determined. The final verification steps compares the proposed method to two different approaches of LSTM-AE. One approach ignores the operating conditions, analysing this version by comparing its metrics with that of the proposed method it is clear that the evaluation metrics decrease significantly. This result emphasize the effect of training the model independently from the operating conditions has positive impact on the performance of the HI construction. The proposed model is trained with the training data of all compressors and could therefore be applied immediately for a newly placed compressor. The version of the method where the weights are trained for each compressor lifecycle separately could only be a applied to a new compressor when the months that are used for collecting training data are passed. However when dealing with real world data each compressor could have a different initial state, which brings extra noise and offsets to the HI construction. This expected difference in performance is visible in Table 6.4, where the evaluation metrics increase with this approach.

The validation of the results is conducted by evaluating the health assessment and fault identification. Health assessment is performed to divide the health state of the compressor using the constructed HI. There is no nuance in health state, there is only healthy or unhealthy, this has as result that the compressor are considered unhealthy relatively early on their lifecycle and operate for a long time before they are overhauled. The first instance of an compressor marked as unhealthy triggers the start of the fault identification, which has resulted in a identification with an accuracy of 73% and a precision of 56% for the three considered failure mechanisms. The performance of the model is increased by training the weights of the model for each compressor lifecycle separately. The trade-off using this approach is that health assessment and fault identification is not possible in the start of a new lifecycle, because this period is used to acquire the training data. To overcome this trade-off a combination of both approaches should be used, where the health assessment during this first period of a new compressor is performed original model and after this initial period the model specifically trained for this lifecycle is used for fault identification with higher accuracy.

To conclude, the proposed LSTM-AE method is able to correctly detect and thereafter identify single or multiple failure mechanism present in chlorine compressors with an accuracy of 73 %, while only being trained with healthy data and is therefore applicable for real world cases with unlabeled data. Therefore the goal of this study has been achieved.

The main contributions of this research are:

- A method is proposed for health indicator construction for compressors with the purpose of health assessment and fault identification. By constructing health indicators for each detectable failure mechanisms the model is able to perform fault identification even when multiple faults are developing. The model is tested with a real world case study of chlorine compressors of which little failure data is available so the model is trained to learn the healthy characteristics of the compressor. In this study it is shown that this method is able to correctly identify the failure mechanism present in the compressor and is therefore applicable for real world cases.
- The health indicators are constructed with the reconstruction loss of the LSTM-AE. The model is trained to reconstruct the measurements independently of the operation conditions, which increases the robustness of the model.
- The collected real world data requires extensive preprocessing to reduce the effect of corrupted data and format it to the correct form before it is used as input to the LSTM-AE. This research proposes the tools to realise this and shows the effect of the quality of the preprocessing.

7.2. Recommendations for further research

Exploring the possibilities for predictive maintenance that are available using machine learning has given insight in what possible improvements and follow up research could occur. In general a lot of the research in literature that try to perform fault diagnosis and prognosis make use of simulated data, which is stable, has Gaussian distribution and a clear degradation path. During this research the lack of research with real-world data is noticed, this provides a lot of opportunity for beneficial future research into the implementation of the these methods in real cases.

Furthermore, the constructed HIs could be used as the basis for RUL predictions, it is however required to establish a maximum for the HI which corresponds to the failure of the equipment. For the determination of this maximum more compressor lifecycles are required to create a better understanding of the behaviour of the compressor towards failure.

For case study specific recommendations there should be started with improving the input data by taking in account sensor failures and process parameter shifts. Also the failures should be better traced to provided a better data base of failure data. This provides a bases to compare the results of this case study with other research to find a possible better method. Lastly, the best option would be to fill the gap of missing interstage pressure measurements, which would provide the opportunity to construct a model-based method or a combined hybrid method.

7.3. Company Implementation

The goal of this research and case study is to develop a model that could improve the decision making for the maintenance of operational chlorine compressors. Although there are limitations to the model, it could be used as a tool by the companies maintenance engineers to gain insight in the health status of the compressors. The strength of the model is to get a fast first indication of changing health condition of the compressors. Since the model is a promising tool for the company an installation and users manual is constructed, so the model can proof its value in the future.

References

Arias Chao, M., Kulkarni, C., Goebel, K., & Fink, O. (2022). Fusing physics-based and deep learning models for prognostics. *Reliability Engineering & System Safety*, *217*, 107961. doi:https://doi.org/10.1016/j.ress.2021.107961

Al-Busaidi, W., & Pilidis, P. (2016). Modelling of the non-reactive deposits impact on centrifugal compressor aerothermo dynamic performance. *Engineering Failure Analysis*, *60*, 57–85. doi:https://doi.org/10.1016/j.engfailanal.2015.11.027

Lei, Y., Li, N., Guo, L., Li, N., Yan, T., & Lin, J. (2018). Machinery health prognostics: A systematic review from data acquisition to rul prediction. *Mechanical Systems and Signal Processing*, *104*, 799–834. doi:https://doi.org/10.1016/j.ymssp.2017.11.016

Jardine, A. K., Lin, D., & Banjevic, D. (2006). A review on machinery diagnostics and prognostics implementing condition-based maintenance. *Mechanical Systems and Signal Processing*, *20*(7), 1483–1510. doi:https://doi.org/10.1016/j.ymssp.2005.09.012

Schwartz, S., Montero Jiménez, J. J., Vingerhoeds, R., & Salaün, M. (2022). An unsupervised approach for health index building and for similarity-based remaining useful life estimation. *Computers in Industry*, *141*, 103716. doi:https://doi.org/10.1016/j.compind.2022.103716

Wang, P., Youn, B. D., & Hu, C. (2012). A generic probabilistic framework for structural health prognostics and uncertainty management. *Mechanical Systems and Signal Processing*, *28*, 622–637. Interdisciplinary and Integration Aspects in Structural Health Monitoring. doi:https://doi.org/10.1016/j.ymssp.2011.10.019

Kim, M., Song, C., & Liu, K. (2019). A generic health index approach for multisensor degradation modeling and sensor selection. *IEEE Transactions on Automation Science and Engineering*, *16*(3), 1426–1437. doi:10.1109/TASE.2018.2890608

Moradi, M., Broer, A., Chiachío, J., Benedictus, R., Loutas, T. H., & Zarouchas, D. (2023). Intelligent health indicator construction for prognostics of composite structures utilizing a semi-supervised deep neural network and shm data. *Engineering Applications of Artificial Intelligence*, *117*, 105502. doi:https://doi.org/10.1016/j.engappai.2022.105502

Eleftheroglou, N., Zarouchas, D., Loutas, T., Alderliesten, R., & Benedictus, R. (2018). Structural health monitoring data fusion for in-situ life prognosis of composite structures. *Reliability Engineering & System Safety*, *178*, 40–54. doi:https://doi.org/10.1016/j.ress.2018.04.031

Liu, C., Sun, J., Liu, H., Lei, S., & Hu, X. (2020a). Complex engineered system health indexes extraction using low frequency raw time-series data based on deep learning methods. *Measurement*, *161*, 107890. doi:https://doi.org/10.1016/j.measurement.2020.107890

Chen, X., Ding, X., Wang, X., Zhao, Y., Liu, C., Liu, H., & Chen, K. (2023). Multi-task data imputation for time-series forecasting in turbomachinery health prognostics. *Machines*, *11*(1). doi:10.3390/machines11010018

de Pater, I., & Mitici, M. (2023). Developing health indicators and rul prognostics for systems with few failure instances and varying operating conditions using a lstm autoencoder. *Engineering Applications of Artificial Intelligence*, *117*, 105582. doi:https://doi.org/10.1016/j.engappai.2022.105582

Arias Chao, M., Kulkarni, C., Goebel, K., & Fink, O. (2021). Aircraft engine run-to-failure dataset under real flight conditions for prognostics and diagnostics. *Data*, *6*(1). doi:10.3390/data6010005

Malhotra, P., TV, V., Ramakrishnan, A., Anand, G., Vig, L., Agarwal, P., & Shroff, G. (2016). Multi-sensor prognostics using an unsupervised health index based on lstm encoder-decoder. arXiv: 1608.06154 [cs.LG]. Retrieved from https://arxiv.org/abs/1608.06154

Ran, Y., Zhou, X., Lin, P., Wen, Y., & Deng, R. (2019). A survey of predictive maintenance: Systems, purposes and approaches. *Comput. Sci. Eng.* Retrieved from https://arxiv.org/pdf/1912.07383.pdf

Achouch, M., Dimitrova, M., Ziane, K., Sattarpanah Karganroudi, S., Dhouib, R., Ibrahim, H., & Adda, M. (2022). On predictive maintenance in industry 4.0: Overview, models, and challenges. *Applied Sciences*, *12*(16). doi:10.3390/app12168081

Brinkmann, T., Santonja, G. G., Schorcht, F., Roudier, S., & Sancho, L. D. (2014). Best available techniques (bat) reference document for the production of chlor-alkali. *JRC (Joint Research Center EU), JRC91156*.

Dokter, T. (1985). Fire and explosion hazards of chlorine-containing systems. *Journal of Hazardous materials*, *10*(1), 73–87.

Talk, T. P. (2020). Centrifugal compressor parts & their function. Retrieved October 24, 2022, from https://thepipingtalk.com/centrifugal-compressor-parts-their-function/

Group, E. (2014). Multi-stage centrifugal compressor modifications and rerates. Retrieved November 11, 2022, from https://www.elliott-turbo.com

Barnard, P. (2001). Centrifugal compressors fouling-understanding, mitigating, and cleaning. In *Compressors and their systems: 7th international conference* (pp. 241–250). John Wiley and Sons.

Bidaut, Y. et al. (2013). The influence of thermal loading on the leak tightness behaviour of horizontally split centrifugal compressors. In *Middle east turbomachinery symposia. 2013 proceedings.* Turbomachinery Laboratory, Texas A&M Engineering Experiment Station.

Qiao, B., Ju, Y., & Zhang, C. (2019). Numerical investigation on labyrinth seal leakage flow and its effects on aerodynamic performance for a multistage centrifugal compressor. *Journal of Fluids Engineering*, *141*(7).

Manikandan, A., & Anwar, Z. (2018). Case Study – To Identify and Fix the Contributing Factors on a Complex Turbo Machinery Driver Misalignment. (Vol. Day 1 Mon, November 12, 2018). doi:10.2118/192641-MS

Walker, R., Perinpanayagam, S., & Jennions, I. K. (2013). Rotordynamic faults: Recent advances in diagnosis and prognosis. *International Journal of Rotating Machinery*, *2013*.

Biglarian, M., MomeniLarimi, M., Ganji, B., & Ranjbar, A. (2019). Prediction of erosive wear locations in centrifugal compressor using cfd simulation and comparison with experimental model. *Journal of the Brazilian Society of Mechanical Sciences and Engineering*, *41*(2), 1–10.

Lu, Y., Wang, F., Jia, M., & Qi, Y. (2016). Centrifugal compressor fault diagnosis based on qualitative simulation and thermal parameters. *Mechanical Systems and Signal Processing*, *81*, 259–273. doi:https://doi.org/10.1016/j.ymssp.2016.03.018

Luo, H., Bo, L., Peng, C., & Hou, D. (2022). Detection and quantification of oil whirl instability in a rotor-journal bearing system using a novel dynamic recurrence index. *Nonlinear Dynamics*, 1–33.

Nguyen, K. T. P. (2022). Feature engineering and health indicator construction for fault detection and diagnostic. In K. P. Tran (Ed.), *Control charts and machine learning for anomaly detection in manufacturing* (pp. 243–269). doi:10.1007/978-3-030-83819-5_10

Firpi, H., & Vachtsevanos, G. (2008). Genetically programmed-based artificial features extraction applied to fault detection. *Engineering Applications of Artificial Intelligence*, *21*(4), 558–568. doi:https://doi.org/10.1016/j.engappai.2007.06.004

Jolliffe, I. (2002). *Principal component analysis*. Springer. Retrieved from https://books.google.nl/books?id=%5C_olByCrhjwIC

He, Q., Yan, R., Kong, F., & Du, R. (2009). Machine condition monitoring using principal component representations. *Mechanical Systems and Signal Processing*, *23*(2), 446–466. doi:https://doi.org/10.1016/j.ymssp.2008.03.010

Chen, H., Huang, W., Huang, J., Cao, C., Yang, L., He, Y., & Zeng, L. (2020). Multi-fault condition monitoring of slurry pump with principle component analysis and sequential hypothesis test. *International Journal of Pattern Recognition and Artificial Intelligence*, *34*(07), 2059019. doi:10.1142/S0218001420590193. eprint: https://doi.org/10.1142/S0218001420590193

Schölkopf, B., Smola, A. J., & Müller, K.-R. (1999). Kernel principal component analysis. In *Advances in kernel methods: Support vector learning* (pp. 327–352). Cambridge, MA, USA: MIT Press.

Feng, D., Xiao, M., Liu, Y., Song, H., Yang, Z., & Zhang, L. (2016). A kernel principal component analysis–based degradation model and remaining useful life estimation for the turbofan engine. *Advances in Mechanical Engineering*, *8*(5), 1687814016650169. doi:10.1177/1687814016650169. eprint: https://doi.org/10.1177/1687814016650169

Tipping, M. E., & Bishop, C. M. (1999). Probabilistic principal component analysis. *Journal of the Royal Statistical Society. Series B (Statistical Methodology)*, *61*(3), 611–622. Retrieved July 25, 2023, from https://www.cs.columbia.edu/~blei/seminar/2020-representation/readings/TippingBishop1999.pdf

Ruiz-Cárcel, C., Jaramillo, V., Mba, D., Ottewill, J., & Cao, Y. (2016). Combination of process and vibration data for improved condition monitoring of industrial systems working under variable operating conditions. *Mechanical Systems and Signal Processing*, *66-67*, 699–714. doi:https://doi.org/10.1016/j.ymssp.2015.05.018

Pilario, K. E. S., & Cao, Y. (2018). Canonical variate dissimilarity analysis for process incipient fault detection. *IEEE Transactions on Industrial Informatics*, *14*(12), 5308–5315. doi:10.1109/TII.2018.2810822

Larimore, W. E. (1983). System identification, reduced-order filtering and modeling via canonical variate analysis. In *1983 american control conference* (pp. 445–451). doi:10.23919/ACC.1983.4788156

Hochreiter, S., & Schmidhuber, J. (1997). Long Short-Term Memory. *Neural Computation*, *9*(8), 1735–1780. doi:10.1162/neco.1997.9.8.1735. eprint: https://direct.mit.edu/neco/article-pdf/9/8/1735/813796/neco.1997.9.8.1735.pdf

Nguyen, H. D., Tran, K. P., Thomassey, S., & Hamad, M. (2020). Forecasting and Anomaly Detection approaches using LSTM and LSTM Autoencoder techniques with the applications in Supply Chain Management. *International Journal of Information Management*. Retrieved from https://hal.science/hal-03083642

Liu, C., Sun, J., Liu, H., Lei, S., & Hu, X. (2020b). Complex engineered system health indexes extraction using low frequency raw time-series data based on deep learning methods. *Measurement*, *161*, 107890. doi:https://doi.org/10.1016/j.measurement.2020.107890

Kong, X., & Yang, J. (2019). Remaining useful life prediction of rolling bearings based on rms-mave and dynamic exponential regression model. *IEEE Access*, *7*, 169705–169714. doi:10.1109/ACCESS.2019.2954915

Bohutska, J. (2021). Anomaly detectionhow to tell good performance from bad. Retrieved February 24, 2024, from https://towardsdatascience.com/anomaly-detection-how-to-tell-good-performance-from-bad-b57116d71a10

AI, E. (2021). How to interpret a confusion matrix for a machine learning model. Retrieved February 24, 2024, from https://www.evidentlyai.com/classification-metrics/confusion-matrix#:~:text=A%20confusion%20matrix%20is%20a%20table%20that%20summarizes%20the%20performance,FN)%20of%20the%20model’s%20predictions.

Sharma, N. (2018). Ways to detect and remove the outliers. Retrieved January 24, 2024, from https://towardsdatascience.com/ways-to-detect-and-remove-the-outliers-404d16608dba

de Cheveigné, A., & Arzounian, D. (2018). Robust detrending, rereferencing, outlier detection, and inpainting for multichannel data. *NeuroImage*, *172*, 903–912. doi:https://doi.org/10.1016/j.neuroimage.2018.01.035

Bilogur, A. (2018). Denoising algorithms. Retrieved January 24, 2024, from https://www.kaggle.com/code/residentmario/denoising-algorithms

Brownlee, J. (2020). How to use standardscaler and minmaxscaler transforms in python. Retrieved January 23, 2024, from https://machinelearningmastery.com/standardscaler-and-minmaxscaler-transforms-in-python/

Vasilev, I. (2019). *Advanced deep learning with python: Design and implement advanced next-generation ai solutions using tensorflow and pytorch*. Packt Publishing Ltd. Retrieved from https://scholar.googleusercontent.com/scholar.bib?q=info:In7B-vrY5dQJ:scholar.google.com/&output=citation&scisdr=ClGORIirEILhn2KGFyU:AFWwaeYAAAAAZs6ADyXNNPpA9by5t02DcOxhYPk&scisig=AFWwaeYAAAAAZs6ADxqxTiIaHif49m6QxwZ6Qeg&scisf=4&ct=citation&cd=-1&hl=nl

Vincrichard. (2020). Lstm-autoencoder-unsupervised-anomaly-detection. https://github.com/vincrichard/LSTM-AutoEncoder-Unsupervised-Anomaly-Detection/tree/master. GitHub.

A

Scientific Paper

Health Indicator construction for health assessment and fault identification of industrial compressors

J. Tas, Dr. ir. X. Jiang, Prof. dr. R.R. Negenborn, B. van den Bogerd
MME Graduation thesis

Abstract: A model has been developed for the health assessment of a chlorine compressor that is capable of constructing Health Indicators (HI). This model is a Long-Short Term Memory AutoEncoder (LSTM-AE), which is an unsuperised machine learning method and works as follows: an LSTM-based encoder maps a multivariate input sequence to a fixed-dimensional vector representation. The decoder, another LSTM network, uses this vector representation to produce the target sequence. The loss between the reconstructed sequence and the input sequence forms the basis for the HI. The model is trained exclusively with healthy data. The LSTM-AE is designed to reconstruct the measurements independently of the operating conditions, enhancing the model's robustness in varying operational contexts. Health assessment is conducted by using the constructed HI to classify the health state of the compressor. The first instance of the compressor being marked as unhealthy triggers the start of fault identification. The proposed method is tested on real-world data through a case study on chlorine compressors, resulting in an identification accuracy of 73% and a precision of 56% for the three considered failure mechanisms.

1. Introduction

A new industrial revolution is ongoing, namely Industry 4.0. This revolution focuses on using resources more efficiently and leveraging data, communication, and new technology to achieve this goal. Industry 4.0 covers all fields of industry and is becoming increasingly relevant and required to compete in today's market. This research focuses on the maintenance part of Industry 4.0, specifically on fault diagnostics methods for turbomachinery such as compressors. Compressors play a crucial role in the industry, and maintaining high reliability and availability is desirable. In the chemical industry, dealing with toxic and corrosive products, maintenance of compressors on-site presents difficulties and is preferably scheduled far in advance. Furthermore, compressors are machines with multiple possible failure mechanisms and different degradation patterns. The mean time between failures is not reliable; the deviation between life cycles is widely spread and highly dependent on the production process, where errors in previous process stages impact the degradation of the compressor. This degradation behavior means that a time-based approach to maintenance could be too late or a waste of time and resources on a well-operating machine. Therefore, developing a fault diagnostic model that provides insight into the health condition of machinery could be beneficial. This opportunity is well known in the industry, and a lot of research is being done in this direction.

1.1. Literature review

As mentioned there are already numerous studies focused on fault diagnostics in compressors, however a lot of these are focused on a single failure mechanism, for example: the study into fouling mechanism by deriving the equivalent compressor performance map at various degrees of fouling with a consideration of gas properties and stage efficiency variation and without prior knowledge of the detailed geometrical features (Al-Busaidi and Pilidis, 2016). An improved qualitative simulation (QSIM) based fault diagnosis method is proposed to diagnose the faults of centrifugal compressors in Lu et al. (2016). This study uses the thermal parameters to detect the occurrence of faults in the gas flow path. The method presented in Luo et al. (2022) is a Dynamic Recurrence Index (DRI) and is used to detect the occurrence and quantify the evolution of oil film instability in the journal bearing system.

An approach that is able to assess the machine as a whole is the construction of Health Indicators(HIs) (Lei et al., 2018, Jardine et al., 2006, Schwartz et al., 2022, Wang et al., 2012). Well constructed Health indicators could also be used as basis for remaining useful life prediction methods. HIs can be divided into two categories based on their construction strategies: physical HIs (PHI) and virtual HIs (VHI) (Lei et al., 2018). PHI correspond to direct underlying degradation factor and the physics of failure and are generally directly extracted from monitoring signals. VHIs are generally built by fusing multiple PHIs or multi-sensor signals. VHIs describe the degradation trend of the equipment, but loses the direct physical meaning. For this research there are no monitoring signals available that directly correspond to a physical degradation, so a VHI should me constructed using multi-sensor signals. This could be achieved by statistical approaches, in Wang et al. (2012) the framework for constructing generic HIs is provided by employing a linear data transformation method. This method is suitable for continuously collected measurements and is a process of information fusion which provides a unified measure being used to characterize the health condition of the system. Schwartz et al. (2022) uses kernel functions in combination with principal component analysis to provide a non linear approach to data fusion as basis for the HI construction. These methods are trained with the help of failure data. Due to preventive maintenance approach limited failure data of compressors is available. This gives the challenge of learning the degradation and failure behaviour without having training data of this. Model should be able to learn the characteristics of a healthy compressor.

A different approach is provided using a machine learning method, where the HIs are constructed with the help of neural networks (NN) Kim et al. (2019). This has the advantage of not requiring the exact failure threshold and does not limit the application of the method for a specific degradation process. Another study uses Semi-Supervised Deep Neural Network (SSDNN) for data fusion in order to create HIs Moradi et al. (2023). Here the model is trained to construct HIs with high prognosability by using evaluation metrics for HIs during the training process, these are often used for this practice (Eleftheroglou et al., 2018). Liu et al. (2020a) proposes the use of a Long-Short Term Memory AutoEncoder (LSTM-AE). The structure of LSTM predicts the next time steps and is able to learn long-term memory information to provide a solution to long-term dependencies Chen et al. (2023), this makes it functional for using the dtaa in an optimal manner. The AE is a reconstruction method that recovers the original input from its compressed representation to measure the reconstruction error. This reconstruction error is used as the basis for the HI. HIs are not only sensitive to degradation, but they also might be influenced by abnormalities in environmental conditions and operations. de Pater and Mitici (2023) extends on this method by making the LSTM-AE feasible for varying operation conditions and applying attention to increase accuracy. Most of these use the same type of data set, which are created by a simulation using a degradation function (Arias Chao et al., 2021) and thus providing a clear degradation behaviour the challenge is to construct accurate HIs for real world applications which are robust enough to deal with impurities in data. Malhotra et al. (2016) also uses LSTM-AE to construct HIs with a different approach. Their goal is to construct a mapping of the reconstruction losses over time, resulting in a HI function that is used for RUL prediction. The limitation here is that the model only assumes one type of degradation curve, which does reflect the occurrence of multiple degradation mechanisms in reality. This highlights the difficulties of performing fault diagnosis and identification in real world cases.

1.2. Research Objective

The aim of this research is to develop a model that is able to asses the health of compressors, which could be used to optimize the maintenance strategy in order to reduce downtime and improve the performance of the production line with the use of data collected by multiple sensors. The focus is establishing a model that gives insight in the health of the asset and is able to identify failure mechanisms of real world cases.

The main contributions of this research are:

- A method is proposed for health indicator construction for compressors with the purpose of health assessment and fault identification. By constructing health indicators for each detectable failure mechanisms the model is able to perform fault identification even when multiple faults are developing. The model is tested with a real world case study of chlorine compressors of which little failure data is available so the model is trained to learn the healthy characteristics of the compressor. In this study it is shown that this method is able to correctly identify the failure mechanism present in the compressor and is therefore applicable for real world cases.

- The health indicators are constructed with the reconstruction loss of the LSTM-AE. The model is trained to reconstruct the measurements independently of the operation conditions, which increases the robustness of the model.
- The collected real world data requires extensive preprocessing to reduce the effect of corrupted data and format it to the correct form before it is used as input to the LSTM-AE. This research proposes the tools to realise this and shows the effect of the quality of the preprocessing.

1.3. Paper outline

The rest of the paper is organised as follows: in Section 2 the proposed methodology is described. Then, the case study is introduced in Section 3 and the HI construction is presented together with the tuning of the model. Thereafter, in Section 4 the results of the health assessment and fault identification are presented and discussed. Finally the conclusion is provided in Section 5.

2. Methodology

In this section the LSTM-AE is introduced first, along with the format of the time series data. Secondly, the reconstruction loss is used to construct the HIs. Then the training and the tuning process for the optimal parameters is described. At last the application of the HIs for health assessment and fault identification is presented.

2.1. LSTM Autoencoder

In this section the characteristics of the LSTM-AE are described. Let $\vec{X}^{c,d} = \vec{X}_t^{c,d}, t \in \{1, 2, ..., n^{c,d}\}$ be the multi-sensor measurement of compressor lifecycle c during sequence d , where t denotes the time step during this sequence. The compressor lifecycle c refers to period that the compressor starts operating after placement till it either fails or is replaced. The input for the LSTM-AE should have a limited length for the model to function effectively, therefore the lifecycle are split in sequences d of size $n^{c,d}$ which are used as input. The $\vec{X}_t^{c,d} = [X_t^{c,d,1}, X_t^{c,d,2}, ..., X_t^{c,d,a^s}]$ is the multi-sensor measurement at time step t, with a^s the amount of considered sensors. Furthermore, the amount of sequences in a compressor lifecycle c is indicated as D^c.

The operation conditions are separated with the purpose of developing a model that constructs the HI independent of these conditions. The sensors that qualify for this purpose are the ones measuring the inlet conditions of the chlorine gas and oil, more precise: the inlet temperature and pressure of the chlorine gas and the inlet temperature of the oil. These are the parameters that could change depending on the season or the production process that precedes the compression and influence the other parameters in the system. The measurements of the operation conditions have their own notification. Let $\vec{O}^{c,d} = \vec{O}_t^{c,d}, t \in \{1, 2, ..., n^{c,d}\}$ be the conditions of sequence d of compressor lifecycle c, then $\vec{O}_t^{c,d} = [O_t^{c,d,1}, O_t^{c,d,2}, ..., O_t^{c,d,a^o}]$ refers to the conditions at time step t of this sequence d and a^o correspond to the amount of operating conditions.

The LSTM-AE consists of an encoder part and a decoder part, which recurrent layers exist of enrolled series of LSTM cells and encodes the input data to the repeat vector and reconstruct the time series at the decoder part, see Fig. 1 where the architecture with one layer is shown.

A. LSTM cell

The LSTM technique is an adapted version of the original LSTM structure by Hochreiter and Schmidhuber (1997). This version described by de Pater and Mitici (2023) consists of two variable states that are

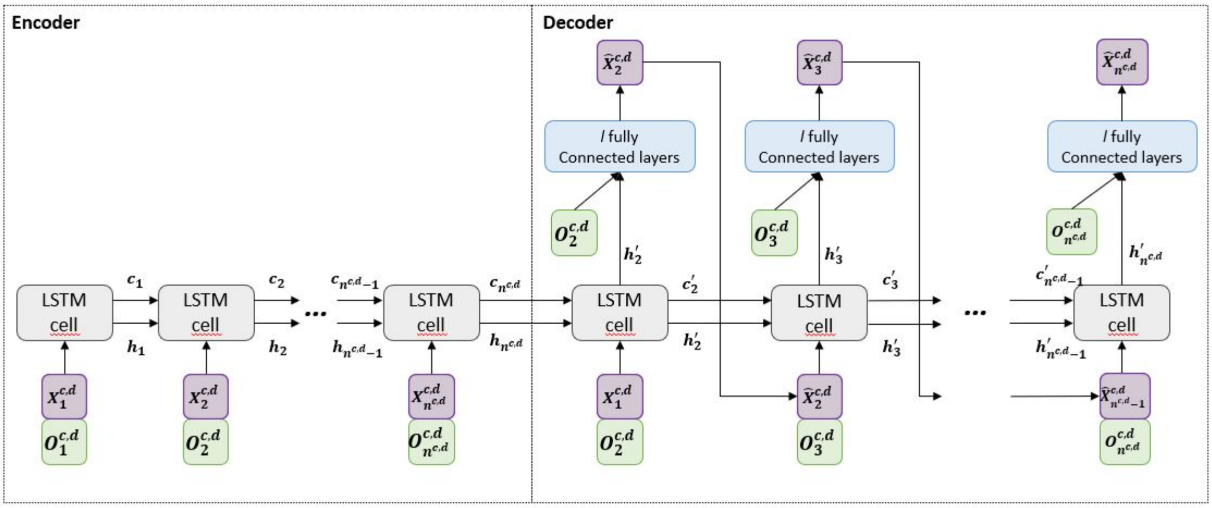

Figure 1. *Architecture of the LSTM-AE*

updated by every cell and than past on to the next cell, these states are the memory state c_t and the hidden state h_t. This results in the situation that every cell has four inputs; the features and operation conditions at the current time step $\vec{X}_t^{c,d}$ and $\vec{O}_t^{c,d}$, the initial memory c_{t-1} and hidden state h_{t-1} and two outputs; the updated memory and hidden state. The LSTM cell is shown in figure 2 and consists of three gates that update the variable states with the use of the inputs and an activation function. The two types of activation functions that are used in the LSTM cell are the simgoid function σ and the tanh function, see Eqs. (1) and (2).

$$\sigma(x) = \frac{e^x}{e^x + 1} \tag{1}$$

$$tanh(x) = \frac{e^x - e^{-x}}{e^x + e^{-x}} \tag{2}$$

The first operation in the LSTM cell is the forget gate, here is decided what old information is removed of the previous memory state. The portion of the memory state that should be forgotten is determined by passing the inputs through the sigmoid function as shown in Eq. (3), here W_g, V_g, U_g are the weights and b_g is the bias of the forget gate.

$$g_t = \sigma(W_g \vec{X}_t^{c,d} + V_g \vec{O}_t^{c,d} + U_g h_{t-1} + b_g) \tag{3}$$

Secondly the input gate provides a potential memory state c_t^{pot} and simultaneously an input state i_t that will decide what part of the potential memory state will be added to update the memory state, see Eqs. (4) and (5) . Here $W_c, V_c, U_c, W_i, V_i, U_i$ are the weights and b_c and b_i are the biases of the input gate.

$$c_t^{pot} = tanh(W_c \vec{X}_t^{c,d} + V_c \vec{O}_t^{c,d} + U_c h_{t-1} + b_c) \tag{4}$$

$$i_t = \sigma(W_i \vec{X}_t^{c,d} + V_i \vec{O}_t^{c,d} + U_i h_{t-1} + b_i) \tag{5}$$

The new memory state c_t is determined with the information of the forget and input gate by, see Eq. (6).

$$c_t = (c_{t-1} \otimes g_t) \oplus (i_t \otimes c_t^{pot}) \tag{6}$$

At last, the output gate generates the new hidden state h_t by determining what part of the new memory state should be used, see Eqs. (7) and (8). Here W_p, V_p, U_p are the weights and b_p is the bias of the output gate.

$$p_t = \sigma(W_p \vec{X}_t^{c,d} + V_p \vec{O}_t^{c,d} + U_p h_{t-1} + b_p) \tag{7}$$

$$h_t = p_t \otimes tanh(c_t) \tag{8}$$

B. Encoder

At the encoder side of the LSTM-AE the sequences are imported into a LSTM cell for every time step together

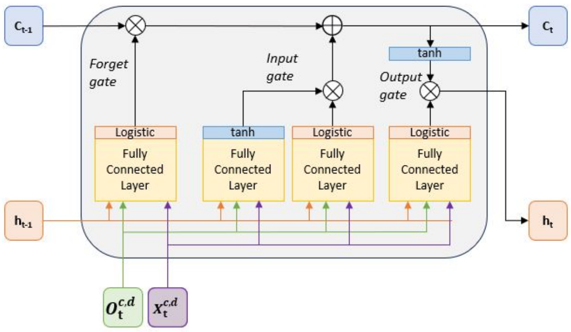

Figure 2. *Schematic overview of the LSTM cell structure.*

with the hidden and memory state of the previous LSTM cell, see Fig. 1. The operation conditions and the sensors measurements are separate inputs so the reconstruction of the data is independent of the operation conditions. The last hidden and memory state at time point $n^{c,d}$ are the starting conditions of the decoder.

C. Decoder

The decoder uses the reconstructed measurements of the previous time step $\hat{X}_{t-1}^{c,d}$ as input, except at $t = 1$, here the original data is used. Furthermore, it also uses the previous hidden and memory state and the operation conditions as inputs. The reconstructed measurement $\hat{X}_t^{c,d}$ is the output of this network and is generated by a fully connected layers of a neural network. This network consist of three layers where the last layer has an output of a^s, corresponding to the number of input sensors. The fully connected layers have the hidden state of the recurrent layer and the original operation conditions as input. By separating the operation conditions the autoencoder is forced to learn that the reconstruction of the sensor data is independent of the operation conditions.

D. Reconstruction losses

The reconstruction loss is determined by the difference between the input measurements and the reconstructed measurements. The mean reconstruction loss $RL_d^{c,s}$ of sensor s in sequence d of compressor lifecycle c is equal to:

$$RL_d^{c,s} = \frac{1}{n^{c,d} - 1} \sum_{t=2}^{n^{c,d}} \left| \hat{\vec{X}}_t^{c,d,s} - \vec{X}_t^{c,d,s} \right| \tag{9}$$

$$HI_d^c = \sum_{s=1}^{m^s} RL_d^{c,s} \tag{10}$$

The LSTM-AE is trained to minimize the reconstruction error, so it learns to capture the essential characteristics of the healthy chlorine compressor, while discarding noise and irrelevant information. During training phase teacher forcing will be applied to improve the training efficiency. Teacher forcing is performed by giving the original $X_{t-1}^{c,d}$ as input at the decoder side of the reconstructed measurements. In this manner the parameters further down the recurring LSTM cells are determined with the exact values instead of the predicted values.

2.2. Health Indicator construction

The data driven health indicators are based on the reconstruction loss of the LSTM-AE following Eq. (10). As previously described there will be constructed four different data driven HIs with the use of the model.

A. Sensor selection

As shown in Eq. (10) the HI is a summation of the reconstruction losses for set of sensors. This subset is specific for a HI. The usefulness of a sensor is dependent on the change of the reconstruction loss towards failure. This can be determined in an objective manner by using the trendability, which will be explained further in section 2.2. The sensors that are included inEq. (10) to construct the HI have a high trendability.

B. Health Indicator Evaluation Metrics

To evaluate the health indicators three metrics are defined: the monotonicity (M), trendability (T) and prognosability (P). These metrics are adopted from the work of Liu et al. (2020b) and de Pater and Mitici (2023) to test the behaviour of the HI during a compressor lifecycle.

Monotonicity. The general increasing or decreasing pattern of a feature over time. For a HI the monotonicity should increase when a incipient fault occurs and evolves.

$$M = \frac{1}{D^c - 1}\left|\sum_{d=1}^{D^c-1} I(HI_{d+1}^c - HI_d^c) - I(HI_d^c - HI_{d-1}^c)\right|,$$
$$\text{where } I(x) = \begin{cases} 1, & \text{if } x > 0 \\ 0, & \text{if } x \leq 0 \end{cases} \tag{11}$$

Trendability. The Spearman correlation coefficient is used between the HI and the sequences $\{1, 2, ..., D^c\}$ to define the trendability.

$$T = \frac{D^c \sum_{d=1}^{D^c} r_d^{HI^c} d - (\sum_{d=1}^{D^c} r_d^{HI^c})(\sum_{d=1}^{D^c} d)}{\sqrt{(D^c \sum_{d=1}^{D^c} (r_d^{HI^c})^2) \times \sqrt{(D^c \sum_{d=1}^{D^c} d^2) - (\sum_{d=1}^{D^c} d)^2}}} \tag{12}$$

Prognosability. The prognosability is the variance of the final state of the HI for each compressor lifecycle divided by the average lifecylce length. This metrics tells how well the HI could be used to detect the fault.

$$P = exp\left[\frac{-std(HI_{D^c}^c, e \in C^{test}}{\frac{1}{|C^{test}|}\sum_{e \in C^{test}} \left|HI_1^c - HI_{D^c}^c\right|}\right] \tag{13}$$

C. Tuning

The architecture of the LSTM-AE depends on the chosen model parameters, these are presented in Table 1. The optimal parameters are found using the approach presented in Fig. 3, where the model parameters are updated after each training process. This optimization loop is executed with the help of grid search, where systematically each logical combination of parameters is evaluated.

2.3. Health Assessment

The purpose of constructing the HI of the compressor is the ability to diagnose the state of the compressor. To determine the difference in the state of the compressor a fault threshold for the HI is proposed. When the upper bound of this threshold is passed the HI is considered unhealthy. The threshold is determined following Eq. (14), which corresponds to the Chebyshev's inequality (Kong and Yang, 2019).

Table 1. *The model parameters of the LSTM-AE that are included in the grid search for the optimal model.*

Architecture parameters
Number of stacked LSTM layers
Size of hidden and memory state
Sequence length of test data
Number of fully connected output layers

$$P(|HI_d^c - \mu \geq k\sigma) \leq \frac{1}{k^2}, \tag{14}$$

where $P()$ is the probability, k determines the confidence interval, μ is the mean and σ is the standard deviation. The mean and standard deviation are retrieved from the healthy training sets. The condition of the threshold is adapted from Chebyshev's inequality to Eq. (15).

$$HI_d^c \geq k\sigma + \mu \tag{15}$$

To filter out outliers of the HI the condition should be met v times in a row for the compressor to be diagnosed as unhealthy. This condition is used for the general HI to determine the state of the entire compressor and to determine whether fault identification is necessary.

2.4. Fault Identification

HIs are constructed in the same manner as described in Section 2.2 for each failure mechanism. Here, the sensor selection for the subset that is used in Eq. (10) is based on both system knowledge and trendability. For each HI of the included failure mechanisms a threshold is determined in the same way as described in Section 2.3. Fault identification takes place if the compressor is considered unhealthy and is the process assess the health of the HIs corresponding to each failure mechanism. Note, by performing the fault identification in this way it is possible to detect multiple developing faults simultaneously. The assess the performance of the fault identification key performance indicators (KPIs) are introduced, that are frequently used in this research field. These

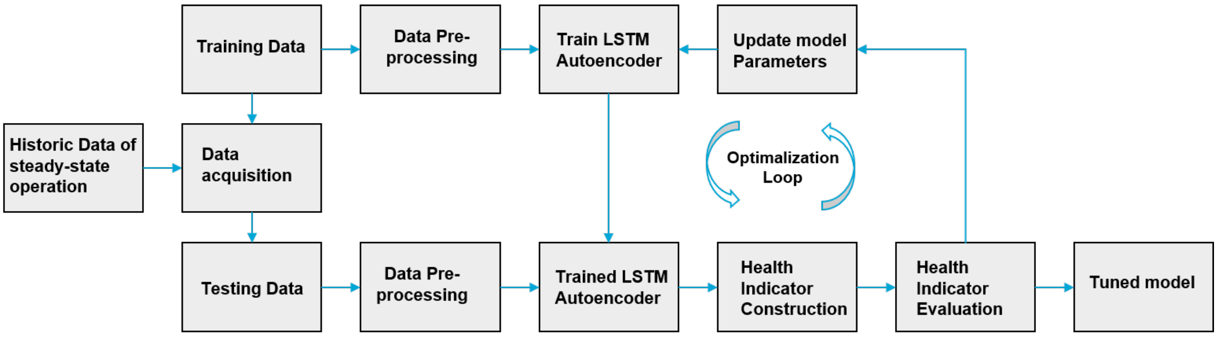

Figure 3. *The approach for tuning the model.*

KPIs are based on the confusion matrix, which is a visualisation of the fault identification results in a tabular representation. The KPIs:

- *Accuracy,* the number of correct predictions made by the model.
- *Precision,* how correctly the model has detected positive outcomes
- *Recall,* evaluates a classification model's effectiveness in identifying all positive instances. It is calculated as the proportion of relevant instances that were correctly detected.
- *F1-score,* identifies overall performance by combining precision and recall.

3. Case Study: Chlorine compressor

The proposed method is tested on the case study of a chlorine production plant, where two chlorine compressors operate parallel to pressurize and cool down chlorine with the purpose of liquefaction. First the characteristics of these compressor are described along with the failure mechanism that are included for the fault identification. Secondly, the data and acquisition of it is explained. The processing of the data is an important aspect when dealing with real world data is described next. Then results of the health indicator construction are described, which includes the tuning of the model, the sensor selection and the evaluation of the HIs.

3.1. Characteristics of the compressor

The compressor used for chlorine liquefaction consists of four compressing stages with cooling between the stages, except after the first stage. It operates at a high rotational speed and is considered as turbomachinery. The compressor is driven by an electrical engine, which is coupled by a gearbox to the rotor of the compressor. The rotor is hold in place by journal bearings on both ends of the compressor and an axial bearing on the non driven end to limit axial movement. These bearing are fed from an auxiliary oil system, this oil functions as both lubricant and coolant of the bearings. Labyrinth seals are used to separate the stages and prevent leakages. At both ends where the rotor leaves the compressor casing a labyrinth gas seal is applied. The failure mechanisms that are included into this research are selected based on occurrence, severity and the ability to be detected with the available data. The following failure mechanisms are included into the fault identification model.

Leakage. Due to the corrosive and toxic nature of chlorine leakages are a great risk for compressors. Most important is that external leakages of chlorine are prevented, since it has a large influence on the direct environment and operating personnel. Multiple types of leakage can occur in the compressor, namely between the two halves of the horizontal split casing, in the cavities between the stages and at the ends of the compressor where the rotor exists the casing. Leakages have effect on the temperature and pressure in the compression stages and on the pressure difference between the dry air and chlorine feedback in the gas seal.

Fouling. Fouling occurs when contaminants enter the compressor system, this results in performance losses of the compressor. Fouling can be divided in two groups, the first being non reactive contaminants that enter the compression circuit and do not change state (Barnard, 2001). This group typically settles in calm places, erode labyrinths and the edges of impeller blades. The other group consists of contaminates in gas or liquid form and these cause problems if they change state as they pass through the compression circuit. The main cause of fouling in chlorine compressors is the presence of moisture in the chlorine which in combination with the cast iron casing and chlorine reacts to ferrochlorine's. These particles can deposit inside the compressor and lead to internal blockages. The effect of fouling is decreasing efficiency of the compressor and is noticeably in the temperature between stages as well by the increase of power consumption.

Bearing failures. Bearing failure is the best known failure mechanism when dealing with rotary equipment and is normally detected with high frequency vibration measurements, these are not included in this case study. The purpose of the axial bearing is to absorb the axial forces and prevent axial movement, so out of bound axial displacement is a sign of a defect. Furthermore, defects on the bearings create extra friction and lead to increasing temperatures.

3.2. Data Acquisition

The data of 5 compressor lifecycles is available with length varying between 2.5 and 5.5 years. The sensor measurements are collected and stored each minute, this rate results in a large amount of data. In this case study the change in measurement values is slow, therefore the measurements are aggregated per hour by considering the mean per hour. There are 56 functional sensors outputting data, resulting in a total of almost 9 million sensor measurements. To reduce the data input for the model, sensor selection is performed. Following industry safety standards critical sensor measurements are executed twice or even three times to implement a safety factor, this brings sensor duplicates of which only one is selected. Also non identical sensors can have a high correlation, only one of two is selected if the correlation is 0.95 or higher. There are a total of $a^s = 16$ sensors selected and $a^o = 3$ are considered as the operation conditions, see Table 2 and Fig. 4.

To train a model to recognise the health state of a system a footprint of the state where the system is considered healthy is required. To establish time intervals in the data from where the training data can be acquired an assumption has to be made. It is assumed that the compressor data is considered healthy the first few months after the compressor is replaced.

Table 2. *The operation conditions and selected sensors. DE stands for Driven End and NDE for non driven end.*

Sensor	Description	Unit
Operation conditions		
P1	Suction pressure	barg
T1	Inlet temperature	°C
T8	Oil temperature	°C
Selected sensors		
dP	Pressure difference dry air and labyrinth	mbar
E1	Power consumption	Amp
P2	Press pressure	barg
P3	Oil pressure	barg
T2	Temperature outlet stage 1	°C
T3	Temperature outlet stage 2	°C
T4	Temperature inlet stage 3	°C
T5	Temperature outlet stage 3	°C
T6	Temperature inlet stage 4	°C
T7	Discharge temperature	°C
T8	Oil temperature	°C
T9	Axial bearing temperature	°C
T10	NDE journal bearing temperature	°C
T11	DE journal bearing temperature	°C
X1	Axial displacement NDE	mm
X2	Rotor vibration NDE	µm
X3	Rotor vibration DE	µm

3.3. Data preprocessing

The preprocessing of the raw data is required to make the model functional by giving it clean data as input. The preprocessing of raw data consists of multiple steps including: outlier removal, noise reduction, normalization and sequencing. The function and method of the preprocess step will be described in this section in the order of application, see Fig. 5.

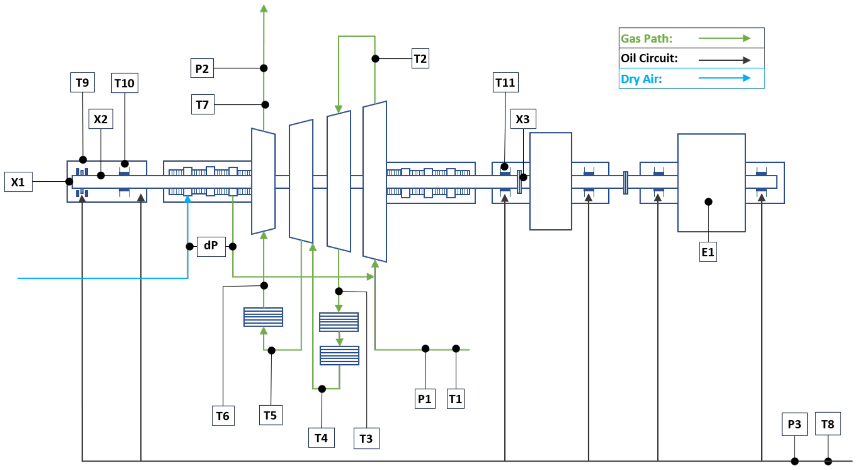

Figure 4. *Schematic of the compressor with the location of the sensors.*

Figure 5. *The order of the preprocessing steps that are applied to prepare the data for the model.*

A. Outlier Removal

The acquired data contains outliers that could be caused by various reasons for example sensor failures. The assumption is made that the training sets do not contain outliers, since these sets are of created of data during relatively short healthy period. To identify potential outliers in the test sets the overall mean and standard deviation of the training sets is used to establish the operation boundaries of the parameters that are measured. The upper and lower boundaries are equal to the mean plus/minus three times the standard deviation. To find the potential outliers the data of the test sets is subjected to these boundaries and the data points outside these boundaries are checked by hand to confirm whether they are outliers or not. In case of outliers the data is replaced by interpolating between the neighbouring non outlier data points.

B. Noise Reduction

The noise reduction will be performed with the moving average method, this makes the time series more smooth and will give a better performance for the model. The moving average replaces data points with the local mean of the window around the point. The window rolls through the time series with the data of each point as middle point and a size $D = 48$. This operation smooths the time series and reduces the noise.

C. Normalization

Normalization is used to scale all features to the same standard. The type of normalisation that will be used is the mean normalisation, also known as standardisation. Here the the mean μ and standard deviation std are calculated from the data and used to normalize the set as shown in Eq. (16). It is important to note that the mean value and standard deviation of the training sets is also used on the testing set, for the reason that these are considered to be the values of the healthy state of the compressor.

$$X_t^{c,s} = \frac{X_t^{c,s} - \mu^{c,s}}{std^{c,s}} \tag{16}$$

D. Sequencing

The time series of a data set can not be fed to the LSTM-AE at once and is therefore split in smaller sequences d of size $n^{c,d}$. The sequences are extracted with a rolling window. The stride and length of this rolling window is different for the training and testing set. The training data has sequences with a length of 48, which corresponds to 2 days worth of data. For the training data the order of the sequences does not matter and overlapping windows are useful to increase the amount of training data. The length of the sequences of the test data is set to $n^{c,d} = 12$, which means that the HI is constructed for every 12 hours.

3.4. Results of Health Indicator construction

First the optimal parameters are determined with a grid search with the help of the metrics described in the methodology 2.2. Next the sensor selection is described, then the health indicators of different versions of the autoencoder are compared.

Plotting the reconstructed time series together with the original input is a way to visualise that the model functions properly. For the healthy state of the compressor the difference between these plots should be minimal. In Fig. 6 the reconstructed sequence of the compressor in a assumed healthy state is shown, note that the reconstruction is similar to the original input, which provides evidence that the autoencoder functions as supposed.

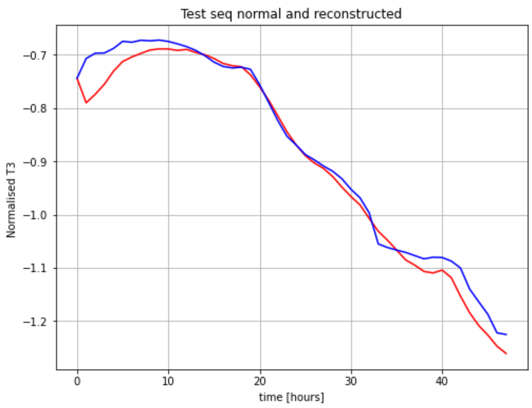

Figure 6. *A reconstructed sequence (blue line) of T3 compared with the original sequence (red line).*

A. Tuning

After the implementation of the model is verified the optimal parameters of the model are determined, these are acquired by performing a grid-search. This optimization loop is shown in the schematic Fig. 3. The grid search is evaluated with the metrics described in the methodology; monotonicity (M), trendability (T) and prognosability (P). The fitness of the model is added to the evaluation metrics, this is equal to the sum of the other metrics. The model parameters in the grid search that had the highest fitness overall are considered to be the optimal parameters, these are presented in Table 3 along with the other important hyperparameters. The weights of the training epoch with the lowest validation losses are applied to the model.

Table 3. *The hyperparameters applied to this case study*

Architecture parameters	value
Number of stacked LSTM layers	3
Size of hidden and memory state	128
Sequence length of test data	12
Number of fully connected output layers	3
Hyperparameters	
Optimizer	Adam
Initial learning rate	0.001
Number of epochs	100
Patience before decreasing the learning rate	5
Decrease the learning rate by factor	0.1

B. Sensor selection for HI construction

Only sensors with a high trendability are included in the construction of the HI. These sensors are added to subset S_{HI} which will be the input for Eq. (10). The trendability provides information over the difference in reconstruction loss at start of a lifecycle and the end of a lifecycle. For features with high trendability it is expected that the reconstructed signal deviation is minimal in the early stage of a lifecycle, this deviation increases with increasing time in the lifecycle, this corresponds to the increasing degradation. On the left in Fig. 7 a feature is shown with a high trendability, this corresponds to described expectation. On the right in Fig. 7 a feature is shown with low trendability, this does not correspond to described expectation and looks more like random noise. The features that are used for the construction of the HI have a high trendability and are included in subset S_{HI}.

C. Health indicator evaluation

The metrics of the HIs of the proposed method are compared with those of different versions of the method (see Table 4. The version of LSTM-AE without the operation conditions ignores the operating conditions.

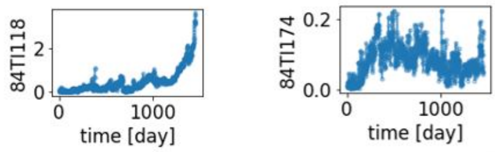

Feature T5 with $T = 0.9$ Feature X4 with $T = 0.05$

Figure 7. *Reconstruction loss per sequence of compressor lifecyle set 1.*

Analysing this version by comparing its metrics with that of the proposed method it is clear that the evaluation metrics decrease significantly. This result emphasize the effect of training the model independently from the operating conditions has positive impact on the performance of the HI construction.
The proposed model is trained with the training data of all compressors and could therefore be applied immediately for a newly placed compressor. The version of the method where the weights are trained for each compressor lifecycle separately could only be a applied to a new compressor when the months that are used for collecting training data are passed. However when dealing with real world data each compressor could have a different initial state, which brings extra noise and offsets to the HI construction. This expected difference in performance is visible in Table 4, where the evaluation metrics increase with this approach.

4. Validation of the results

After the implementation and verification of the model, the validation takes place. Since the model has two main purposes, namely assessment of the health and fault identification, the validation should cover both of these purposes. Lastly the value of the results is discussed.

4.1. Health Assessment

The health state division of the compressor lifecycle is shown in Fig. 8. There is no nuance in health state, when applying the threshold for the division between a healthy and unhealthy state as proposed in the methodology, this has as result that the compressor are considered unhealthy relatively early and operate for a long time before they are overhauled. The threshold could be increased or established in an entire different way to overcome this. The health state division could be used as bases for RUL prediction, since it indicates that degradation is taking place. To realise RUL prediction for this case study more failure data is required and in the best case addition of run-to-failure data. For generalisation and ease of implementation the original method has advantages over the method where for each lifecycle the model has to be retrained, while the latter has better performance.

4.2. Fault Identification

The process of fault identification is started from the moment the compressor lifecycle is marked unhealthy for the first time. This section first describes the selected sensors for each HI following and then the process of identifying the faults is presented along with the final results.

A. Sensor selection

The HI is based on the reconstruction losses of a subset of sensors that are considered for each HI of a failure mechanism. These subsets are based on the expected effect and location of the failure mechanism as described in section 3.1. Furthermore the trendability of the reconstruction loss has to be higher than 0.5 for the sensor to be included. The HI for detecting leakages will be constructed from the sensors that are relevant to the gas sealing. The selected sensor for fouling are measuring parameters of the gas path in the compressor. The subset for the bearing HI includes the temperature and pressure of the oil, the bearing temperatures and the position of the rotor. The subsets of the selected sensors are shown in Table 5.

B. Fault Identification

This model has the possibility to identify what fault is developing in the compressor. As mentioned multiple times before there is no clear data of failures available, adding to this the documentation of failures that occurred in the compressors are also lacking. This makes it hard to objectify this validation step, therefore it is chosen to discuss the occasions where the fail mechanisms of the compressor are known to a certain

Table 4. *Evaluation of the different version of LSTM-AE architecture. Here the sets corresponds to the compressor lifecycle. Mon, Tre and Pro stand for the monotinicity, trendability and prognosability respectively.*

	Set 1		Set 2		Set 3		Set 4		Set 5		Mean			
	Mon	Tre	Mon	Tre	Mon	Tre	Mon	Tre	Mon	Tre	Mon	Tre	Pro	Fitness
proposed LSTM-AE	0.01	0.88	0.02	0.87	0.02	0.51	0.00	0.91	0.03	0.86	0.02	0.81	0.519	0.612
proposed LSTM-AE without operating conditions	0.03	0.79	0.05	0.91	-0.01	0.51	-0.01	0.65	0.05	0.47	0.02	0.67	0.398	0.525
proposed LSTM-AE with trained weights per compressor lifecycle	0.03	0.94	0.05	0.88	0.04	0.72	0.04	0.88	0.08	0.92	0.05	0.87	0.704	0.764

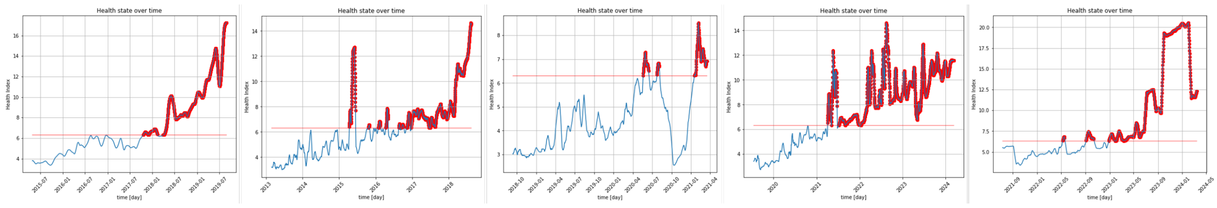

Figure 8. *The health state division of the compressor lifecycles sets 1 to 5 from the left to the right. The unhealthy state is marked by the red circles.*

Table 5. *The subsets for each type of constructed health indicator (HI).*

Health indicator	Sensor subset
General HI	{dP, P2 T2, T4, T5, T6, T7,T9, T10, T11, X2}
Leakage HI	{dP, P2}
Fouling HI	{P2, T2,T3, T4, T5, T6, T7}
Bearing HI	{P3, T9, T10, T11, X1, X2, X3}

degree. These are found by analysing the notifications and inspection reports of the compressors. The identification is performed by checking whether the separate HIs of the test sets cross the health threshold. Instances of the passing the threshold for each HI are shown in Fig. 9. In the left graph of Fig. 9 fouling HI of set 1 is shown, it is clearly visible that the HI passes the threshold, so fouling is identified. This lifecycle has been diagnosed with fouling so this identification is correct. The middle and right graph of Fig. 9 are both of lifecycle set 5 and show the presence of bearing damage and leakage respectively. These failure mechanisms are diagnosed for this compressor lifecycle so the identification is correct. The fault identification is performed by analysing the failures per set for each constructed HI, the results of analysis is presented in Table 6. The results of the fault identification are used to calculate the KPIs proposed in Section 2.4 and are shown in Table 7.

Table 6. *Confusion matrix of the fault identification*

Confusion matrix		Diagnosed Fault	
		Fault is present	*Fault is absent*
Identified fault	*Fault is identified*	5 True Positives	4 False Positives
	Fault is not identified	0 False Negatives	6 True Negatives

Table 7. *Case study results of the fault identification.*

KPI	Score
Accuracy	0.73
Precision	0.56
Recall	0.45
F1-score	0.5

4.3. Discussion

The results of the case study are validated to determine the quality of the model. In section 3.4 the performance of the proposed method is presented. The LSTM-AE which is trained for each compressor lifecycle separately performs considerably than the original proposed method, it has a mean monotonicity of 0.05, a mean trendability of 0.87 and a prognosability of 0.704. The health assessment and fault

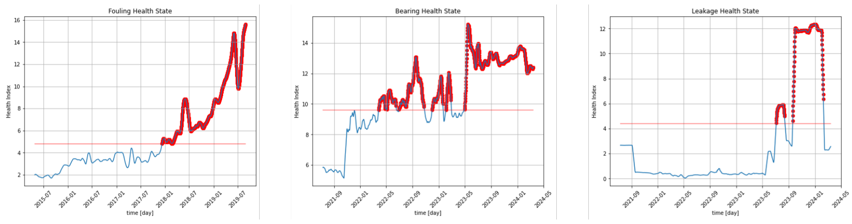

Figure 9. *Fault identification instances. The left figure shows that fouling is detected in lifecycle set 1. The figure in the middle and on the right show that bearing damages and leakage are detected in compressor lifecycle set 5.*

identification are therefore executed with this version. The health state division as shown in Fig. 8 functions as start signal for the fault identification. The HIs behave as expected with increasing reconstruction losses towards the end of life, however it is noticeable that the HI is not only increasing over time. The HI corresponds to the degradation of the compressor and degradation can not be undone without repairs, therefore this decreases of the HI are in theory not logical. However, they can be explained acknowledging that this is real data of compressors in a controlled process, this means that performance can be boosted by changing the process parameters. For the fault identification it is required to identify and couple the failure mechanism for each test set. However, there is no clear data of failures available, adding to this the documentation of failures that occurred in the compressors are also lacking, this has the effect that is hard to objectively quantify the performance. To make the validation of the fault identification possible educated assumptions based on the data that is available, are made on the failure mechanism of the compressor lifecycles. These are then analysed for compressor lifecycle and the results are presented in a confusion matrix (see Table 6). This results in a identification with an accuracy of 73% and a precision of 56%, which means that the proposed method could successfully identify faults in real world compressors even when multiple faults are occurring simultaneously. The use of the HI construction as basis for RUL prediction is not possible to be tested with the lack of run to failure instances in the available data.

5. Conclusion

The maintenance history of the chlorine compressors is analysed, which has resulted in 3 main failure mechanisms being identified. The sensor measurements of 5 historical compressor lifecycles have been acquired, preprocessed and used as input for HI construction. The proposed method for the HI construction is unsupervised machine learning LSTM-AE model, where the model is trained with healthy data only. The LSTM-AE is trained to reconstruct the measurements independently of the operation conditions, which increases the robustness of the model in varying operation conditions. Health assessment is performed to divide the health state of the compressor using the constructed HI. The first instance of an compressor marked as unhealthy triggers the start of the fault identification, which has resulted in a identification with an accuracy of 73% and a precision of 56% for the three considered failure mechanisms. The performance of the model is increased by training the weights of the model for each compressor lifecycle separately. The trade-off using this approach is that health assessment and fault identification is not possible in the start of a new lifecycle, because this period is used to acquire the training data. To overcome this trade-off a combination of both approaches should be used, where the health assessment during this first period of a new compressor is performed original model and after this initial period the model specifically trained for this lifecycle is used for fault identification with higher accuracy. To conclude, the proposed LSTM-AE method is able to correctly identify single or multiple failure mechanism present in chlorine compressors with an accuracy of 73 %, while only being trained with healthy data and is therefore applicable for real world cases with unlabeled data.
Therefore the goal of this study has been achieved.
Furthermore, the constructed HIs could be used as the basis for RUL predictions, it is however required to establish a maximum for the HI which corresponds

to the failure of the equipment. For the determination of this maximum more compressor lifecycles are required to create a better understanding of the behaviour of the compressor towards failure.

Exploring the possibilities for predictive maintenance that are available using machine learning has given insight in what possible improvements and follow up research could occur. In general a lot of the research in literature that try to perform fault diagnosis and prognosis make use of simulated data, which is stable, has Gaussian distribution and a clear degradation path. During this research the lack of research with real-world data is noticed, this provides a lot of opportunity for beneficial future research into the implementation of the these methods in real cases.

References

Al-Busaidi, W., and Pilidis, P., "Modelling of the non-reactive deposits impact on centrifugal compressor aerothermo dynamic performance," *Engineering Failure Analysis*, Vol. 60, 2016, pp. 57–85. doi: https://doi.org/10.1016/j.engfailanal.2015.11.027, URL https://www.sciencedirect.com/science/article/pii/S1350630715301527.

Lu, Y., Wang, F., Jia, M., and Qi, Y., "Centrifugal compressor fault diagnosis based on qualitative simulation and thermal parameters," *Mechanical Systems and Signal Processing*, Vol. 81, 2016, pp. 259–273. doi: https://doi.org/10.1016/j.ymssp.2016.03.018, URL https://www.sciencedirect.com/science/article/pii/S0888327016300176.

Luo, H., Bo, L., Peng, C., and Hou, D., "Detection and quantification of oil whirl instability in a rotor-journal bearing system using a novel dynamic recurrence index," *Nonlinear Dynamics*, 2022, pp. 1–33.

Lei, Y., Li, N., Guo, L., Li, N., Yan, T., and Lin, J., "Machinery health prognostics: A systematic review from data acquisition to RUL prediction," *Mechanical Systems and Signal Processing*, Vol. 104, 2018, pp. 799–834. doi: https://doi.org/10.1016/j.ymssp.2017.11.016, URL https://www.sciencedirect.com/science/article/pii/S0888327017305988.

Jardine, A. K., Lin, D., and Banjevic, D., "A review on machinery diagnostics and prognostics implementing condition-based maintenance," *Mechanical Systems and Signal Processing*, Vol. 20, No. 7, 2006, pp. 1483–1510. doi: https://doi.org/10.1016/j.ymssp.2005.09.012, URL https://www.sciencedirect.com/science/article/pii/S0888327005001512.

Schwartz, S., Montero Jiménez, J. J., Vingerhoeds, R., and Salaün, M., "An unsupervised approach for health index building and for similarity-based remaining useful life estimation," *Computers in Industry*, Vol. 141, 2022, p. 103716. doi: https://doi.org/10.1016/j.compind.2022.103716, URL https://www.sciencedirect.com/science/article/pii/S0166361522001130.

Wang, P., Youn, B. D., and Hu, C., "A generic probabilistic framework for structural health prognostics and uncertainty management," *Mechanical Systems and Signal Processing*, Vol. 28, 2012, pp. 622–637. doi: https://doi.org/10.1016/j.ymssp.2011.10.019, URL https://www.sciencedirect.com/science/article/pii/S088832701100450X, interdisciplinary and Integration Aspects in Structural Health Monitoring.

Kim, M., Song, C., and Liu, K., "A Generic Health Index Approach for Multisensor Degradation Modeling and Sensor Selection," *IEEE Transactions on Automation Science and Engineering*, Vol. 16, No. 3, 2019, pp. 1426–1437. doi: 10.1109/TASE.2018.2890608.

Moradi, M., Broer, A., Chiachío, J., Benedictus, R., Loutas, T. H., and Zarouchas, D., "Intelligent health indicator construction for prognostics of composite structures utilizing a semi-supervised deep neural network and SHM data," *Engineering Applications of Artificial Intelligence*, Vol. 117, 2023, p. 105502. doi: https://doi.org/10.1016/j.engappai.2022.105502, URL https://www.sciencedirect.com/science/article/pii/S0952197622004924.

Eleftheroglou, N., Zarouchas, D., Loutas, T., Alderliesten, R., and Benedictus, R., "Structural health monitoring data fusion for in-situ life prognosis of composite structures," *Reliability Engineering & System Safety*, Vol. 178, 2018, pp. 40–54. doi: https://doi.org/10.1016/j.ress.2018.04.031, URL https://www.sciencedirect.com/science/article/pii/S0951832017306737.

Liu, C., Sun, J., Liu, H., Lei, S., and Hu, X., "Complex engineered system health indexes extraction using low frequency raw time-series data based on deep learning methods," *Measurement*, Vol. 161, 2020a, p. 107890. doi: https://doi.org/10.1016/j.measurement.2020.107890, URL https://www.sciencedirect.com/science/article/pii/S0263224120304280.

Chen, X., Ding, X., Wang, X., Zhao, Y., Liu, C., Liu, H., and Chen, K., "Multi-Task Data Imputation for Time-Series Forecasting in Turbomachinery Health Prognostics," *Machines*, Vol. 11, No. 1, 2023. doi: 10.3390/machines11010018, URL https://www.mdpi.com/2075-1702/11/1/18.

de Pater, I., and Mitici, M., "Developing health indicators and RUL prognostics for systems with few failure instances and varying operating conditions using a LSTM autoencoder," *Engineering Applications of Artificial Intelligence*, Vol. 117, 2023, p. 105582. doi: https://doi.org/10.1016/j.engappai.2022.105582, URL https://www.sciencedirect.com/science/article/pii/S0952197622005723.

Arias Chao, M., Kulkarni, C., Goebel, K., and Fink, O., "Aircraft Engine Run-to-Failure Dataset under Real Flight Conditions for Prognostics and Diagnostics," *Data*, Vol. 6, No. 1, 2021. doi: 10.3390/data6010005, URL https://www.mdpi.com/2306-5729/6/1/5.

Malhotra, P., TV, V., Ramakrishnan, A., Anand, G., Vig, L., Agarwal, P., and Shroff, G., "Multi-Sensor Prognostics using an Unsupervised Health Index based on LSTM Encoder-Decoder," , 2016. URL https://arxiv.org/abs/1608.06154.

Hochreiter, S., and Schmidhuber, J., "Long Short-Term Memory," *Neural Computation*, Vol. 9, No. 8, 1997, pp. 1735–1780. doi: 10.1162/neco.1997.9.8.1735, URL https://doi.org/10.1162/neco.1997.9.8.1735.

Liu, C., Sun, J., Liu, H., Lei, S., and Hu, X., "Complex engineered system health indexes extraction using low frequency raw time-series data based on deep learning methods," *Measurement*, Vol. 161, 2020b, p. 107890. doi: https://doi.org/10.1016/j.measurement.2020.107890, URL https://www.sciencedirect.com/science/article/pii/S0263224120304280.

Kong, X., and Yang, J., "Remaining Useful Life Prediction of Rolling Bearings Based on RMS-MAVE and Dynamic Exponential Regression Model," *IEEE Access*, Vol. 7, 2019, pp. 169705–169714. doi: 10.1109/ACCESS.2019.2954915.

Barnard, P., "Centrifugal compressors fouling-understanding, mitigating, and cleaning," *Compressors and Their Systems: 7th International Conference*, John Wiley and Sons, 2001, pp. 241–250.

B Correlation matrix

Here the correlation matrix that is used for sensor selection is shown.

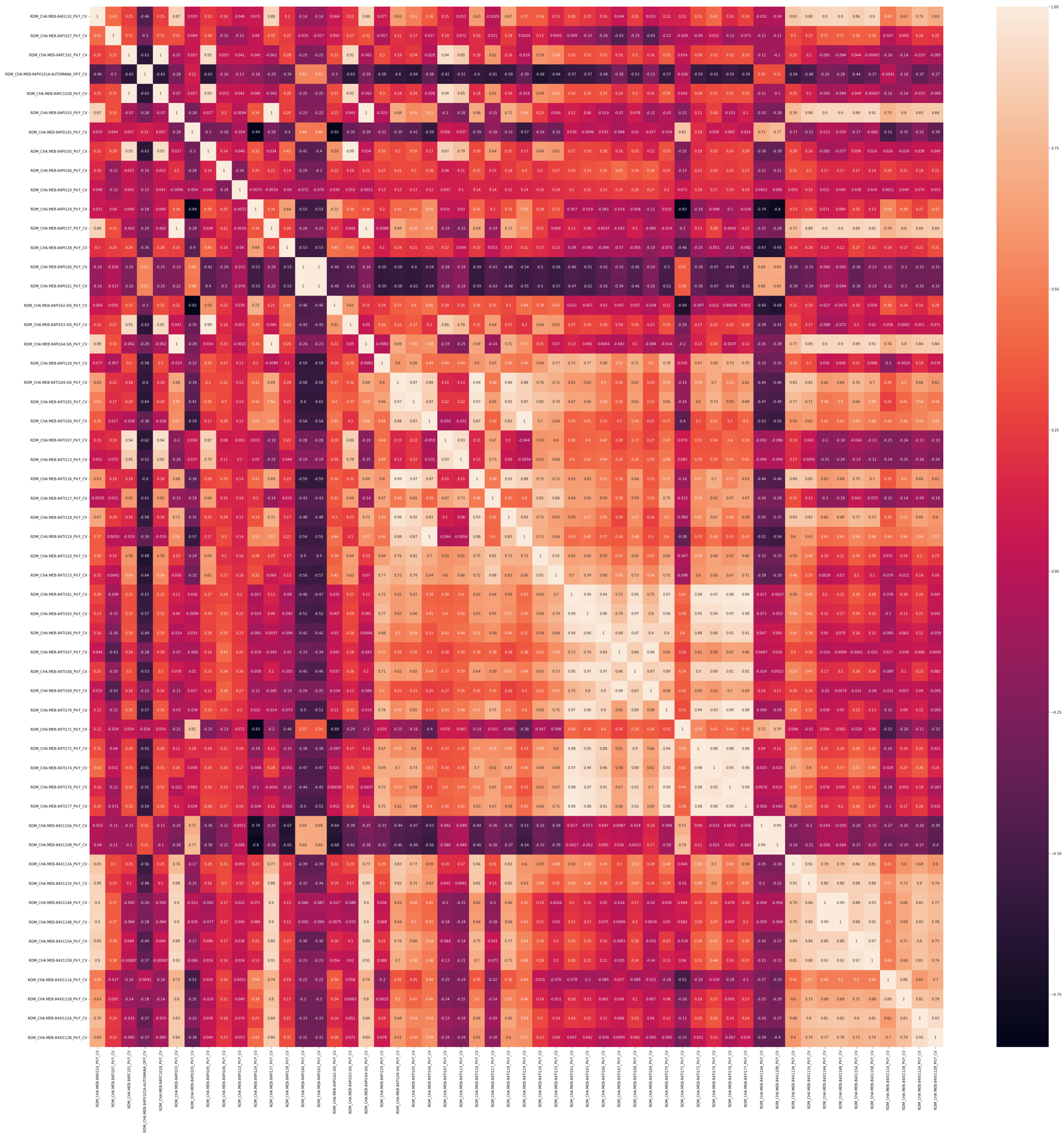

Figure B.1: Correlation matrix of the 56 sensors

C
Data preprocessing

The preprocessing of raw data consists of multiple steps including: outlier removal, noise reduction, normalization and sequencing. The effect of the preprocess step are presented in Figures C.1 to C.4 following the order of Figure 5.3.

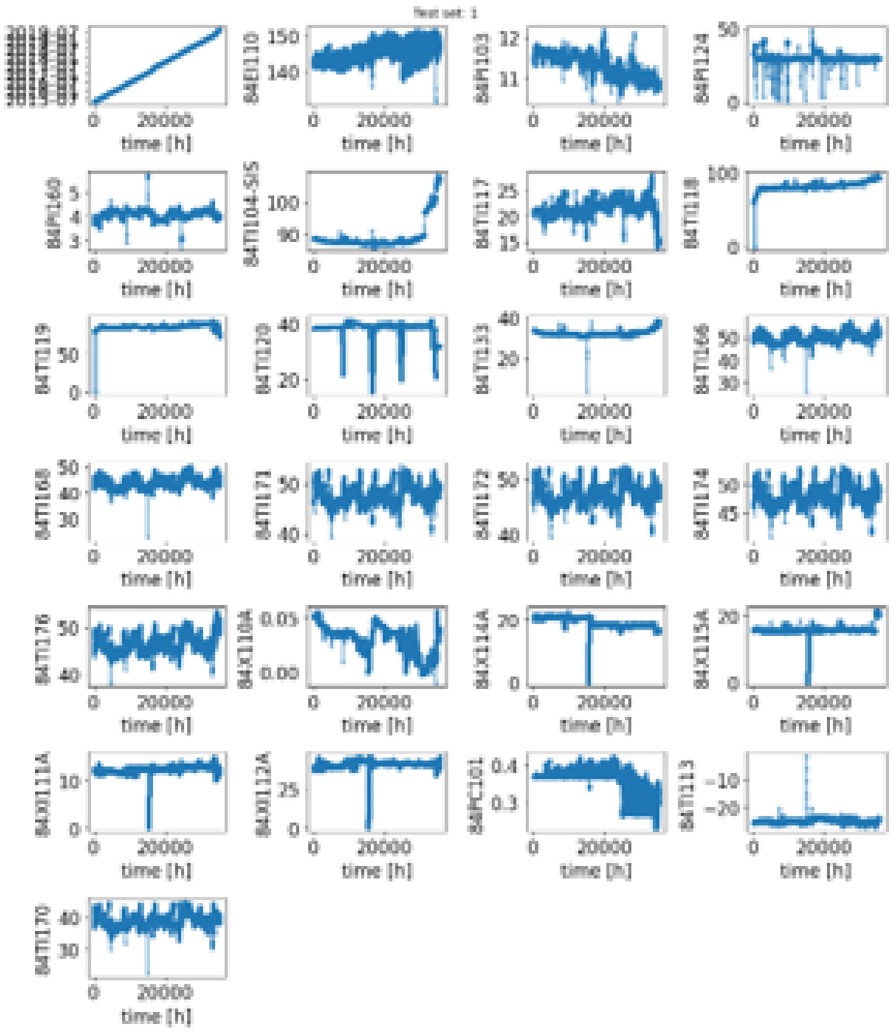

Figure C.1: Raw data that is the input of the model before the data preprocessing.

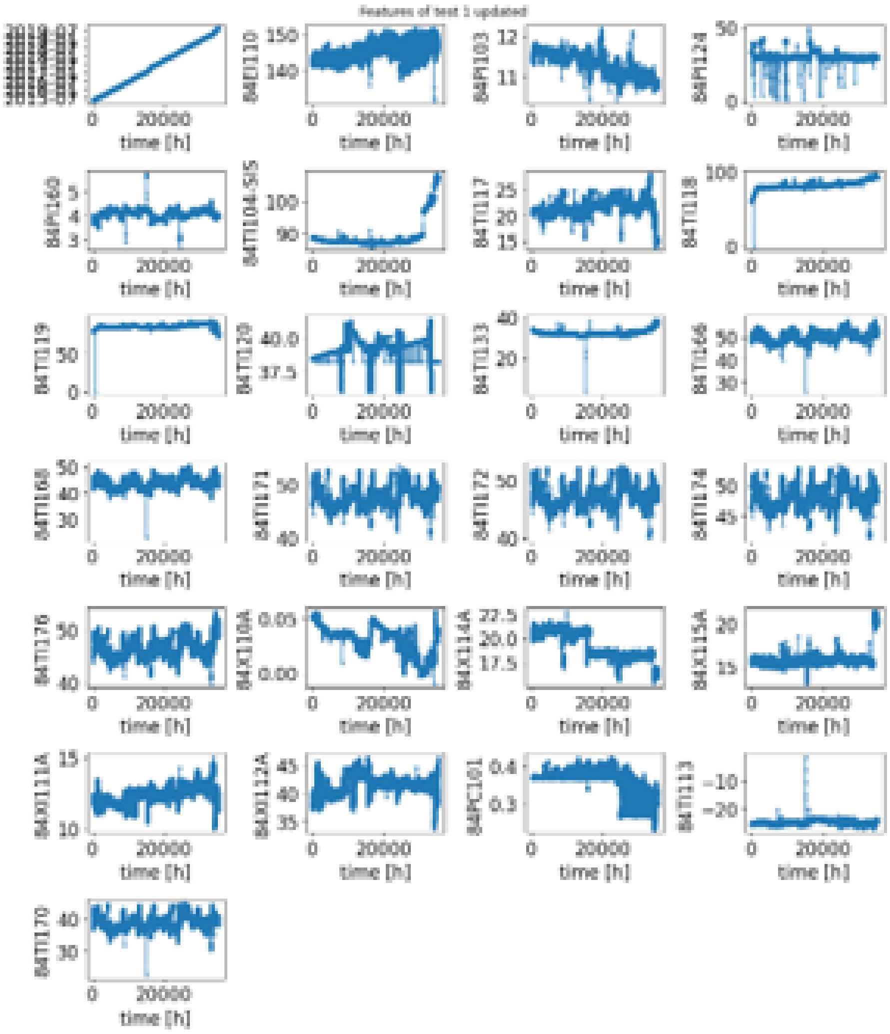

Figure C.2: The time series of the features of data set 1 after outlier removal

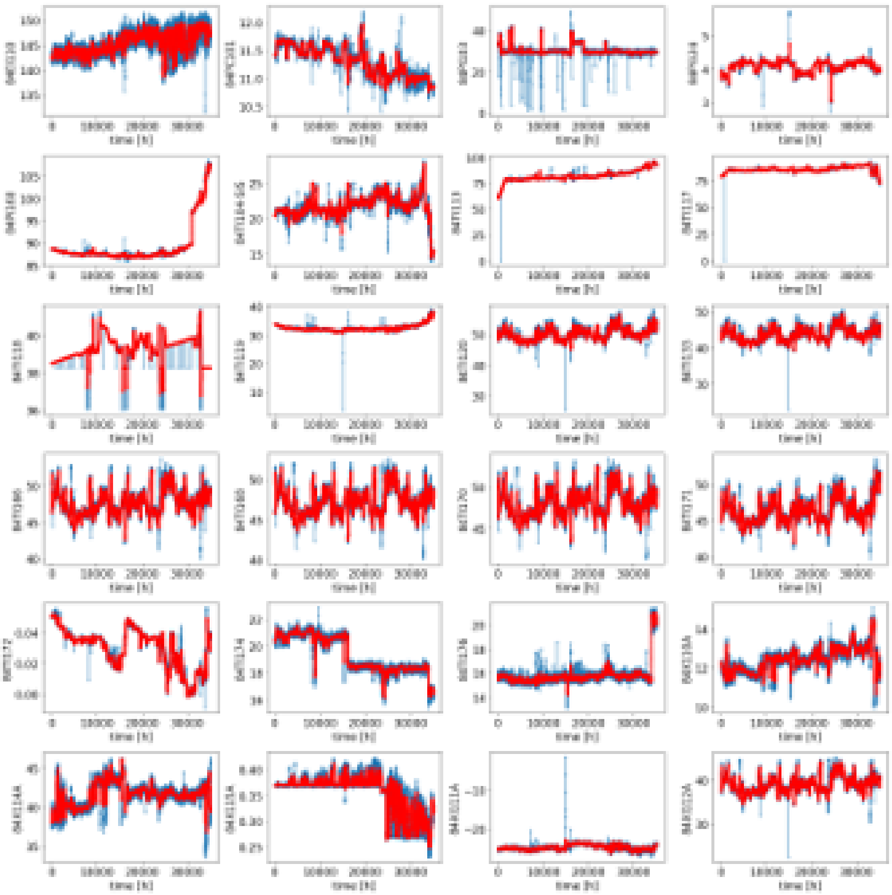

Figure C.3: The time series of the features of data set 1 after applying the moving average

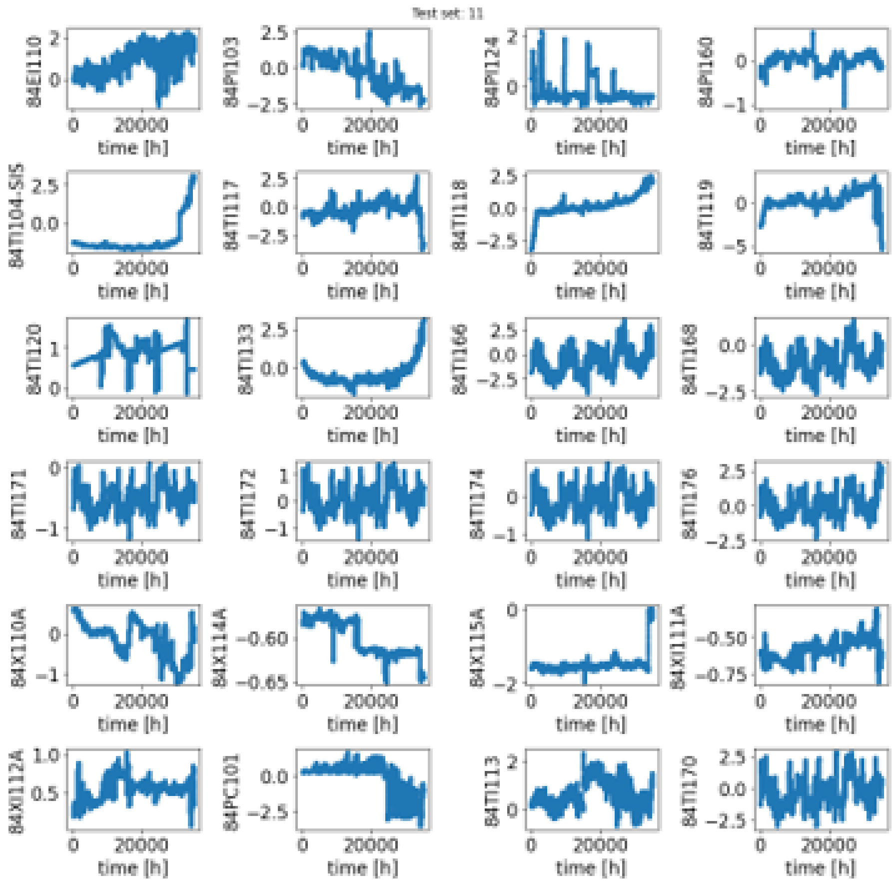

Figure C.4: The time series of the features of data set 1 after normalization

It is observable that the trend of the data has become more visible after the preprocessing steps. An interesting thing to note is the trend of the temperature sensors, which corresponds to the seasons, since it is depended on the cooling water temperature. Learning and identifying this seasons trend

D
Grid search for parameter tuning

This appendix contains the grid search used for the parameter tuning. The model parameters that are adjustable for model optimization are presented in Table D.1 along with the possible values that are considered, note that there are parameters in the architecture of the model that could be optimized, however to limit the grid search these are determined by assumption.

Table D.1: The adjustable parameters for model optimization

Parameters	Possible values
Number of stacked layers	1-5
Size of hidden and memory state	32,64,128,256
sequence length of test data	12,14,24,48
sample rate test data	12,1

The grid search is evaluated with the metrics described in the methodology; monotonicity (M), trendability (T) and prognosability (P). The fitness of the model is added to the evaluation metrics, this is equal to the sum of the other metrics. The results of the grid search are presented in table D.2. When analysing the results it can be seen that version 19 has the highest fitness value, however before appointing this as the optimal settings the training speed and the risk for overfitting should be considered. Due to the 5 stacked layers and the large hidden size the time to train increases immensely and overfitting becomes a problem. When excluding the versions with 5 layers, version 8 has the highest fitness.

Table D.2: Grid search for optimal parameters settings of the LSTM-AE

Version	seq len	sample rate	nr. layers	Hidden size	Monotinicity	Trendability	Prognosability	Fitness
1	14	12h	2	32	0.07	0.77	0.423	1.263
2	14	12h	2	64	0.05	0.738	0.444	1.230
3	14	12h	2	128	0.10	0.742	0.492	1.336
4	14	12h	2	256	0.05	0.792	0.481	1.319
5	14	12h	1	32	0.02	0.666	0.398	1.086
6	14	12h	1	128	0.08	0.738	0.445	1.261
7	14	12h	3	32	0.06	0.754	0.456	1.272
8	14	12h	3	128	0.11	0.764	0.566	1.438
9	14	12h	4	32	0.10	0.766	0.431	1.293
10	14	12h	4	128	0.04	0.774	0.516	1.334
11	14	12h	3	128	0.10	0.794	0.455	1.347
12	14	12h	3	128	0.08	0.81	0.543	1.433
13	48	1h	3	128	0.02	0.692	0.475	1.189
14	24	1h	3	128	0.02	0.746	0.503	1.267
15	24	1h	5	128	0.04	0.834	0.575	1.449
16	24	1h	5	256	0.03	0.784	0.586	1.402
17	24	1h	3	256	0.02	0.728	0.546	1.292
18	12	1h	3	128	0.01	0.806	0.519	1.339
19	12	1h	5	128	0.03	0.838	0.590	1.460
20	12	1h	5	256	0.03	0.814	0.574	1.415

E

Extra verification and validation results

E.1. Trendability

The trendability is highly depended on the reconstruction loss of each feature. The reconstruction losses of compressor lifecyle set 1 are displayed in Figure E.1. The average trendability per feature are shown in table E.1, the features that are used for the construction of the HI have a high trendability and are included in subset S_{HI}, the trendability per lifecycle of the features of this subset are shown in figure E.2.

Table E.1: Average trendability of all features

Feature	Trendability	Feature	Trendability
84EI110	0.447541	84TI170	0.497934
84PI103	0.537791	84TI171	0.613885
84PI124	0.33705888	84TI172	0.507401
84TI104	0.41878486	84TI174	0.459196
84TI117	0.5687834	84TI176	0.577804
84TI118	0.48005	84X110A	0.687018
84TI119	0.5817658	84X114A	0.597977
84TI120	0.6288814	84X115A	0.65348
84TI133	0.7545174	84XI111A	0.605298
84TI166	0.4750996	84XI112A	0.308984
84TI168	0.4120144		

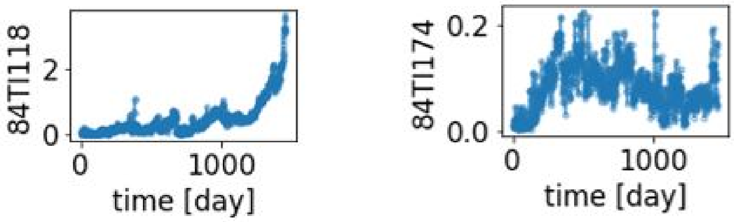

Feature T5 with $T = 0.9$ Feature X4 with $T = 0.05$

Figure E.1: Reconstruction loss $RL_d^{c,s}$ per daily sequence of compressor lifecyle set 1.

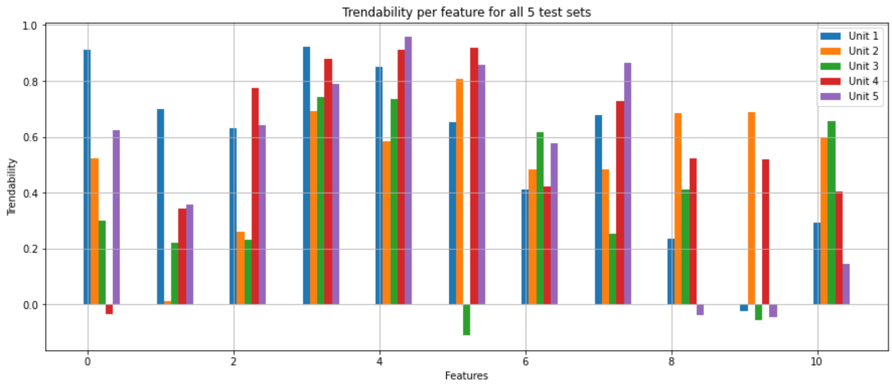

Figure E.2: Trendability of features

E.2. Manual fault identification

The identification is performed by checking whether the separate HIs of the test sets cross the health threshold. The HIs for fouling, leakage and bearings are shown in figures E.3, E.4 and E.5 respectively. The fault identification is performed by analysing the failures per set for each constructed HI, this analysis is presented in table E.2. While the analysis is not quantified it provides a good insight in performance of the model.

Figure E.3: The fouling HI for the 5 cases

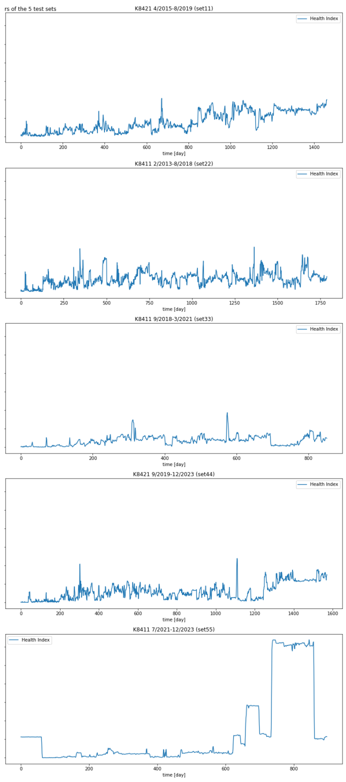

Figure E.4: The leakage HI for the 5 cases

Figure E.5: The bearing HI for the 5 cases

Table E.2: The analysis of the HIs per lifecycle

Set	Fail mechanism	Analysis of the HI		
		Fouling	**Leakage**	**Bearing**
df11	Fouling	Clear rise of the HI towards the end of the lifecycle, which indicates the occurrence of fouling	A minimal trend is visible, which is not enough to indicate a leakage	No trend is visible, the bearings can be considered healthy
df12	Fouling	Clear rise of the HI towards the end of the lifecycle, which indicates the occurrence of fouling	No trend is visible, which indicates that there are no significant leakages present	No trend is visible, the bearings can be considered healthy
df13	Unknown	A minimal trend is visible, which is not enough to indicate fouling	No trend is visible, which indicates that there are no significant leakages present	An increasing trend is visible, which indicate bearing problems
df14	Fouling	Clear rise of the HI towards the end of the lifecycle, which indicates the occurrence of fouling	No trend is visible, which indicates that there are no significant leakages present	The HI is constant, with the exception of a jump in the constant, which could be explained by calibration of the measuring instrument
df15	Bearing Leakage	A small trend is visible, which could point to the occurrence of fouling	Some large jumps are visible which indicates the possibility of a leakage	An increasing trend is visible, which indicate bearing problems